The isolation of antibiotic survivors in *Mycobacterium tuberculosis* using fluorescence activated cell sorting (FACS).

Patience Shumba

211546494

Submitted for complete fulfilment of the requirements for the degree of Master of Medical Science (Medical Microbiology) in the School of Laboratory Medicine and Medical Sciences, Nelson R. Mandela School of Medicine, University of KwaZulu-Natal.

November 2016

Declaration

I, Patience Shumba, declare that the work reported in this thesis is a result of my own research under the supervision of Dr Alexander Pym. This work has not been previously submitted to UKZN or any other tertiary institution for purposes of obtaining a degree.

Signed:

…...…… ……

Patience Shumba Dr Alexander Pym

Dedication

This work is dedicated to the Lord Almighty, my Saviour and my God without Him, I would have never made it this far.

Not to us Lord, Not to us but to Your name be the glory, because of Your love and faithfulness (Psalms 115:1, The Holy Bible, New International Version, 2011)

Acknowledgements

I am very grateful to the LORD, God Almighty for granting me the grace and the opportunity to study. I am thankful to Dr Alexander Pym for being my mentor and supervising the experimental work which was done in this project and the compiling of this thesis. Many thanks to the Africa Health Research Institute (AHRI) and Sub-Saharan Africa Network for TB/HIV Research Excellence (SANTHE) for funding.

I extend my gratitude to the following:

Dr Hollis Shen, Dr Adam Yadon and Dr Sary el Daker for teaching me about flow cytometry, assisting with the sorting and setting up the flow cytometer.

Dr John Adamson for teaching me a lot about mass spectrometry and assisting me with the mass spectrometry experiments.

Vanisha Munsamy and Pamla Govendor for the preliminary work you did.

The Pym lab at AHRI (Dr Sary el Daker, Kashmeel Maharaj, Lynne De Welsen, Vanisha Munsamy, Kayleen Brien, Darren Chetty) for all the ideas and support you provided.

Dr Dennis Chopera, Shepard Nhamoyebonde and Darren Chetty for proof reading this dissertation and the suggestions you provided.

My friends and colleagues at AHRI and UKZN whose names have not been written (because you are many ☺).

My parents Maxwell and Emma Shumba for your love, support and prayers.

My siblings Majury, Talbert and Loreen for cheering me all the way.

May the good Lord bless you for all the assistance you offered during my studies.

Once again THANK YOU, NGIYABONGA, NDINOTENDA.

Presentations related to this work

P. Shumba, S. el Daker, A. Yadon & A. Pym. The isolation of antibiotic survivors in Mycobacterium tuberculosis using Fluorescence Activated Cell Sorting (FACS), Poster to be presented at the Keystone Symposia Conference A5: New Developments in Our Basic Understanding of Tuberculosis, Vancouver (Canada), January 2017.

P. Shumba, S. el Daker, A. Yadon & A. Pym. The isolation of antibiotic survivors in Mycobacterium tuberculosis using Fluorescence Activated Cell Sorting (FACS), Poster and short talk presented at the Sub-Saharan Africa Network for TB/HIV Research Excellence Annual Meeting in Nairobi (Kenya), October 2016.

P. Shumba, A. Yadon & A. Pym. The isolation of antibiotic survivors in Mycobacterium tuberculosis using Fluorescence Activated Cell Sorting (FACS), short talk presented at the K-RITH/IDM Scientific Symposium – Human Disease Pathogenesis in Durban (South Africa), November 2015.

TABLE OF CONTENTS

LIST OF FIGURES

LIST OF TABLES

LIST OF ABBREVIATIONS

ACP	Enoyl-Acyl carrier protein
AMK	Amikacin
CCCP	Carbonyl cyanide-*m*-chlorophenylhydrazone
CFU	Colony Forming Units
CFZ	Clofazimine
CHP	Cumene hydroperoxide
CTC	5-cyano-2,3-ditoyl tetrazolium chloride
DAPI	4´,6-diamidino-2-phenylindole
$DiBAC_4$ (3)	Bis -1,3-dibutylbarbituric acid trimethine oxonol
$DiOC_2$(3)	3,3´-diethyloxacarbocyanine iodide
DNA	Deoxyribonucleic acid
EMB	Ethambutol
FACS	Fluorescent Activated Cell Sorting
FDA	Fluorescein Diacetate
FISH	Fluorescence *in situ* hybridisation
FITC	Fluorescein isothiocyanate
FSC	Forward scatter
GFP	Green Fluorescent Protein
H_2O_2	Hydrogen peroxide
INH	Isoniazid
LVX	Levofloxacin
MDR–TB	Multi-drug resistant tuberculosis
MIC	Minimum Inhibitory Concentration
MOX	Moxifloxacin
NAC	N-acetyl- L- Cysteine
NAD	Nicotinamide adenine dinucleotide
NO	Nitric oxide
OADC	Oleic acid – Albumin – Dextrose – Catalase
OD	Optical Density
OFX	Ofloxacin
OH·	Hydroxyl radical
$\cdot O_2^-$	Superoxide anion
$ONOO^-$	Peroxynitrite
PBS	Phosphate Buffered Saline
PI	Propidium Iodide

PZA	Pyrazinamide
RIF	Rifampicin
ROS	Reactive oxygen species
RNA	Ribonucleic acid
SSC	Side scatter
STR	Streptomycin
TB	Tuberculosis
TCA	Tricarboxylic acid
UV	Ultraviolet
WHO	World Health Organisation
XDR–TB	Extensively-drug resistant tuberculosis
mM	millimolar
µM	micro molar
mg/ml	milligrams per millilitre
µg/ml	micrograms per millilitre
mV	millivolts
ml	millilitre
µl	microlitre
m/z	mass to charge ratio

ABSTRACT

The current chemotherapy for drug susceptible Tuberculosis (TB) does not rapidly eradicate the entire *Mycobacterium tuberculosis* population. It is not clear how a small fraction of bacteria (antibiotic survivors) can evade prolonged exposure to anti-TB drugs. The mechanisms which are responsible for this phenotype are unknown mainly because isolating this rare subpopulation of bacteria is extremely difficult. We hypothesised that fluorescent activated cell sorting (FACS) can be used to identify and isolate this subpopulation. In our approach, we first sought to identify fluorescent dyes which would distinguish viable from non-viable bacteria after antibiotic treatment. *M. tuberculosis* was grown to log phase and exposed to antibiotic treatment for 72 or 168 hours. At different time points cells from the treated cultures were stained individually and in combination with dyes for membrane integrity, membrane potential, reactive oxygen species, and esterase activity. We observed drug specific staining patterns with marked heterogeneity for most of the stains and antibiotics tested. Our results also indicate that staining with fluorescent dyes can provide information about the potential mode of action of new antimycobacterial drugs. When we evaluated CellROX Deep red as a marker for viability we observed that the CellROX Deep red negative cells were enriched for viable bacteria after 24 hours of treatment with clofazimine. CellROX Deep red, is a dye which detects reactive oxidative species in cells. Further work is now underway to characterise the mechanisms which are responsible for this phenotype.

CHAPTER 1

INTRODUCTION

1.1. Tuberculosis

Mycobacterium tuberculosis is the pathogen which causes the global health problem Tuberculosis (TB). Despite the availability of intense drug treatment, TB resulted in the deaths of 1.5 million people among the estimated 9.6 million incident cases of TB in 2014 (WHO, 2015). South Africa is among the six countries that had the largest number of annual incident TB cases globally (WHO, 2015). TB is normally diagnosed using sputum smear microscopy and culture or a rapid genetic diagnostic test such as GeneXpert (Helb *et al.*, 2010) before anti-TB chemotherapy is started.

The current treatment regimen for drug susceptible TB involves 2 months' intensive phase of orally administered isoniazid (INH), rifampicin (RIF), pyrazinamide (PZA) and ethambutol (EMB) followed by 4 months' continuation phase of INH and RIF. These antibiotics are also referred to as the first-line drugs for TB management. Anti-mycobacterial drugs vary in their mode of action targeting different cellular processes (Table 1). This long treatment regimen results in poor patient adherence which may lead to the emergence of drug-resistant TB (WHO, 2015). The need for such lengthy treatment is not clear but may include poor tissue penetration of antibiotics (Dartois and Barry, 2010), suboptimal pharmacokinetics (Boeree *et al.*, 2015) as well as the presence of a rare subpopulation of *M. tuberculosis* which is drug tolerant (Chengalroyen *et al.*, 2016). Recent studies to shorten TB therapy were not successful and resulted in relapse after completion of therapy (Gillespie *et al.*, 2014). Efforts to shorten TB therapy will require a better understanding of how *M. tuberculosis* can survive such prolonged exposure to antibiotics (Zhang *et al.*, 2012;Honeyborne *et al.*, 2016).

1.2. Drug-resistant TB

The emergence of drug-resistant TB poses a major threat to the public health sector's aim to control TB (WHO, 2015). Multi-drug resistant (MDR) TB is when *M. tuberculosis* is resistant to INH and RIF. Extensively drug resistant (XDR) TB is defined as *M. tuberculosis* that is resistant to INH and RIF as well as a quinolone and one of the injectable second-line agents (CDC, 2006). Drug resistance is a result of genetic mutations in *M. tuberculosis* which results in reduced permeability of the membrane to the antibiotic, production of enzymes that degrade the antibiotic, modification of the antibiotic activation pathways or modification of the drug target (Zhang *et al.*, 1993;Caugant *et al.*, 1995;Cohen *et al.*, 2014). Drug-resistant TB is treated by combining the first-line drugs to which the strain is still susceptible and second-line drugs. Treatment for drug resistant TB can last between 18- 24 months (Mitchison and Davies, 2012) although newer and shorter regimens are under clinical evaluation.

Table 1.1. Summary of mechanism of action of some of the anti-mycobacterial drugs used in TB treatment.

Drug	Mechanism of action	Cellular process targeted
First-line drugs		
Isoniazid (INH)	INH is activated by a catalase-peroxidase enzyme to forms an adduct with NAD that inhibits InhA an enzyme required for fatty acid elongation and mycolic acid synthesis (Knox *et al.*, 1952;Heym *et al.*, 1993).	Cell wall synthesis
Rifampicin (RIF)	RIF binds to *rpoB* gene product (RNA polymerase) and prevents elongation of RNA (Miller *et al.*, 1994).	Transcription
Pyrazinamide (PZA)	PZA is converted to pyrazinoic acid but its mechanism of action is not clear, although interaction with the ribosome is one possibility (Zhang and Mitchison, 2003)	Translation and probably other processes
Ethambutol (EMB)	EMB binds arabinosyl transferases interrupting arabinan synthesis. Arabinan is a component of arabinogalactan the major polysaccharide of the mycobacterial cell wall (Mikusová *et al.*, 1995;Takayama and Kilburn, 1989).	Cell wall synthesis
Other drugs		
Fluoroquinolones: Ofloxacin (OFX), Moxifloxacin (MOX), Levofloxacin (LVX)	Fluoroquinolones inhibit DNA supercoiling by binding to DNA gyrase (Drlica, 1999).	DNA replication and transcription
Clofazimine (CFZ)	CFZ binds to NADH dehydrogenase resulting in production of reactive oxidative species* (Yano *et al.*, 2011).	Respiration
Aminoglycosides: Streptomycin (STR) Kanamycin (KAN) Amikacin (AMK)	STR, KAN and AMK bind to the 16S ribosomal RNA on the 30s ribosomal subunit inhibiting the initiation of translation (Chan *et al.*, 2003) (Nair *et al.*, 1993).	Protein synthesis

***** possible mechanism of action

1.3. Persisters in TB

In contrast to drug resistance, antibiotic tolerance is a non-heritable mechanism by which bacteria can survive antibiotics. This phenotype was first described with penicillin treatment (Hobby *et al.*, 1942) (Bigger, 1944). Despite prolonged exposure to antibiotics a small proportion of bacteria survived. Critically when these survivors were re-grown in the absence of drug and then re-challenged with antibiotics their minimum inhibitory concentration (MIC) was not elevated and the same kill kinetics were observed. This type of experiment has been reproduced in many bacteria and critically shows that antibiotic tolerance is not due to the hereditable acquisition of drug resistance conferring mutations (Balaban *et al.*, 2004;Wayne and Hayes, 1996;Keren *et al.*, 2004). The antibiotic survivors selected were originally called persisters, and this term has stuck. Balaban *et al.* (2004) described Type I persisters as a preexisting population of non-growing cells generated during the stationary phase of growth and Type II persisters as a subpopulation of slowly growing cells that are continuously being generated in all stages of the growth. Unfortunately, in the study of TB, the term persister has also been used to describe *M. tuberculosis* during clinical latency. However, for the purposes of this thesis persister will be used to describe antibiotic tolerant bacteria that have been selected by antibiotics.

Persisters are the rare subpopulation of bacteria which survive the antibiotic treatment that kills their genetically identical siblings (Mc Dermott, 1958). Thus persisters are phenotypic variants of the drug susceptible bacteria (Zhang *et al.*, 2012;Lewis, 2010). Unlike resistant bacteria, persisters do not proliferate in the presence of an antibiotic (Figure 1). When the antibiotic is removed, persisters give rise to a genetically identical population which exhibits the same kill curve as the original population (Keren *et al.*, 2004). Importantly the decline in bacterial load in the sputum from TB patients initiating therapy is biphasic similar to that seen in killing by antibiotics of bacteria grown in liquid media. It has been proposed that this is due to the presence of a heterogeneous population of bacteria and the selection of persisters that take greater antibiotic exposure to kill (Jindani *et al.*, 2003). Transcriptional profiling of the response of *M. tuberculosis* to drug treatment has been used to define the mechanism of action of antibiotics and it has also been used to understand drug tolerant populations in sputum (Honeyborne *et al.*, 2016;Tudó *et al.*, 2010;Wakamoto *et al.*, 2013). In this study, we also use the term antibiotic survivors to refer to the drug tolerant population (persisters).

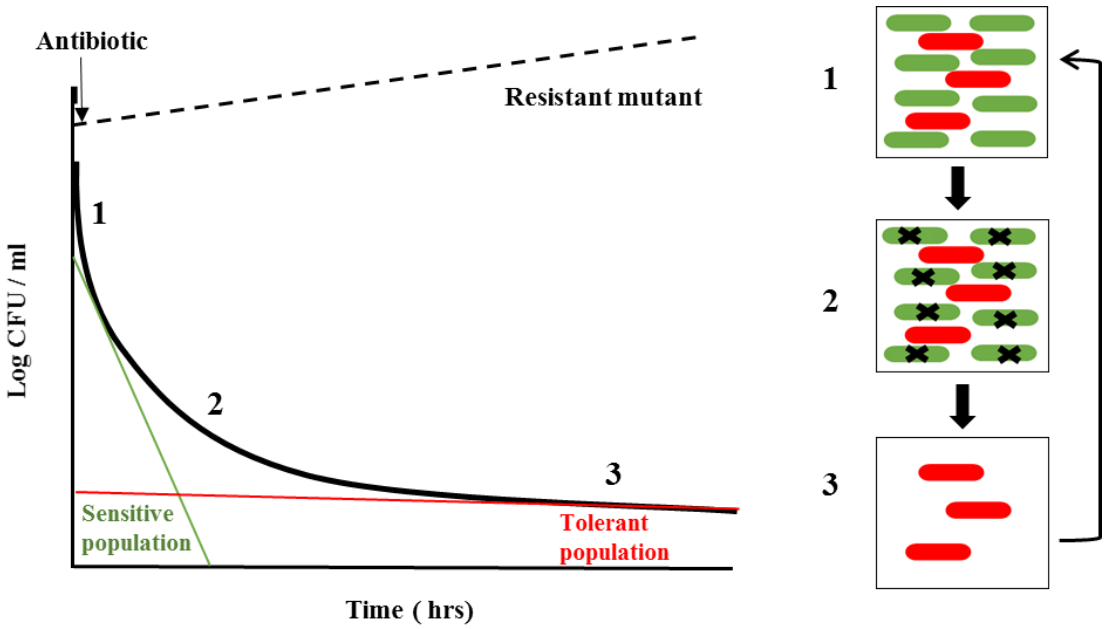

Figure 1.1. Killing kinetics during treatment with a bactericidal antibiotic. The panels to the right show: 1. The initial population of bacteria being exposed to a bactericidal antibiotic contains normally growing cells (green) and persisters (red) 2. Killing of the normally growing cells (green) on exposure to antibiotics but not the persisters (red). 3. Persistent cells (red) are killed with very slow kinetics and are therefore still present after antibiotic exposure. The arrow flanking the panels on the right shows that if persister cells are regrown without antibiotic they give rise to a population which is similar to the original population. In the graph the bold line shows the timing of killing after exposure to a bactericidal antibiotic. Initially there is rapid killing (1) until persister cells become enriched (2) and finally slow killing of the selected persisters (3). The black dashed line shows the growth of a drug resistant mutant strain in the presence of an antibiotic. The green line shows the kill kinetics of a drug susceptible population. The red line shows that persister cells are a preexisting population in the bacterial population. CFU/mL – Colony forming units /mL (Lewis, 2010;Maisonneuve and Gerdes, 2014).

Single gene mutation *in vitro* and *in vivo* studies have identified several pathways which may be involved in persister formation in *M. tuberculosis*. The pathways which have been implicated include energy related pathways, the stringent response regulator, cell wall synthesis, transporter systems and protein degradation pathways (Zhang *et al.*, 2012). Some of the identified genes include *sucB* a subunit of the pyruvate dehydrogenase complex involved in the TCA cycle (Bryk *et al.*, 2008), *cyd*C involved in cytochrome *bd* assembly (Dhar and McKinney, 2010), *pcaA* and *tgs* 1 which code for proteins involved in cell wall synthesis (Glickman *et al.*, 2000;Deb *et al.*, 2009) and toxin-antitoxin (TA) modules like RelA and RelE (Singh *et al.*, 2010;Keren *et al.*, 2011;Dahl *et al.*, 2003).

1.3.1. Challenges in eradicating persisters in TB

Bigger (1944) initially proposed intermittent drug dosing as a strategy of eliminating persisters assuming that this would allow persisters to become susceptible again once the antibiotic was removed (Zhang *et al.*, 2012). This strategy worked *in vitro* under defined conditions however *in vivo* the complex environment and pharmacokinetics of different antibiotics would present a potential risk of the emergence of drug resistance (Cogan, 2006;Zhang *et al.*, 2012). The inclusion of pyrazinamide (PZA) in TB treatment contributed greatly to the reduction of chemotherapy duration to 6 months (Fox, 1981). PZA is thought to primarily target persisters and is less effective against actively growing bacteria and is therefore referred to as a drug with sterilizing activity (Zhang and Mitchison, 2003). Rifampicin is also a critical drug in short course chemotherapy and is considered to have sterilizing activity. There are many *in vitro* assays that have been used to try and replicate the persister state in humans including starvation, hypoxia, and other models of slowly dividing bacteria. Other drugs have been found to have activity in these models including bedaquiline and fluoroquinolones and are considered therefore to have activity against persisters (Zhang, 2005;Dhar and McKinney, 2010;Singh *et al.*, 2010). However, the inclusion of fluoroquinolones in chemotherapy regimens didn't shorten therapy duration below 6 months so it is still unclear how *in vitro* models relate to drug activity against persisters in humans (Ji *et al.*, 1998;Zhao *et al.*, 1999;Chan *et al.*, 2004).

While the use of drug screens to identify agents that target persisters is important, it is also very important to identify the mechanisms that lead to persister formation in mycobacteria (Zhang *et al.*, 2012). This could lead to a more rational approach to eliminate persisters if we understood better the key metabolic pathways required to maintain viability in the face of antibiotics. Depending on the conditions and the drug, persisters usually represent less than 1% of a population of actively growing cells. The major barrier to the discovery of mechanisms responsible for persister formation is the lack of methods for isolating persister cells (Lewis, 2007) from cells that are dead or dying.

1.3.2. Single cell approaches in studying persisters

Single cell analysis is an approach that can provide insight into the heterogeneity of bacterial cells within a bacterial population. This heterogeneity may arise as an adaptive trait to counteract environmental disturbances (Manina *et al.*, 2015;Trouillon *et al.*, 2012). Microfluidic technologies and real time imaging have been used separately or in combination to show heterogeneity in microbial populations (Rusconi *et al.*, 2014;Lin *et al.*, 2014;Balaban *et al.*, 2004). Wakamoto *et al.* (2013), used microfluidics to show the production of heterogeneous responses from a population of genetically identical mycobacteria after exposure to antibiotics. Fluorescent reporter tags have been used in microfluidic cultures in conjunction with time lapse fluorescent microscopy to study the metabolic

activity in replicating and dormant cells (Jain *et al.*, 2016;Golchin *et al.*). Although these microscopy based approaches have the advantage of being able to track the fate of single cells after antibiotic treatment, they are essentially low-throughput. Most experiments that have been conducted to date report on hundreds of cells. But if the frequency of true persisters is less than 1%, the current format of single cell analysis may not be sufficiently sensitive to track rare subpopulations. An alternative technique which has emerged for higher throughput bacterial single cell analysis is flow cytometry (Ambriz-Aviña *et al.*, 2014;Rehse *et al.*, 1995;Czechowska *et al.*, 2008). Since its introduction in the mid-1900s flow cytometry has gained popularity in the identification and characterization of microorganisms at single cell level (Shapiro, 2015;Vives-Rego *et al.*, 2000). This is mainly because flow cytometry offers extremely high-throughput (millions of cells can be rapidly analyzed) quantitative and qualitative multi-parameter analysis (Wu *et al.*, 2016).

1.4. Flow cytometry

Flow cytometry is a process for measuring the physical and chemical properties of cells in a fluid stream (Shapiro, 2003). This technique is a fast and effective way for single cell analysis making it suitable for assays involving numerous cells. The fluidics system of a flow cytometer causes hydrodynamic focusing of particles (cells) on a laser beam which interrogates one cell at a time. The cell can be subjected to one or multiple laser beams at the interrogation point (Tracy *et al.*, 2010). The signals from the cell are detected by photomultiplier tubes and converted into quantitative electronic signals. Sophisticated software exists to interpret these signals (Virgo and Gibbs, 2012). Flow cytometry data can be displayed on a logarithmic or linear scale in the form of histograms, contour plots, density plots or dot plots. Dot plots have been most popular in graphical display compared to other forms (Maher and Fletcher, 2005).

Light scattering properties of cells are measured to give the side scatter (SSC) signal which shows the granularity of the cells and forward scatter (FSC) signal which represents the size of the cell (Shapiro, 2003). The relationship between light scatter and cell morphology can be complicated by the many factors such as the scatter angle geometry of the cytometer. Therefore, it should be noted that the FSC signal does not always produce a linear correlation with cell size (Müller and Nebe-von-Caron, 2010;Becker CL *et al.*, 2002). In spite of these factors, measuring scatter properties has been used to show that there was a change in the FSC signal due to impaired cell division after antibiotic treatment (Wickens *et al.*, 2000). SSC has also been used as measure the accumulation of metabolites an indirect measure of the metabolic state of cells (Fouchet *et al.*, 1993). In addition to identifying subpopulations with similar properties, flow cytometers can be used to locate and separate rare events from heterogeneous populations (Müller and Nebe-von-Caron, 2010).

Some flow cytometers use electrical or mechanical means to isolate and collect cells with desired characteristics and this is referred to as cell sorting (Shapiro, 2003). The combination of measuring fluorescent signals and cell sorting resulted in the formation of the core concept of modern flow cytometry referred to as fluorescence activated cell sorting (FACS) (Tracy *et al.*, 2010). The most common type of single cell sorting is droplet sorting which is based on the assigning of a charge to a droplet containing the particle of interest (Figure 2). The droplet is charged via the stream-charging wire attached to the flow cell. As the charged droplet passes through the charged deflection plates, electrostatic attraction and repulsion cause the charged droplet to be deflected to the left or right depending on its polarity (BDFACSAria™). This process allows for direct sorting into appropriate liquid media or onto solid agar (Müller and Nebe-von-Caron, 2010). The sorted cells can be used for further assays for example transcriptomics or viability. Tzur *et al.* (2011), has shown that combining the measurement of multiple parameters produced better results when sorting when compared to just measuring one parameter.

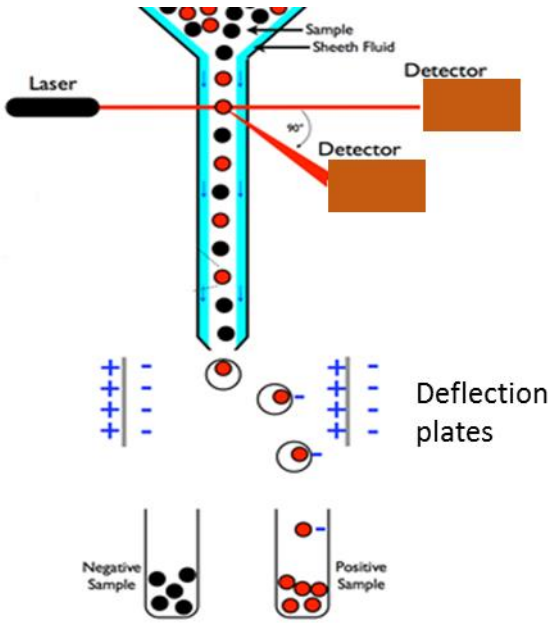

Figure 1.2. The principles of Fluorescence activated cell sorting (FACS). A sample containing cells is injected into the sheath fluid where the cells are funnelled to a single line of cells. The cells pass through the laser beam where signals of the light scattering and fluorescent properties of the cells are sent to detectors. At this point the nozzle generates droplets containing one cell per drop. When a particle which meets the sorting criteria is identified, an electrical charge is applied to the droplet containing the particle. When the charged droplet gets to the deflection plates (electromagnets), the polarity of the droplet causes the path of the droplet to be deviated so that the droplet is collected in the appropriate sample tube. Uncharged droplets are collected in the waste vial (not shown in diagram). (Sabban, 2011); http://nptel.ac.in/courses/102103015/module7/lec8/3.html

Physical parameters, sometimes called intrinsic factors, are measured without dyes. Structural and functional information on cells also called extrinsic factors can be measured using fluorescent stains or reporters (Shapiro, 2003). Fluorescent indicators are an established tool for distinguishing phenotypes at single cell level however very few fluorescent stains have been used to study bacterial physiology(Joux and Lebaron, 2000) (Maglica *et al.*, 2015). Flow cytometers with multicolour laser diodes have a wide variety of wavelengths which allow for the use of multiple fluorescent probes hence analysis of multiple parameters (Telford *et al.*, 2015). Flow cytometry has been used to study many biological organisms including multicellular organisms e.g. Drosophila embryos, eukaryotic cells, bacteria and viruses (Shapiro, 2005;Virgo and Gibbs, 2012;Nebe-von-Caron *et al.*, 2000;Strober, 2001). Flow cytometry with fluorescent stains has been used to measure DNA content, enzyme activity, cell membrane integrity, proliferative activity, oxidative stress, membrane polarity, total protein and many other factors (Shapiro, 2005).

1.5. Microbiological applications of flow cytometry

1.5.1. Cell count and cell proliferation measurements

Enumeration of cells can be achieved reliably with statistical confidence using flow cytometry (Wang *et al.*, 2010). Although changes in turbidity in opaque media are commonly used to estimate cell count, the presence of abiotic particles may overestimate the cell number (Müller and Nebe-von-Caron, 2010). Flow cytometry is more reliable than the classical method of determining cell number by counting of CFU. The major drawback of the CFU method is the exclusion of some cells which may not be able to grow under the experimental conditions (Barer, 1997). This has resulted in flow cytometry being widely used in the routine monitoring of drinking water and food safety (Czechowska *et al.*, 2008;Hammes and Egli, 2010). To improve the sensitivity of enumeration, nucleic acid stains such as 4´,6-diamidino-2-phenylindole (DAPI) and SYBR® Green 1 can be incorporated to stain cells and this excludes interference signals from the instrument or sample cells (Hammes and Egli, 2010;Völsch *et al.*, 1990).

Bacterial growth can be evaluated by monitoring the DNA content of the cell (Cooper, 2006). The DNA distribution pattern represents the chromosome number in a cell and this can be used to show the cell cycle stage of the bacteria (Cooper, 1969;Button and Robertson, 2001). DAPI and Hoechst dyes are cell membrane permeant which fluoresce blue upon binding to the minor groove of double stranded DNA (Arndt-Jovin and Jovin, 1989;Wolfe *et al.*, 1987). These dyes which are excited using the UV laser are non-toxic to cells nevertheless they exhibit a higher affinity for binding to AT clusters in DNA (Shapiro and Perlmutter, 2001;Loontiens *et al.*, 1990).

1.5.2. Drug susceptibility testing and analysis of efflux pump activity using flow cytometry

Norden *et al.* (1995) were the first to determine the susceptibility of *M. tuberculosis* to antibiotics agents within 24 hours. This is based on the ability of cellular esterase to hydrolyse fluorescein diacetate (FDA). FDA is a non-fluorescent molecule based on fluorescein. After cleavage of side chains by intracellular esterases FDA becomes fluorescent (Kirk *et al.*, 1998;Moore *et al.*, 1999;Veal *et al.*, 2000). Recent attempts to improve drug susceptibility testing in sputum samples incorporated a bacteriophage with a fluorescent reporter (O'Donnell *et al.*, 2015). Phage infection in the presence of drug could be detected by flow cytometry and predicted resistance. In addition to predicting susceptibility, flow cytometry coupled with fluorescent stains can be used to predict the mechanism of action of new antibiotics (Hendon-Dunn *et al.*, 2016).

Over expression of efflux pumps is one of the mechanisms responsible for the emergence of drug-resistant bacteria (Piddock, 2006;Machado *et al.*, 2012). Flow cytometry has been used to measure the rate of efflux pump expression by measuring the rate of efflux and accumulation of ethidium bromide(Paixão *et al.*, 2009). This may be an important technique to identify persisters as Szumowski *et al.* (2012), reported that drug tolerance in *M. tuberculosis* could be associated with the emergence of macrophage-induced mycobacterial efflux pumps and efflux pump inhibitors could potentially be used to shorten the chemotherapy for drug susceptible TB (Szumowski *et al.*, 2012).

1.5.3. Viability testing using flow cytometry

The conventional method for measuring cell viability is plating a small volume of the culture and incubating at the appropriate conditions then counting the number of colonies (Postgate, 1969). This technique may be ideal for fast growing organisms like *E. coli* or *M. smegmatis*. However for slow growing microorganisms like *M. tuberculosis*, which take at least 21 days to form visible colonies, this technique is not ideal and has impaired drug screens and the clinical evaluation of new drugs (Davey *et al.*, 2004). The CFU method may also be limiting when there is a subpopulation which is viable but non-culturable under the plating conditions used (Amann *et al.*, 1995). These and other disadvantages CFU enumeration have attracted the use of viability stains which provide a rapid method of determining viability and other physiological characteristics of the cell (Davey *et al.*, 2004). The common viability stains are based on assessing membrane permeability, enzyme activity or membrane polarity. Thus, assessing the dynamics of the molecular events (Figure 2) that are necessary to sustain cell survival and proliferation could serve as reliable evidence of cell viability (Manina and McKinney, 2013).

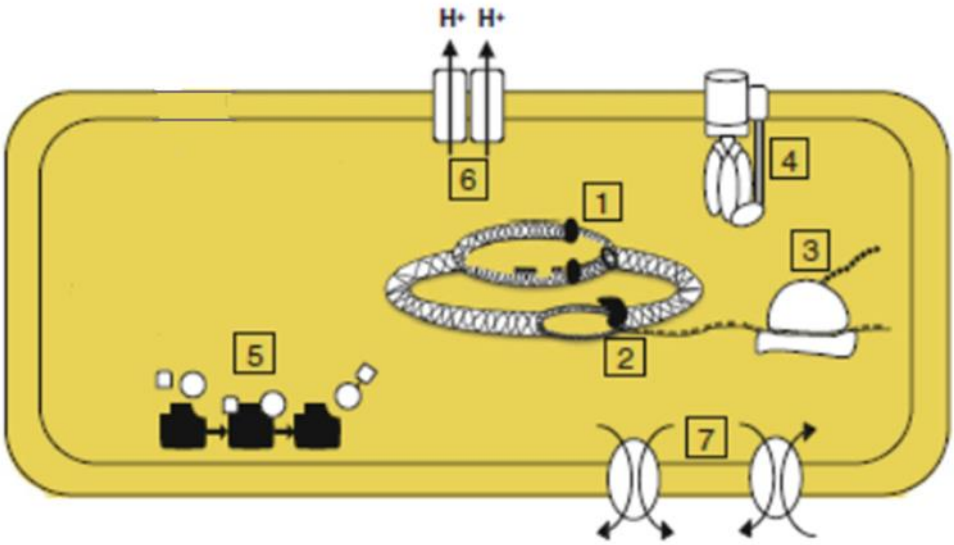

Figure 1.3. Schematic illustration of fundamental cellular processes. Cellular processes essential for survival, include: DNA replication (1), transcription (2), translation (3), ATP synthesis (4), enzymatic reactions involved in metabolic processes (5), respiration (6), symport and antiport of various molecules (7) (Manina and McKinney, 2013). It is not clear what role these processes play in the survival of persisters.

1.5.4. Evaluating cell membrane integrity

The ability of the cell to retain or exclude dyes from the cell has been used to discriminate live or dead bacteria. The exclusion of propidium iodide (PI), ethidium bromide and Sytox dyes from bacterial cells is used to assess membrane integrity (Bunthof *et al.*, 2001;Shu *et al.*, 2012). PI and Ethidium bromide are hydrophilic cationic, DNA intercalating dyes that bind at a stoichiometry of 4-5 base pairs per molecule (Comas and Vives-Rego, 1998;Horobin *et al.*, 2006;Waring, 1965). Both dyes are excluded from viable cells and fluoresce red when they bind to DNA. Sytox nucleic acid stains are cyanine based and cell impermeant dyes, as well binding non-selectively to DNA. These dyes are commonly used as dead cell stains and fluoresce either red, green, blue or orange making them favourable for multiple colour analysis (Hendon-Dunn *et al.*, 2016;Hammes and Egli, 2010;Chan *et al.*, 2012).

Though PI and ethidium bromide are assumed to be excluded from viable cells they have been found to stain intact cells (Nebe-von-Caron *et al.*, 2000). Determining membrane integrity by assessing the retention of dyes may be limiting due to variable uptake of the substrate, lack of enzymes for dye activation and active efflux of the dye (Nebe-von-Caron *et al.*, 2000). In order to interpret the staining results with these stains have been used in combination with nucleic acid binding dyes that are permeable to the cell or markers of enzyme activity (Müller and Nebe-von-Caron, 2010;Soejima *et al.*, 2009).

1.5.5. Enzyme activity as a measure of viability

Measuring the ability of cells to hydrolyse substrates for dehydrogenases or esterases has been used to indicate metabolic activity (Nebe-von-Caron *et al.*, 2000). These substrates are non-polar, permeable non-fluorescent molecules which become fluorescent and are retained within the cell upon hydrolysis. The redox dye 5-cyano-2,3-ditoyl tetrazolium chloride (CTC) has been used to detect respiring bacteria in aquatic environments. Dehydrogenases reduce CTC to a red fluorescent formazan product. Yamaguchi and Nasu (1997) reported that CTC is toxic to cells and some bacteria can not reduce the dye. These factors have limited its use in identifying bacteria (Joux and Lebaron, 2000).

Fluorescein diacetate (FDA) and its derivatives are the commonly used fluorophores for measuring non-specific esterase activity (Clarke *et al.*, 2001;Sträuber and Müller, 2010). The hydrolysis of FDA produces a fluorescent product, fluorescein. However, some media components e.g. tryptone result in FDA hydrolysis in the absence of live cells and other culture media quench the signal of fluorescein (Clarke *et al.*, 2001). These and other factors have reduced the use of FDA as a stain for evaluating esterase activity. Calcein acetoxymethyl esters are more widely used esterase substrates because calcein, the fluorescent product is brighter and has superior cell retention compared to fluorescein (Joux and Lebaron, 2000;Krämer *et al.*, 2015). In addition, calcein acetoxymethyl esters come in variable colours which allows multiparameter staining to be done using a palate of either calcein blue, green, violet, red or orange (Probes, 2010;Roth *et al.*, 1997;Krämer *et al.*, 2015;Johnson, 2010).

1.5.6. Measuring membrane polarity using flow cytometry

The electrical potential of the membrane is an important property for the cell as it governs signal transduction, nutrient uptake, respiration and other processes (Epps *et al.*, 1994). Fluorescent dyes have been used to measure membrane potential as an indicator of the physiologic state of cytoplasmic membrane and viability of the bacteria. Bacteria maintain a membrane potential > 100 mV across the membrane. Charged lipophilic dyes readily pass through the membrane (Shapiro and Nebe-von-Caron, 2004). Bis -1,3-dibutylbarbituric acid trimethine oxonol $DiBAC_4$ (3), is an anionic, lipophilic probe for measuring membrane potential. The dye is excluded by healthy polarized cells and upon entering depolarized cells it binds to lipid rich surfaces (Breeuwer and Abee, 2000).

A cationic cyanine based dye 3,3´-diethyloxacarbocyanine iodide $DiOC_2$ (3), is also used to measure the membrane potential of bacteria (Mason *et al.*, 1995). Metabolically active bacteria maintain an electrically negative charge on the cytosolic surface of the cell membrane. The positively charged $DiOC_2$ (3) aggregates on the cytosolic membrane causing the red fluorescence and the monomeric form of the dye gives rise to the green fluorescence (Novo *et al.*, 1999). This dye has both green and red fluorescence, the former is dependent on cell size whereas the latter is dependent on both cell size and membrane potential (Shapiro and Nebe-von-Caron, 2004;Novo *et al.*, 2000). Measuring the ratio of red

to green fluorescence is a more accurate way of measuring membrane potential using $DiOC_2(3)$ (Nebe-von-Caron *et al.*, 2000). Comparison of the staining with membrane potential uncouplers like carbonyl cyanide *m*-chlorophenyl hydrazine (CCCP) improves the reliability of the staining by providing a positive control (Joux and Lebaron, 2000). In addition to uncouplers membrane potential dyes can be used in conjunction with nucleic acid binding dyes like SYTO 17 as a way of improving the reproducibility (Comas and Vives-Rego, 1997).

1.5.7. Measuring oxidative stress using flow cytometry

Cellular metabolism in aerobic organisms generates toxic radicals called reactive oxidative species (ROS). ROS species include superoxide anion (O_2^-), hydroxyl radical (·OH), peroxynitrite ($ONOO^-$), hydrogen peroxide (H_2O_2) and nitric oxide ($NO^·$) (Korshunov and Imlay, 2006;Dwyer *et al.*, 2009). ROS levels are controlled by the activity of enzymes like superoxide dismutase, catalase and other free radical quenching agents such as glutathione (Cabiscol *et al.*, 2010). When cells experience oxidative stress, there is an imbalance between production of reactive oxygen species (ROS) and the ability of cells to scavenge them. This in turn causes oxidative damage to the membrane lipids, protein and nucleic acids and can lead to cell death (Belenky *et al.*, 2015).

Bactericidal antibiotics have been reported to produce ROS as part of their lethality in *Escherichia coli* and *Staphylococcus aureus* (Kohanski *et al.*, 2007;Dwyer *et al.*, 2014;Lobritz *et al.*, 2015). Although it is unclear to what extent this is the lethal mode of action of antibiotics or a by-product of the failure of other essential metabolic pathways (Keren *et al.*, 2013). Either way the detection of ROS could be a method of identifying a terminal event in antibiotic treatment. CellROX dyes, 4-amino-5-methylamino-2´,7´-difluorescein diacetate (DAF-FM) and dihydroethidium are some of the dyes that have been used to measure the oxidative status of cells (Lagman *et al.*, 2015;Dwyer *et al.*, 2014). Table 2 shows the characteristics of some widely used fluorescent stains for detecting oxidative stress.

Table 1.2. Summary of the properties of some stains used to detect oxidative stress.

Dye	**Chemistry**	**Ex/Em (λ)**	**Species detected**
CellROX Green	• Binds to DNA upon oxidation. • Signal localised to nucleus and mitochondria. • Can be used with fixed cells.	508/525	HO· $·O_2^-$
CellROX Orange	• Localised to cytoplasm • Cannot be used on fixed cells	545/565	$·O_2^-$ NO $ONOO^-$
CellROX Deep Red	• Localised to cytoplasm • used on fixed cells	644/665	HO· $·O_2^-$
Dihydroethidium (DHE)	• Binds to DNA upon oxidation. • Localised to nucleus.	518/605	Not known

Grant *et al.* (2012), reported that mycobacterial persisters can be eradicated by treating with antibiotics which generate ·OH and it has been suggested that INH and PZA induce ROS formation in the cell leading to autophagy (Goletti *et al.*, 2013). Piccaro *et al.* (2014), used electro paramagnetic resonance to show that there is production of ·OH after RIF interacts with its target the β- subunit of RNA polymerase and this could participate in the killing of *M. tuberculosis*. The activation of INH by KatG has been shown to result in the production of $NO^{\cdot}$ which potentially results in its antimycobacterial activity (Timmins and Deretic, 2006). FACS is therefore a promising approach to evaluate if the presence of ROS after antibiotic treatment would be able to predict cell death in *M. tuberculosis*.

1.5.8. The use of reporter systems in flow cytometry

Fluorescent proteins (FP) are used in flow cytometry to measure some cell parameters directly or indirectly (Dhandayuthapani *et al.*, 1995;Valdivia and Falkow, 1997). Enhanced mutants of the green fluorescent protein (GFP) from *Aequorea victoria* jellyfish, which is introduced into cells by cloning, has been used as a reporter for gene expression (Wu *et al.*, 2016;Patterson and Lippincott-Schwartz, 2002). Modification of GFP has led to a wide range of FPs with variable excitation and emission characteristics which have allowed investigators to combine FPs with fluorescent stains. Reporter systems have been used to measure gene expression, cell division and the metabolic status of cells (Southward and Surette, 2002;Vromman *et al.*, 2014). Recently fluorescent dilution of induced GFP has been used to measure single cell growth and this has been successfully used in *Salmonella* and mycobacteria (Helaine *et al.*, 2014;Mouton *et al.*, 2016). Another type of reporter are fluorescent oligonucleotide hybridisation probes which have been used to detect bacterial nucleic acids to identify species in mixed populations (Amann *et al.*, 1990) and quantify messenger RNA. Combining flow cytometry with fluorescence *in situ* hybridisation (FISH) has generated a technique called Flow-FISH which can quantify fluorescent hybridization levels at the single cell level (Nettmann *et al.*, 2013). These latter reporters have been used to investigate bacteria abundance or to distinguish specific properties of bacteria from environmental samples (Foladori *et al.*, 2015;Wang *et al.*, 2010;Decamp and Warren, 2001).

1.6. Problem statement

Treatment for drug susceptible TB lasts for at least six months in part due to the presence of a subpopulation of *M. tuberculosis* which is drug tolerant (Keren *et al.*, 2011). The mechanisms which are responsible for this phenotype are unknown mainly because there are no methods for isolating this rare subpopulation of bacteria (Mouton *et al.*, 2016;Grant *et al.*, 2012). Identification of such subpopulations so that they can be characterized is a major challenge as they represent less than 2% of the bacterial population (Keren *et al.*, 2004). Flow cytometry and fluorescent stains have been successfully used to distinguish physiological states of bacteria in environmental microbiology so we sought to apply similar techniques in *M. tuberculosis* to isolate antibiotic survivors.

1.7. Research rationale

The basis of this study was to develop an *in vitro* flow cytometry and fluorescent based technique for identifying and isolating *M. tuberculosis* persisters. As mentioned earlier, the major advantage of flow cytometry over other techniques like microscopy, plating for CFU and PCR is the rapid and accurate multiparameter analysis of many cells at single cell level. Fluorescent indicators are an established tool for distinguishing phenotypes at single cell level (Joux and Lebaron, 2000) however very few fluorescent stains have been used to study *M. tuberculosis* physiology. Bacterial flow cytometry is still developing and this study would be a significant advance in the field. The ability to isolate antibiotic survivors will enable us to identify mechanisms which cause this phenotype and possibly new targets for TB drug development. This study may also result in the identification of new protocols for viability staining in *M. tuberculosis*.

1.6. Hypothesis

We hypothesised that fluorescent stains can be used to predict the viability of bacteria and FACS can be used to isolate antibiotic cell survivors in *M. tuberculosis*. This approach would enable us to characterize the physiological differences between antibiotic tolerant (viable) and susceptible (non-viable) bacteria using for example transcriptomics, lipidomics and other techniques.

1.6.1. Aims

(i) To identify the fluorescent stains which can be used to predict the viability of antibiotic treated *M. tuberculosis.*

(ii) To use FACS to isolate single cell antibiotic survivors in *M. tuberculosis*.

(iii) To identify physiological mechanisms associated with *M. tuberculosis* antibiotic survivors.

CHAPTER 2

MATERIALS AND METHODS

2.1. Materials

All chemical reagents and antibiotics were obtained from Sigma Aldrich. Fluorescent dyes were obtained from Life Technologies. All chemical reagents and antibiotics were of analytical grade. The centrifuge was from Beckman Coulter®. Liquid chromatography was done using C18 column-ZORBAX Eclipse Plus C18 (2.1 mm x 50 mm; Agilent Technologies, USA) SN-USUX MO2122 and HILIC column-ZORBAX HILIC Plus (2.1 mm x 50 mm; Agilent Technologies, USA) SN-USCJR01187. Mass Spectrometry was done using the Triple Quad instrument (AB Sciex QTrap® 5500). Flow cytometry analysis and cell sorting was done using the BD FACS ARIA III cell sorter-Special Order Research Product (BD Biosciences, USA) located in a biosafety cabinet at the KwaZulu Natal Research Institute for TB and HIV situated in a biosafety level 3 (BSL-3) laboratory. All work done with *M. tuberculosis* was done in a biosafety cabinet in the BSL-3 laboratories.

2.2. Methods

2.2.1. M. tuberculosis strain and culturing

M. tuberculosis H37Rv strain was used in this project.

2.2.1.1. Glycerol stocks preparation

M. tuberculosis was grown to OD_{600} > 1 to ensure the cells were in stationary phase. Culture aliquots (1 mL) were added to 50% glycerol (500 µl) to make 25% glycerol stocks of the culture in cryovials. The stock culture was gently mixed by vortexing and stored at -80ºC.

2.2.1.2. Culturing of M. tuberculosis from glycerol stock

A cryovial containing 25% glycerol stock was thawed and added to a 30 mL inkwell containing 10 mL 7H9 media supplemented with 10% oleic acid- albumin-dextrose-catalase (OADC), 0.5 % glycerol and 0.05% Tween 80 (Appendix A). The culture was incubated at 37 ºC with shaking at 100 revolutions per minute for 7 days prior to sub culturing.

2.2.2. Liquid Chromatography – Mass Spectrometry (LCMS)

The stability of antibiotics was evaluated by monitoring the concentration of INH, RIF and ofloxacin (OFX) over 336 hours in 7H9 media and culture incubated at 37 ºC. Samples from both culture and media were analysed by liquid chromatography and mass spectrometry to measure the drug concentration.

2.2.2.1. Culture preparation

M. tuberculosis was sub cultured from a glycerol stock culture and grown to OD_{600} ~ 0.3. Culture aliquots (10 mL) were treated with either minimum inhibitory concentration (MIC) or 10X MIC of INH, RIF or OFX. Preparation of antibiotic stock solutions and MIC values are outlined in Appendix

B. Media controls were prepared by adding the antibiotics to 10 mL of 7H9 supplemented with OADC. The experiment was done in triplicate and all inkwells were incubated at 37 °C with shaking for 336 hours.

2.2.2.2. Culture and media samples

At baseline, 168 and 336 hours of incubation, 1 mL samples were taken in duplicate from each treatment condition for LCMS analysis. Culture samples were centrifuged at 10 000*g* for 10 minutes at room temperature to pellet the cells. The supernatant was filtered through a 0.2 micron filter into 1.5 mL Eppendorf tubes and samples were stored at -80 ºC. Media samples were filtered through 0.2 micron filters and stored at -80 ºC. On the day of analysis samples from 10X MIC were diluted 10 fold.

2.2.2.3. High Performance Liquid Chromatography (HPLC) and Mass Spectrometry

Chromatography was done on a HILIC column with a mobile phase of 75% Acetonitrile (ACN) in water for INH and RIF samples. The internal standard was 6-amino-nicotinic acid. The sample was mixed with 100% ACN containing internal standard in a ratio of 1:2 and gently mixed by vortexing. The samples were centrifuged at 16 000 rpm for 7 minutes to pellet precipitated proteins. The supernatant was mixed with deionised water at a ratio of 4:1 in a sample vial. The sample vial was then loaded on the auto sampler. Chromatography for OFX samples was done on a C18 column with a mobile phase of 15% ACN in water using the same internal standard. OFX samples were prepared in the same manner as INH and RIF samples until centrifugation. The supernatant was mixed with deionised water at a ratio of 1:3 in a sample vial. The sample was injected into the respective column for separation by high performance liquid chromatography then the samples were directly injected into the mass spectrometer which is attached to the column. Here the sample was fragmented into ions with different transitions. The transitions for detection and analysis for INH, RIF and OFX were of *m/z* 138.118/93.000, 823.280/791.400 and 361.958/318.100 respectively. Data acquisition, peak integration and calibration were performed using the Analyst software 1.6.2 (SCIEX, USA). Standard curves were generated to calculate the drug concentration in the samples.

2.3. Viability staining

2.3.1. Flow cytometry sample preparation and acquisition

Staining was done using 1 mL aliquots from three biological replicates and each replicate was analysed by flow cytometry. Cells were filtered through a 10 micron filter prior to acquisition on the flow cytometer. Single cells were identified by exploiting the relationship between height and width in the forward and side scatter signals (Figure 3.2.). This gating strategy excluded doublets and was followed during acquisition and sorting on the BD DIVA Software (BD Biosciences). The cells were acquired at a threshold rate ~ 5000–7000 events per second and 100 000 events were recorded. Photomultiplier tube (PMT) voltages which we used for all parameters are listed in Appendix C.

2.3.2. Evaluating antibiotic treated cells for esterase activity

Optimisation of the calcein green and calcein blue staining protocols was done by Vanisha Munsamy and Pamla Govender. *M. tuberculosis* was grown to log phase (OD_{600} ~ 0.4) and treated with INH, EMB, clofazimine (CFZ) and RIF at 10X MIC and incubated at 37 ºC for 72 hours. At baseline, 24 and 72 hours samples were stained with calcein blue or calcein green at 5 µg/mL for 1 hour at room temperature then filtered through a 10 micron filter and analysed on the BD FACS ARIA III. Calcein blue was excited with a 355 nm UV laser and fluorescence monitored using a DAPI filter. Calcein green was excited with a 488 nm laser and fluorescence intensity monitored using a FITC filter. We initially optimised the staining protocol by staining with FDA concentrations ranging from 0.01 – 10 µg/mL. FDA staining log phase cultures were treated with INH, RIF, moxifloxacin (MOX) and streptomycin (STR) at 10X MIC. At baseline, 72 and 168 hours samples were stained with FDA at 2.5 mg/mL for 1 hour at room temperature then filtered and analysed on the BD FACS ARIA III. FDA was excited with a 488 nm blue laser and fluorescence monitored using the FITC filter.

2.3.3. Analysis of membrane integrity and membrane potential after antibiotic treatment

Membrane integrity was evaluated using propidium iodide and Sytox red. The staining protocol was optimised by Vanisha Munsamy and Pamla Govender. *M. tuberculosis* was grown to log phase and treated with INH, EMB, CFZ and RIF at 10X MIC and incubated at 37 ºC for 72 hours. At baseline, 24 and 72 hours samples were stained with propidium iodide at 2 µg/mL or Sytox red at 5 µg/mL for 1 hour at room temperature then filtered and analysed on the BD FACS ARIA III. PI was excited with a 561 nm yellow green laser and fluorescence monitored using a PI filter. Sytox red was excited with a 640 nm red laser and fluorescence monitored using an Alexa Fluor 647 filter.

We evaluated membrane polarity using $DiOC_2$ (3) which emits both red and green fluorescence and $DiBAC_4$(3) which emits green fluorescence. We modified the BacLight Bacterial Membrane Potential kit protocol (Thermo Fisher Scientific) for $DiOC_2$ (3) staining. We initially compared the membrane potential changes in log phase *M. tuberculosis*, *E. coli* and *S. aureus* by treating the cells with 10 µM CCCP for 30 minutes to depolarise the membrane. Untreated cells were used as the hyperpolarised control. Untreated cells and depolarised cells were stained with 15 µM $DiOC_2$ (3) for 1 hour at room temperature then filtered and analysed on the flow cytometer. $DiOC_2$ (3) was excited with a 488 nm blue laser and fluorescence monitored using the PercP-Cy5.5 (red) and Alexa Fluor 488 (green) filters. The median fluorescence intensity was used to calculate the red: green ratio. *M. tuberculosis* was grown to log phase and treated with INH, RIF, MOXI and STR at 10X MIC then stained with 15 µM $DiOC_2$ (3) for 1 hour at baseline, 24 and 72 hours. We optimised the $DiBAC_4$ (3) staining protocol by staining bacteria with concentrations ranging from 0.03-10 µg/mL. Antibiotic treated samples were stained with 0.05 µg/mL $DiBAC_4$ (3) for 1 hour at room temperature then filtered and analysed. The depolarised control for $DiBAC_4$ (3) staining was prepared by incubating cells at 95 ºC for 30 minutes then re-

suspending the pellet in 1 mL PBS. $DiBAC_4(3)$ was excited with the 488 nm blue laser and fluorescence monitored using the FITC filter.

2.3.4. Analysis of ROS formation using DHE and CellROX oxidative stress reagents

Initially we optimised the concentrations for the positive control cumene hydroperoxide (CHP) which induces ROS formation and the negative control N-Acetyl-L-cysteine (NAC) which increases the anti-oxidative capacity of the cells. Cells were incubated with 5 mM CHP or 10 mM NAC for 1 hour at room temperature. We then stained untreated cells with CellROX dyes at a final concentration of 5 µM according to the manufacturers protocol (Life Technologies) and incubated at room temperature for either 30 minutes or 1 hour. We compared CHP versus 5 mM tert-butyl-hydroperoxide (TBHP) as positive controls. We also compared the staining patterns with or without washing. Subsequently, we stained 1 mL of cells with 5 µM of CellROX reagent for 1 hour at room temperature. This was followed by a washing step in which the cells were centrifuged at 10 000*g* for 10 minutes then the pellet was re-suspended in 1 mL of 7H9 media then filtered and analysed by flow cytometry.

We next evaluated ROS formation after antibiotic treatment as a marker a potential marker for viability. Log phase cultures were treated with INH, EMB, CFZ, OFX, levofloxacin (LVX), MOX, STR and RIF at 10X MIC and incubated at 37 ºC for 72 hours. Samples were collected for staining with CellROX Deep red and CellROX green reagents at baseline, 3, 6, 24 and 72 hours. The staining protocol described above was performed followed by flow cytometry analysis. We also stained untreated cells with different concentrations of DHE ranging from 5-50 µM for 30 minutes or 1 hour at room temperature. We compared the flow cytometry analysis with or without a washing step after staining.

2.3.5. Dual staining of calcein stains and membrane integrity stains

We simultaneously evaluated the esterase activity and membrane integrity of antibiotic treated *M. tuberculosis* by staining with combinations of either calcein blue and Sytox red or calcein green and PI. Log phase cultures were treated with INH, EMB, CFZ and RIF at 10X MIC and incubated at 37 ºC for 72 hours. At baseline, 24 and 72 hours samples were stained for 1 hour at room temperature then filtered through a 10 micron filter and analysed by flow cytometry. The same stain concentrations were used as with single staining and cytometer settings were not changed during acquisition.

2.4. Evaluating fluorescent dyes as viability markers

Initially we evaluated the effect of the fluorescent stains on the viability of untreated cells. Cells were grown to log phase and incubated with each stain at the appropriate concentration (Appendix D) for 1 hour at room temperature. Staining was done in triplicate. The sorting protocol was done using the four-way purity precision mode. Events were sorted into 2.5 mL Eppendorf tubes. The purity of sorted events was evaluated by reflowing a small proportion from the sorted events. The negative (low staining) subpopulation was collected from the events one log away from the positive (high staining) subpopulation on the histogram. Serial dilutions were performed and 100 µL from each dilution was

plated on Middlebrook 7H10 agar supplemented with 2.5% glycerol and 10% OADC. The plates were incubated for 21 days at 37 ºC. Plates containing between 20-200 visible colonies were used to calculate the colony forming units (CFU) per mL.

$$CFU\ per\ mL = \ Number\ of\ colonies\ \times\ Dilution\ factor\ \times 10$$

2.4.1. PI and Sytox red as viability markers

We evaluated the ability of membrane integrity stains PI and Sytox red to detect non-viable bacteria after antibiotic treatment. We compared the differences in the culturability of PI negative versus PI positive bacteria and Sytox red negative versus Sytox red positive bacteria. We treated log phase cells with OFX, RIF and INH at 10X MIC then incubated at 37 °C with shaking. Samples were collected at baseline, 72 and 168 hours after treatment and stained with PI. We sorted 500 000 events from the PI negative and PI positive subpopulations into 2.5 mL Eppendorf tubes. The sorted events were centrifuged at 10 000*g* for 10 minutes and the pellet was then re-suspended in 150 µL 7H9 media. Serial dilutions were performed as shown in Figure 2.1 and 100 µL was plated from each dilution. Plates were checked for growth after 21 days of incubation at 37 ºC.

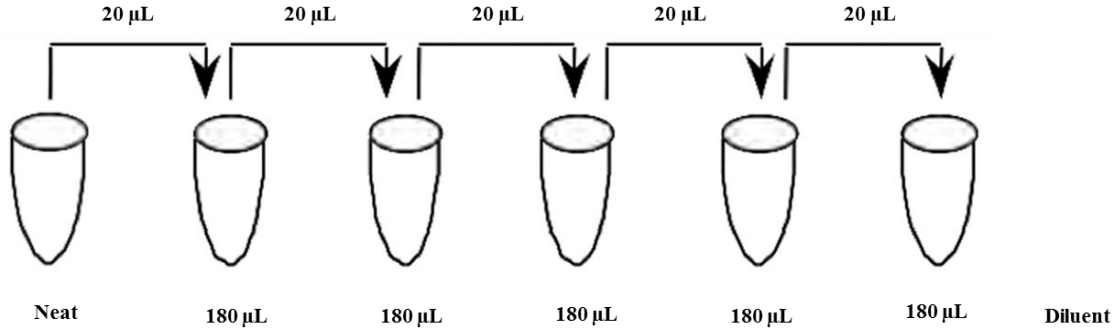

Figure 2.1. Schematic illustrating dilutions done after sorting. After sorting of required events and centrifugation the pellet was re-suspended in 7H9 media (neat). Tenfold dilutions were done using 7H9 media followed by plating.

CFU was calculated as shown below. Growth ratio was calculated by dividing the CFU by the number of sorted events. The ratio of survival of PI positive cells to PI negative cells was calculated as shown below. This ratio was calculated separately for each antibiotic and at each time point.

$$CFU = \ Number\ of\ colonies\ \times\ Dilution\ factor\ \times 1.5$$

$$Growth\ ratio = \frac{CFU}{Number\ of\ sorted\ events}$$

$$Ratio\ of\ survival\ of\ PI\ positive\ to\ PI\ negative = \frac{Mean\ growth\ ratio\ of\ PI\ positive\ (t = x)}{Mean\ growth\ ratio\ of\ PI\ negative\ (t = x)}$$

We also treated log phase bacteria with RIF and OFX at 10X MIC then incubated at 37 °C with shaking. Samples were collected at baseline, 24 and 72 hours after treatment and stained with Sytox red. We sorted 250 000 events from the Sytox red negative and Sytox red positive subpopulations into 2.5 mL Eppendorf tubes. Sorted events were treated as previously described and plated. Plates were incubated at 37 °C for 21 days and checked for CFUs. CFU and growth ratio were calculated as described above. The ratio of survival of Sytox red positive cells to Sytox red negative cells was calculated as shown below.

$$Ratio\ of\ survival\ of\ Sytox\ red\ positive\ to\ Sytox\ red\ negative = \frac{Mean\ growth\ ratio\ of\ Sytox\ red\ positive\ (t = x)}{Mean\ growth\ ratio\ of\ Sytox\ red\ negative\ (t = x)}$$

2.4.2. Calcein blue as a viability marker

We next analysed if the presence or absence of metabolic activity could be used to identify viable bacteria after antibiotic treatment. To carry out this aim, log phase bacteria were treated with CFZ and RIF at 10X MIC then incubated at 37 °C with shaking. Samples were collected at baseline, 24 and 72 hours after treatment and stained with calcein blue. We sorted 250 000 events from the calcein blue negative and calcein blue positive subpopulations into 2.5 mL Eppendorf tubes. Sorted events were treated as previously described and plated. Plates were incubated at 37 °C for 21 days and checked for CFUs. CFU and growth ratio were calculated as described above. The ratio of survival of calcein blue negative cells to calcein blue positive cells was calculated as shown below.

$$Ratio\ of\ survival\ of\ Calcein\ blue\ negative\ to\ Calcein\ blue\ positive = \frac{Mean\ growth\ ratio\ of\ Calcein\ blue\ \ negative\ (t = x)}{Mean\ growth\ ratio\ of\ Calcein\ blue\ positive\ (t = x)}$$

2.4.3. CellROX Deep red as a viability marker

We finally evaluated if the presence of ROS would be in indicator of cell death. We did this by treating log phase bacteria with CFZ and RIF at 10X MIC then incubated at 37 °C with shaking. Samples were collected at baseline, 24 and 72 hours after treatment and stained with calcein blue. We sorted 250 000 events from the CellROX Deep red negative and CellROX Deep red positive subpopulations into 2.5 mL Eppendorf tubes. Sorted events were treated as previously described and plated. Plates were incubated at 37 °C for 21 days and checked for CFUs. CFU and growth ratio were calculated as described above. The ratio of survival of CellROX Deep red positive cells to CellROX Deep red negative cells was calculated as shown below.

$$Ratio\ of\ survival\ of\ CellROX\ deep\ red\ positive\ to\ CellROX\ Deep\ red\ negative = \frac{Mean\ growth\ ratio\ of\ CellROX\ Deep\ red\ positive\ (t = x)}{Mean\ growth\ ratio\ of\ CellROX\ Deep\ red\ negative\ (t = x)}$$

2.5. Flow cytometry and Statistical analysis

The same gating strategy used during acquisition was used during analysis of FCS files using FlowJo versions 9 and 10 (Tree Star, OR, USA). GraphPad Prism 6 was used for statistical analysis. Multiple t-tests were performed (at the 95% confidence interval) on the data and P values < 0.05 were considered significant.

CHAPTER 3

RESULTS

3.1. Mass spectrometry analysis of drug stability

We initially sought to establish the stability of antibiotics in culture and media at different concentrations. Too low a concentration might result in selection of resistant mutants over the longer time courses required to study phenotypic tolerance, especially if drugs were labile in culture conditions. This would also enable us to determine the duration of treatment for these drugs. Other drugs were used in this study but we selected INH that is known to be unstable, RIF and OFX. We used these antibiotics to define a concentration relative to MIC that could be applied for many drugs.

We found OFX to be stable in both media and culture at 37 ºC for at least 336 hours. In contrast, RIF and INH exhibited a decrease in the drug concentration with time during culture and with media alone. The results were similar at both concentrations (at 1X MIC and 10X MIC) for all the antibiotics. Based on these results we decided to use 10X MIC for all antibiotics and treat for at most 168 hours without adding more antibiotic.

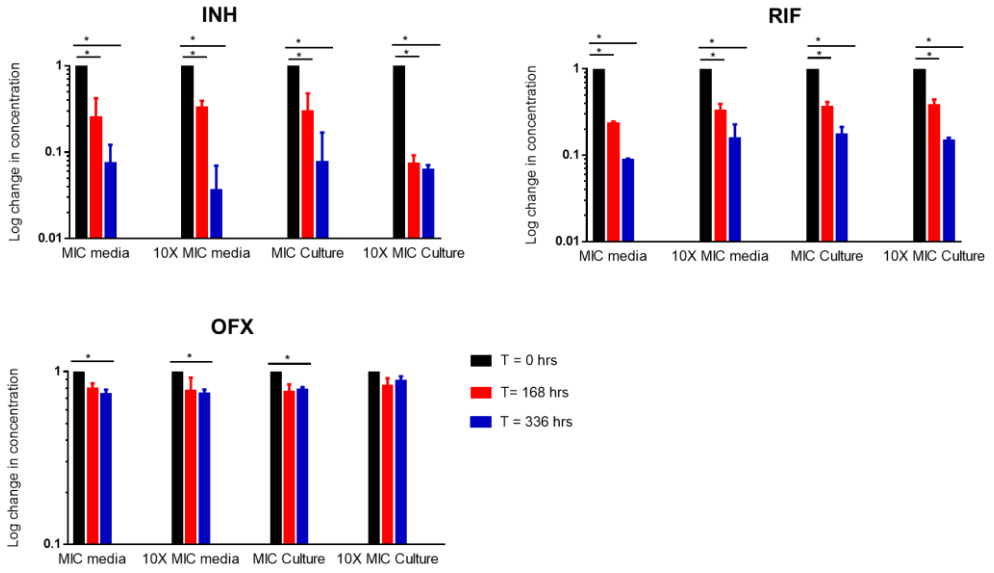

Figure 3.1. Assessing antibiotic stability over time in media and in culture. Cells or 7H9 media were incubated at 37 °C with antibiotic at 1X MIC or 10X MIC in triplicate. Antibiotic concentration was measured by collecting samples after 168 and 336 hours of incubation then analysed by mass spectrometry. There was a 90% decrease in the concentration of INH and RIF after 336 hours. However, the concentration of OFX was stable over the 336 hours of incubation. The log change in concentration was calculated as a fraction of the baseline concentration (y axis). Bars show the mean of three replicates and standard deviation. * P value < 0.05. Error bars represent standard deviation.

3.2. Staining patterns of drug treated cells

Antibiotic treated cells were stained with a range of fluorescent stains which measure enzyme activity, membrane integrity, membrane potential and oxidative stress. These stains were either used alone or in conjunction with others. The gating strategy was specific for single cells during acquisition on the BD DIVA software and during analysis of fcs files in FlowJo (Figure 3.2.). The doublet bacteria were excluded from analysis based on the relationship between height and width in the forward and side scatter signals. In preliminary experiments done in the laboratory this strategy was shown to exclude doublets using *M. tuberculosis* expressing red and green fluorescent proteins. The same strategy was used in subsequent analysis.

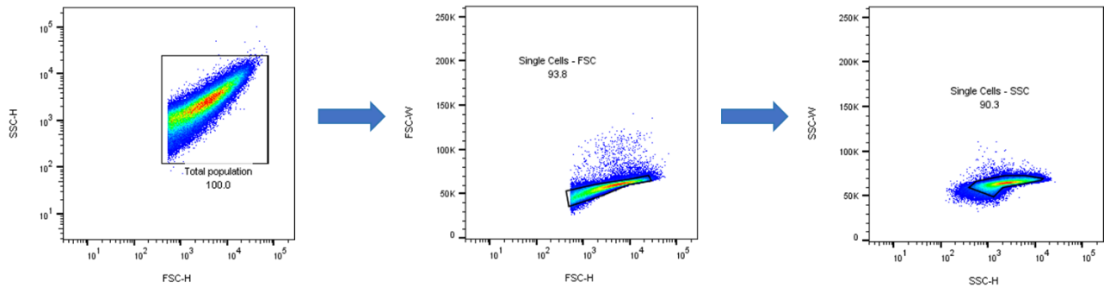

Figure 3.2. The gating strategy used to analyse flow cytometry files and define single cells. The total population was gated on the relationship between cell size (forward scatter - FCS) and granularity (side scatter - SSC). Doublets were excluded by gating twice on the single cells using the width to height relationship in both FCS and SSC. The green to red area shows the highest cell density. SSC-H – side scatter height, SSC-W – side scatter width, FSC-H – forward scatter height, FSC-W – forward scatter width.

3.2.1. Esterase activity stains

We evaluated calcein blue, calcein green and FDA for non- specific esterase enzyme activity. These fluorescent stains are thought to enter cells passively after which the activity of intracellular bacterial esterases cleave acetoxymethyl ester groups resulting in fluorescence. The continued presence of esterase activity after drug treatment could indicate viability. In untreated cells, we observed very similar bimodal patterns for both calcein green and calcein blue with approximately 60% cells positive for either stain, relative to unstained controls. After drug treatment, we observed marked drug specific staining patterns and considerable heterogeneity (Figure 3.3.; Figure 3.4. and Figure 3.5). There was no difference between calcein blue and green staining patterns after treatment with INH, EMB, CFZ and RIF at all time points. Strikingly for INH and EMB nearly all cells became calcein blue or green positive after 24 and 72 hours of treatment indicating the presence of ongoing esterase activity in all cells. In contrast the staining patterns for CFZ and RIF treated cells changed less with a slight reduction in the proportion of cells that were calcein blue or green positive.

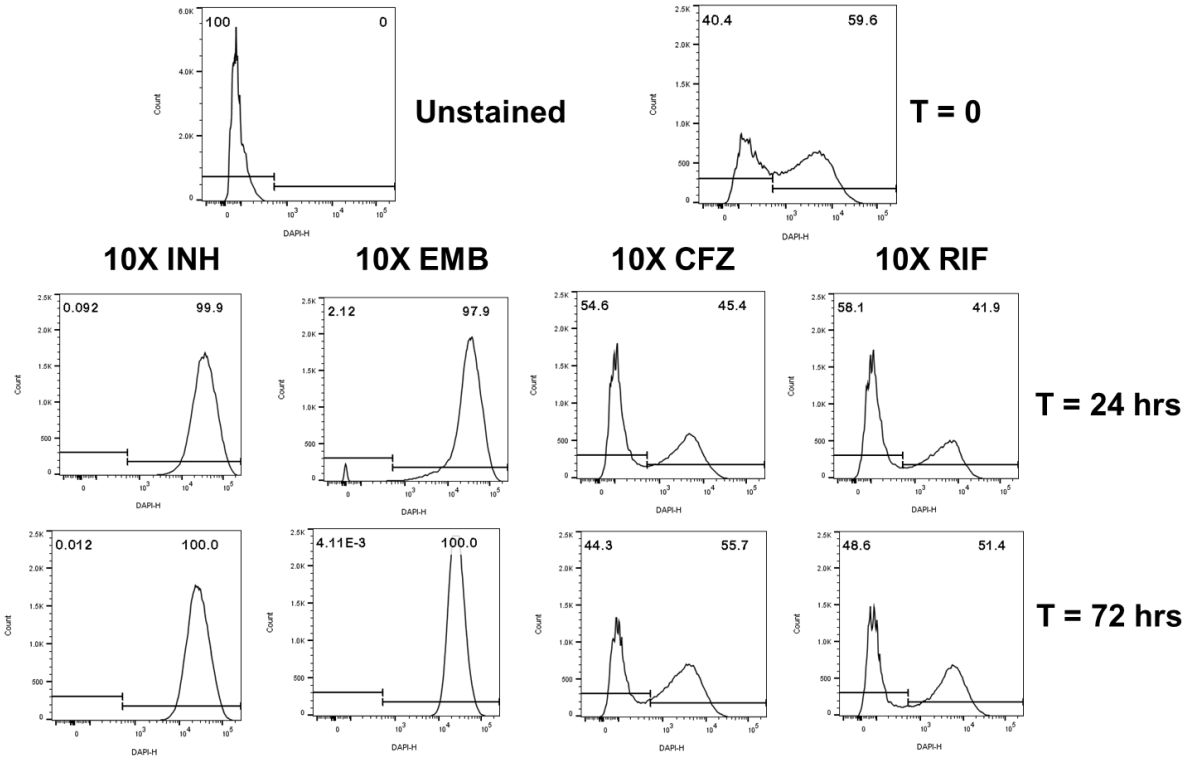

Figure 3.3. Evaluation of esterase activity using calcein blue. Cells were stained in triplicate with calcein blue as a measure of esterase activity after 24 and 72 hours of drug treatment. The histograms show that INH and EMB treatment causes the entire population to become calcein blue positive. RIF and CFZ treatment results in a small decrease in the calcein blue positive subpopulation. The fluorescence intensity of calcein blue (x axis) was measured with the DAPI filter. The y axis shows the cell count. Gates are based on the unstained control. The numbers show the percentages of the calcein blue negative and calcein blue positive subpopulations respectively.

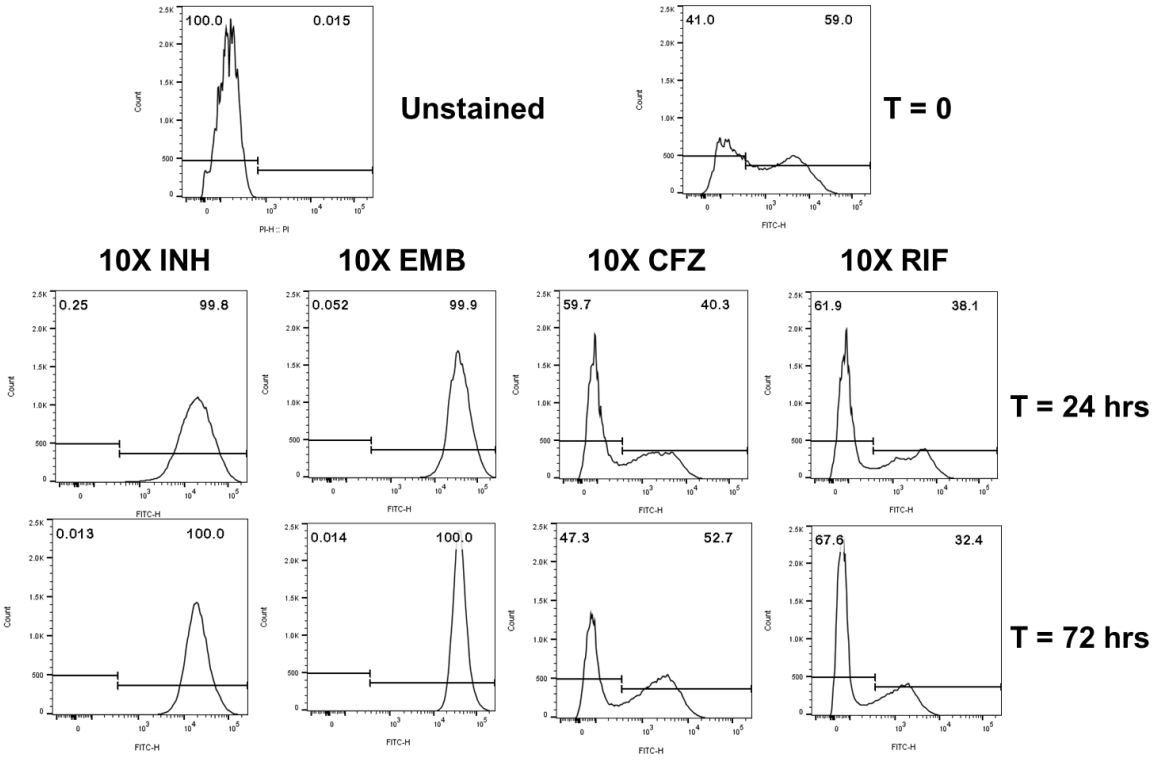

Figure 3.4. Evaluation of esterase activity using calcein green. Cells were stained in triplicate with calcein green as a measure of esterase activity after 24 and 72 hours of drug treatment. The histograms show that INH and EMB treatment caused all cells to be calcein green positive. RIF and CFZ treatment resulted in a slight decrease in the calcein green positive subpopulation. The y axis shows the cell count and the x axis shows the calcein green intensity measured with the FITC filter. Gates are based on the unstained control. The numbers show the percentages of the calcein green negative and calcein green positive subpopulations respectively.

We then evaluated FDA staining, which also depends on the same esterases for fluorescent activation. Interestingly in contrast to the calcein stains all cells were positive for FDA staining in the absence of drug although there was marked heterogeneity in the intensity of fluorescence (Figure 3.5). After treatment, the changes in staining patterns with FDA were roughly similar to those found with the calcein stains. In the case of INH treated cells there was an increase in staining and a reduction in heterogeneity indicated by a narrowing in the peak width. After treatment with the other drugs (RIF, MOX, STR) most the cells remained positive for FDA staining but there was a slight decrease in the mean fluorescent intensity. Taken together these results indicate that staining for esterase activity within 72 hours of treatment is drug specific. The increase in staining observed with cell wall synthesis inhibitors such as INH and EMB, in contrast to drugs with other modes of action, suggests that changes in bacterial cell wall permeability might have influenced fluorescent staining.

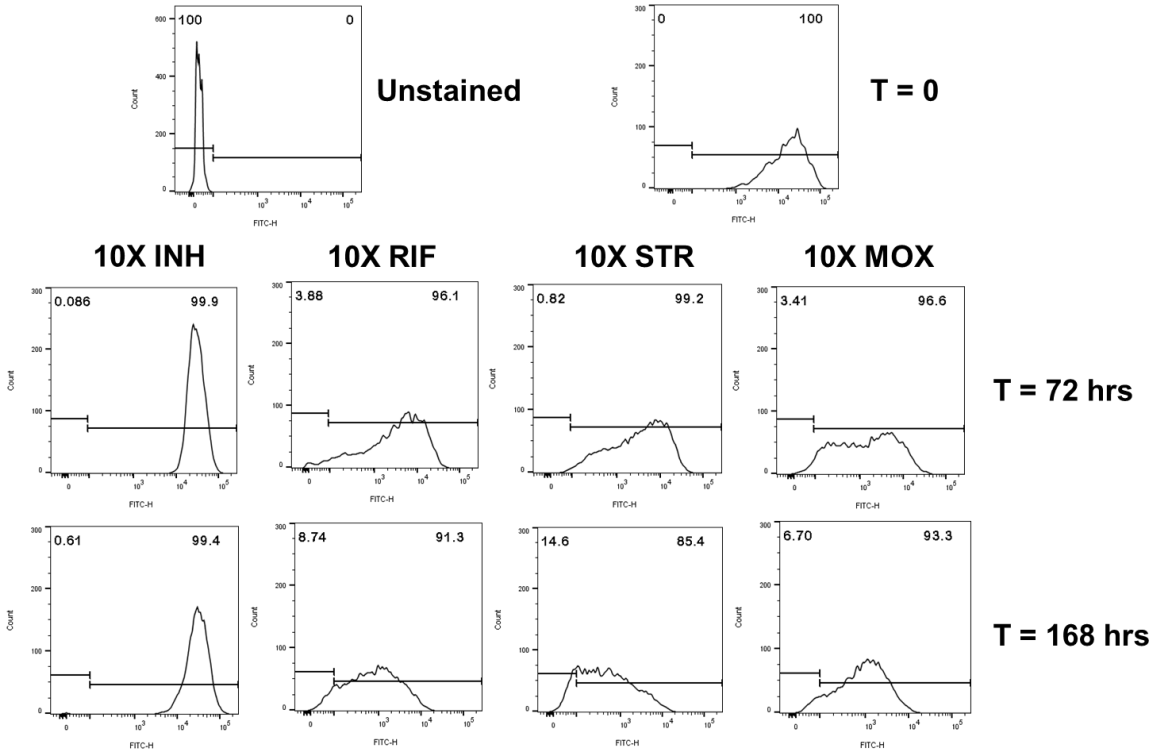

Figure 3.5. Evaluation of esterase activity using FDA. Cells were stained in triplicate with FDA to measure esterase activity after 72 and 168 hours of drug treatment. All cells were positive at baseline and approximately 90% of cells remained positive after 168 hours of antibiotic treatment. There was a reduction in the heterogeneity of staining in INH treated cells. FDA fluorescence intensity (x-axis) was measured with the FITC filter. The y axis shows the cell count. Gates are based on the unstained control. The numbers represent the percentages of the FDA negative and FDA positive subpopulations.

3.3.2. Membrane integrity and membrane potential stains

Positively charged stains that fluoresce on binding to DNA, but are excluded from cells that have intact membranes, have been used successfully as viability markers in other microorganisms. To evaluate two such "membrane integrity" markers, we compared the staining patterns of PI and Sytox red after treatment with drugs. In the absence of drug less than 5% of cells stained positively for PI. Surprisingly the proportion of cells positive for PI did not substantially increase after treatment with EMB, RIF, CFZ or INH with the PI positive population greatest after treatment with EMB. Remarkably for all the treated cultures, most of the cells were PI negative after 72 hours suggesting that the cells still had intact membranes (Figure 3.6).

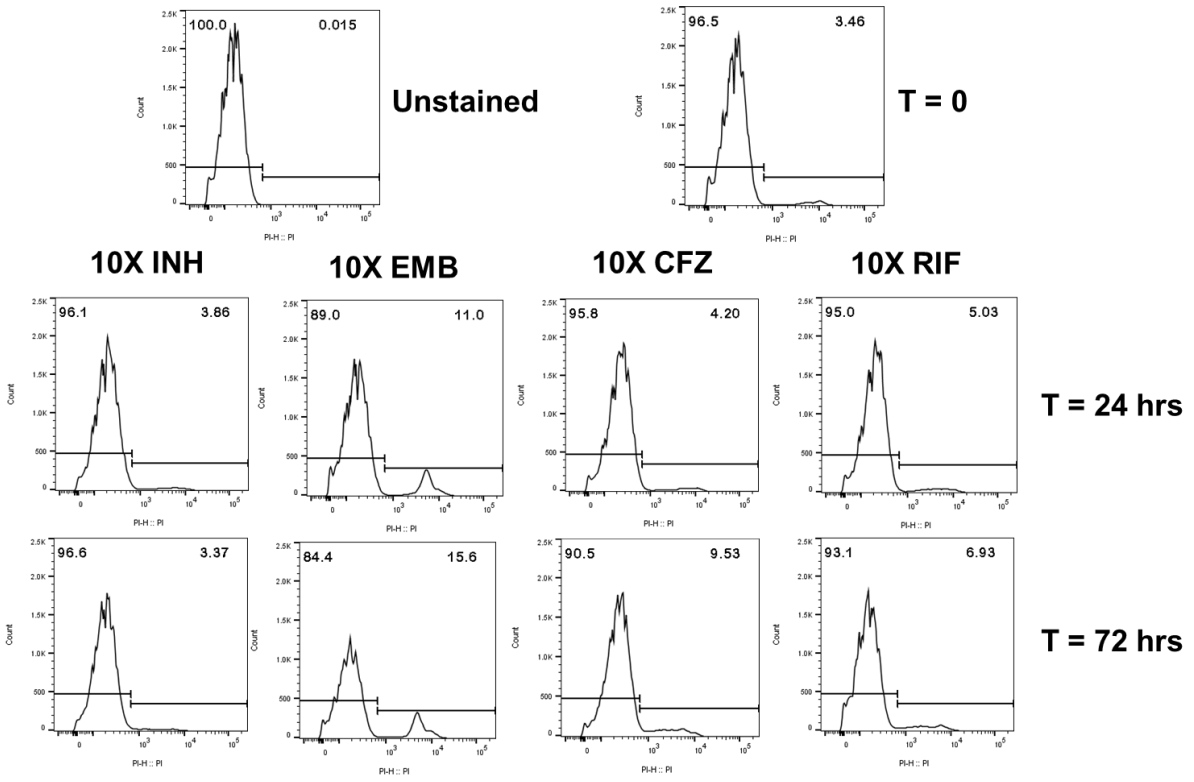

Figure 3.6. Membrane integrity assessment after antibiotic treatment using PI. Cells were stained in triplicate with PI to measure of membrane integrity after 24 and 72 hours of drug treatment. There was a general increase in the PI positive population with EMB treated cells producing the highest percent increase. There was no change in the PI staining patterns after INH treatment relative to baseline. The fluorescence intensity of PI (x axis) was measured using the PI filter. The y axis shows the cell count. Gates are based on the unstained control. The numbers show the percentages of the PI negative and PI positive subpopulations respectively.

Like PI staining, we also observed similar patterns of staining with Sytox red. Baseline staining resulted in a slight right shift in the overall staining but also a distinct small subpopulation with high staining. The gating was based on the untreated (T= 0) because the unstained and untreated were not similar as observed with PI. RIF and CFZ treated cells produced similar staining patterns (Figure 3.7). Although both EMB and INH target cell wall synthesis, EMB treated cells produced two distinct subpopulations whereas with INH treated cultures there was a general shift of the entire population to the right. The staining patterns at baseline suggested that the cell membrane was approximately five times more permeable to Sytox red than PI. Hence the percentages of Sytox red positive cells at all time points were higher than the corresponding PI positive. Despite this minor difference between the two stains, we continued to use both stains.

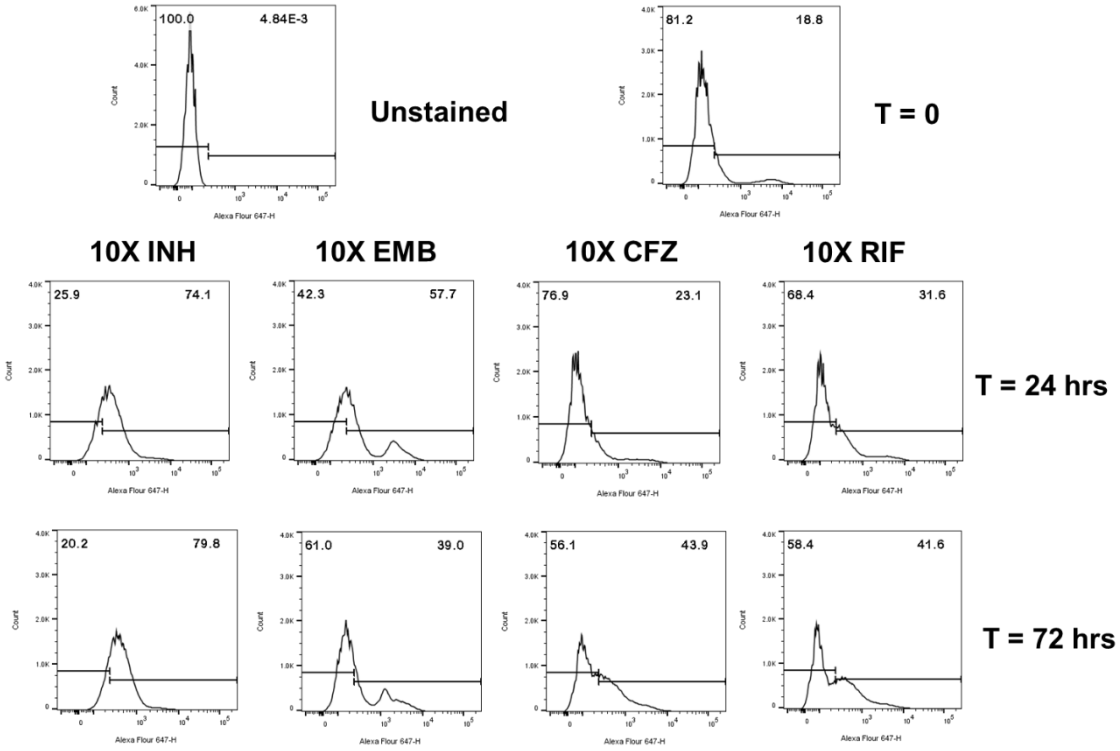

Figure 3.7. Evaluating membrane integrity after antibiotic treatment using Sytox red. Cells were stained in triplicate with Sytox red to measure membrane integrity after 24 and 72 hours of drug treatment. There was a general shift towards positivity in the overall staining at all timepoints. However, there were distinct low and high staining cells after EMB treatment. The histograms are showing changes in the fluorescence intensity of Sytox red (x axis) measured with the Alexa Fluor 647 filter. The y axis shows the cell count. Gates are based on the untreated control (T =0). The numbers show the percentages of Sytox red negative and Sytox red positive cells.

PI and Sytox red are indirect measures of membrane polarity, in that their exclusion from cells is partly due to their polarity. Other stains were used to measure membrane polarity more directly i.e. $DiOC_2$ (3). To determine if $DiOC_2$ (3) could be used in Mycobacteria we compared the differences between depolarised and hyperpolarised cells in *M. tuberculosis* staining with *E. coli* and *S. aureus*. $DiOC_2$ (3) is thought to bind to the inner membrane and emits a red-green fluorescence. After depolarization, the dye is more diffusely bound resulting in a decreased emission in the red spectrum. Thus, depolarisation is detected by a reduction in the red to green fluorescent ratio. With *S. aureus*, we found a six-fold reduction in the red to green ratio as described previously for this assay. In contrast, there were only subtle changes in the red: green ratio of depolarised and hyperpolarised cells for *E. coli* and *M. tuberculosis* which could be due to differences in the structure of the cell wall (Figure 3.8).

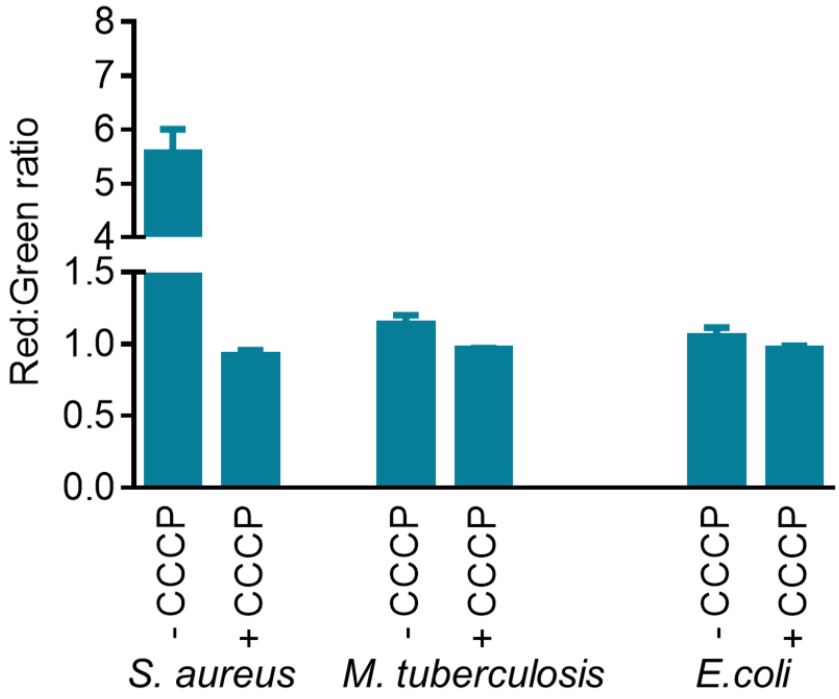

Figure 3.8. Comparing membrane potential changes between *M. tuberculosis* and other bacteria. Cells were stained in triplicate with $DiOC_2$ (3) to evaluate changes in membrane potential. The red: green ratio was calculated by dividing the median of the red fluorescence by the median of the green fluorescence. *S. aureus* had the highest difference between polarised (untreated) and depolarised cells (CCCP treated). There was a very small difference in the red: green ratio of *M. tuberculosis* and *E. coli*. Error bars represent standard deviation.

Although there were only subtle changes in the fluorescent ratio after depolarization we decided to evaluate if these changes could be used to identify potentially viable organisms after drug treatment. For the five drugs tested there was a modest paradoxical increase in the red: green ratio, rather than decrease as would be expected in a depolarized membrane. The largest effect was seen after INH treatment (Figure 3.9). We further analysed this by doing a dot plot for the INH treated cells. This showed that there was an increase in the red as well as green emission spectra (Figure 3.10). This might be due to the mechanism of action of INH on the cell wall that alter stain penetration, similar to that observed with calcein.

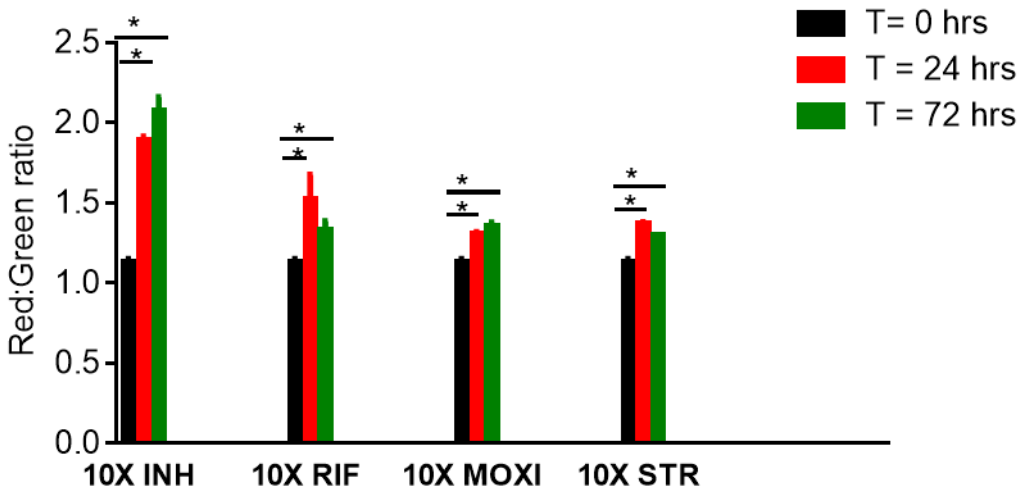

Figure 3.9. Analysis of changes in membrane polarity after drug treatment using $DiOC_2$ (3). Cells were stained in triplicate with $DiOC_2$ (3) to evaluate changes in membrane potential after 24 and 72 hours of drug treatment. The red: green ratio was calculated by dividing the median of the red fluorescence by the median of the green fluorescence. The red: green ratio generally increased with antibiotic treatment and INH treatment produced the highest change. * significant, P values < 0.05. Error bars represent standard deviation.

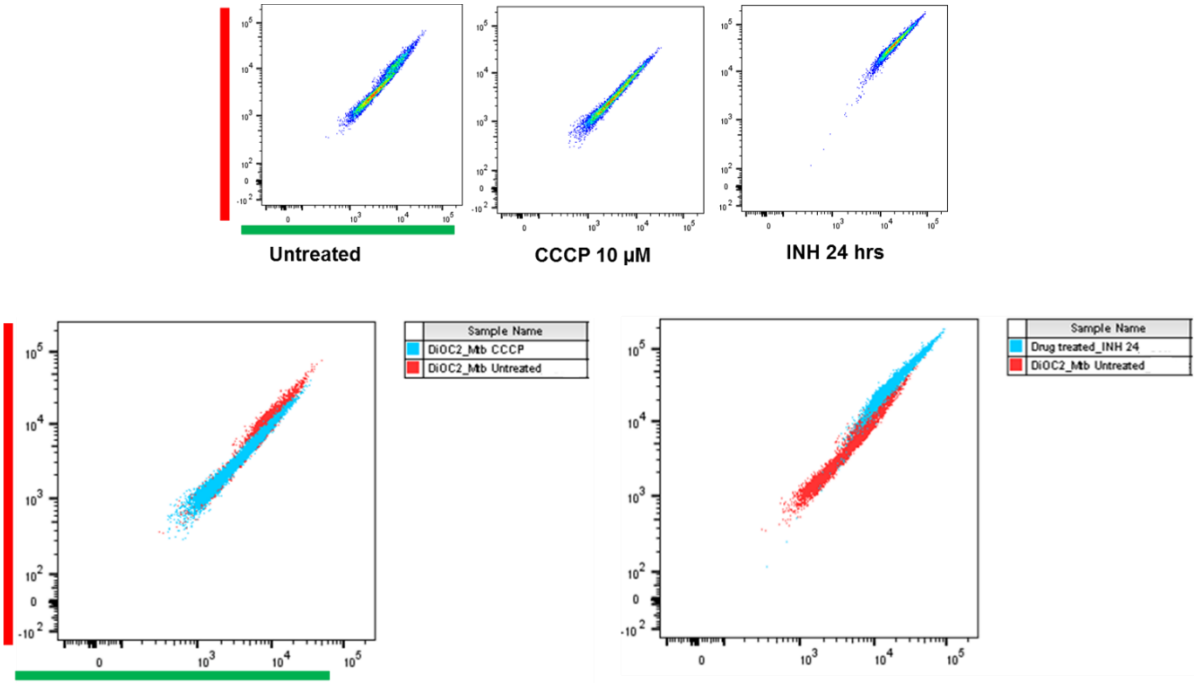

Figure 3.10. Overlays of dot plot diagrams showing the differences between polarised and depolarised cells. Cells were depolarised by incubating with CCCP for 30 minutes or treated with INH for 24 hours. Cells were stained in triplicate with $DiOC_2$ (3) to measure the changes in membrane polarity compared with the untreated. $DiOC_2$ (3) staining produces red fluorescence (y axis) and green fluorescence (x axis). The overlays show that there was heterogeneity in staining and no clear difference in the localisation of polarised cells and depolarised cells in *M. tuberculosis*. INH treatment caused both the red and green fluorescence to increase compared to the untreated.

We also stained cells with $DiBAC_4$ (3), another dye with single colour fluorescence which has been used to detect changes in membrane polarity. Heat killed cells were the depolarised control and untreated cells were the hyperpolarised control, although there was only a modest increase in fluorescence in the heat treat control. Like $DiOC_2$ (3), there were minimal changes after antibiotic treatment (Figure 3.11).

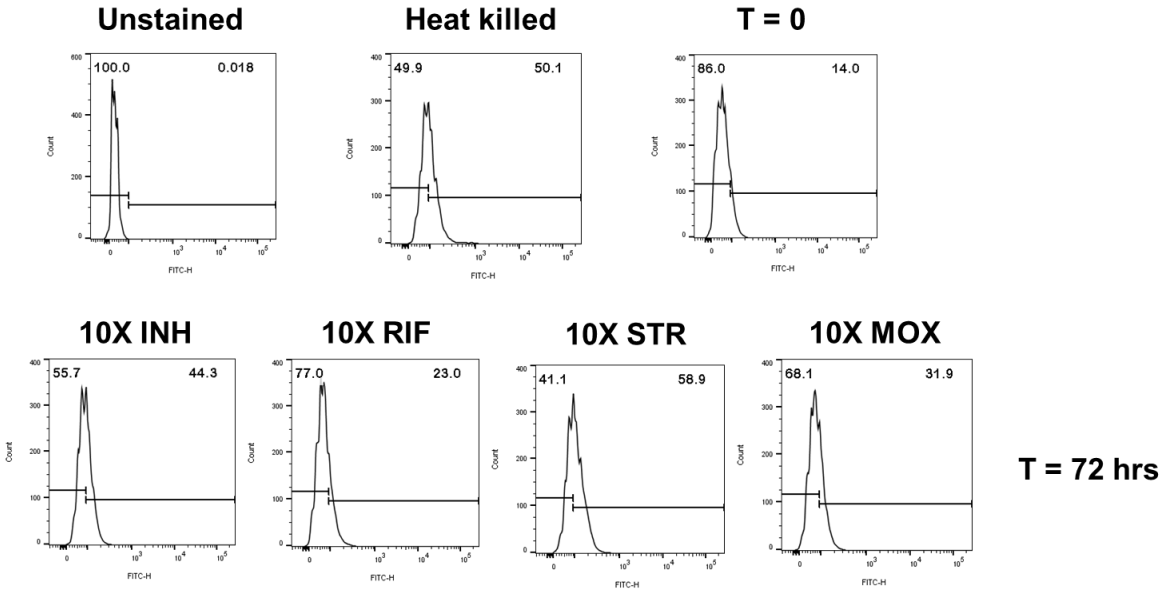

Figure 3.11. Evaluating membrane polarity after antibiotic treatment using $DiBAC_4$ (3). Cells were stained in triplicate with $DiBAC_4$ (3) to measure changes in membrane potential after 72 hours of drug treatment. The histograms show that there was a slight change in the fluorescence intensity of $DiBAC_4$ (3) in heat killed and drug treated cells compared to the untreated (T = 0). The y axis shows the cell count and x axis shows $DiBAC_4$ (3) fluorescence intensity measured with the FITC filter. The gates were based on the untreated. The numbers show the percentages of the $DiBAC_4$ (3) negative and $DiBAC_4$ (3) positive subpopulations respectively.

3.3.3. Oxidative stress stains

Previous studies in *E. coli* have suggested that the generation of ROS in bacteria may precede killing by many antibiotics. We therefore decided to evaluate antibiotic treated cells for the presence of ROS as a potential marker of viability using fluorescent stains which can detect ROS. We hypothesized that antibiotic survivors would be negative or have lower levels of oxidative stress after antibiotic therapy. We initially stained with DHE but were unable to establish a low concentration of DHE to distinguish between induced oxidative stress (CHP treated) and cells treated with an antioxidant (NAC treated) (Figure 3.12.I). However, CellROX dyes produced staining patterns which could differentiate between cells undergoing oxidative stress (CHP treated) and untreated cells (Figure 3.12.II). We observed that CHP produced stronger fluorescence than TBHP with all the CellROX dyes tested. CellROX Deep red produced a more reproducible and intense fluorescent signal than CellROX Green with CHP (Figure 3.12.III). CellROX Orange also produced an intense signal but with a greater heterogeneity.

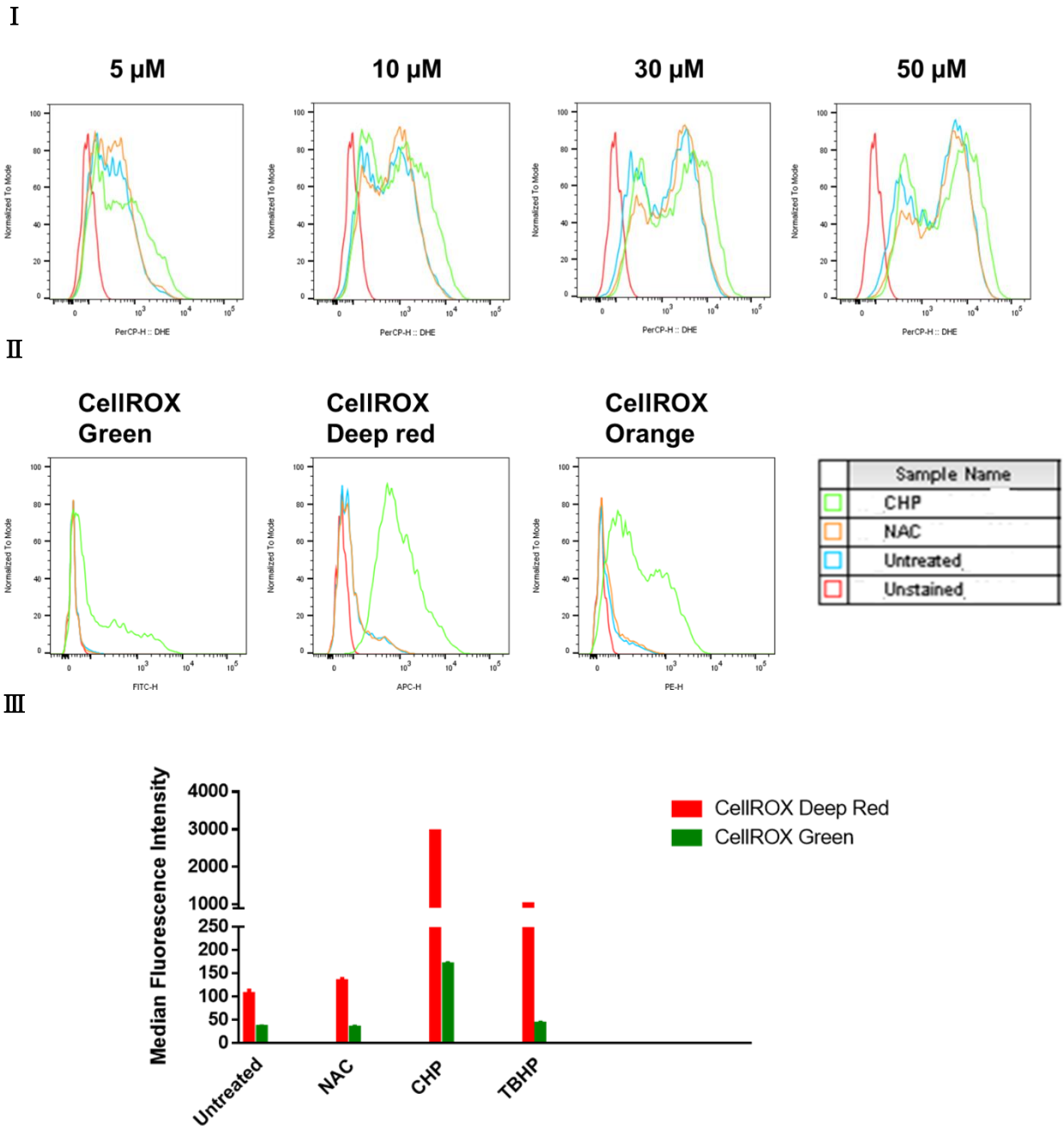

Figure 3.12. Comparison of DHE, CellROX Deep red and Green in detecting oxidative stress. Cells were stained in triplicate with ROS detecting dyes (DHE, CellROX Deep red and CellROX green) to identify the best dye to use. **(I)** There was no clear-cut distinction between the positive control (CHP) and the negative controls (NAC and untreated) at all DHE concentrations. (**II)** CellROX stains produced a better distinction between the controls and unstained sample. (**III)** CellROX Deep red produced a better fluorescent intensity than CellROX Green and CHP was a better positive control than TBHP. The y axis on the histograms in **I** and **II** shows the percentage of cells normalised to mode. The x axis shows the DHE fluorescence measured with the PerCP-Cy5.5 filter (**I**), CellROX Green, Deep red and Orange fluorescence measured with FITC, APC and PE filters respectively (**II**). Error bars represent standard deviation.

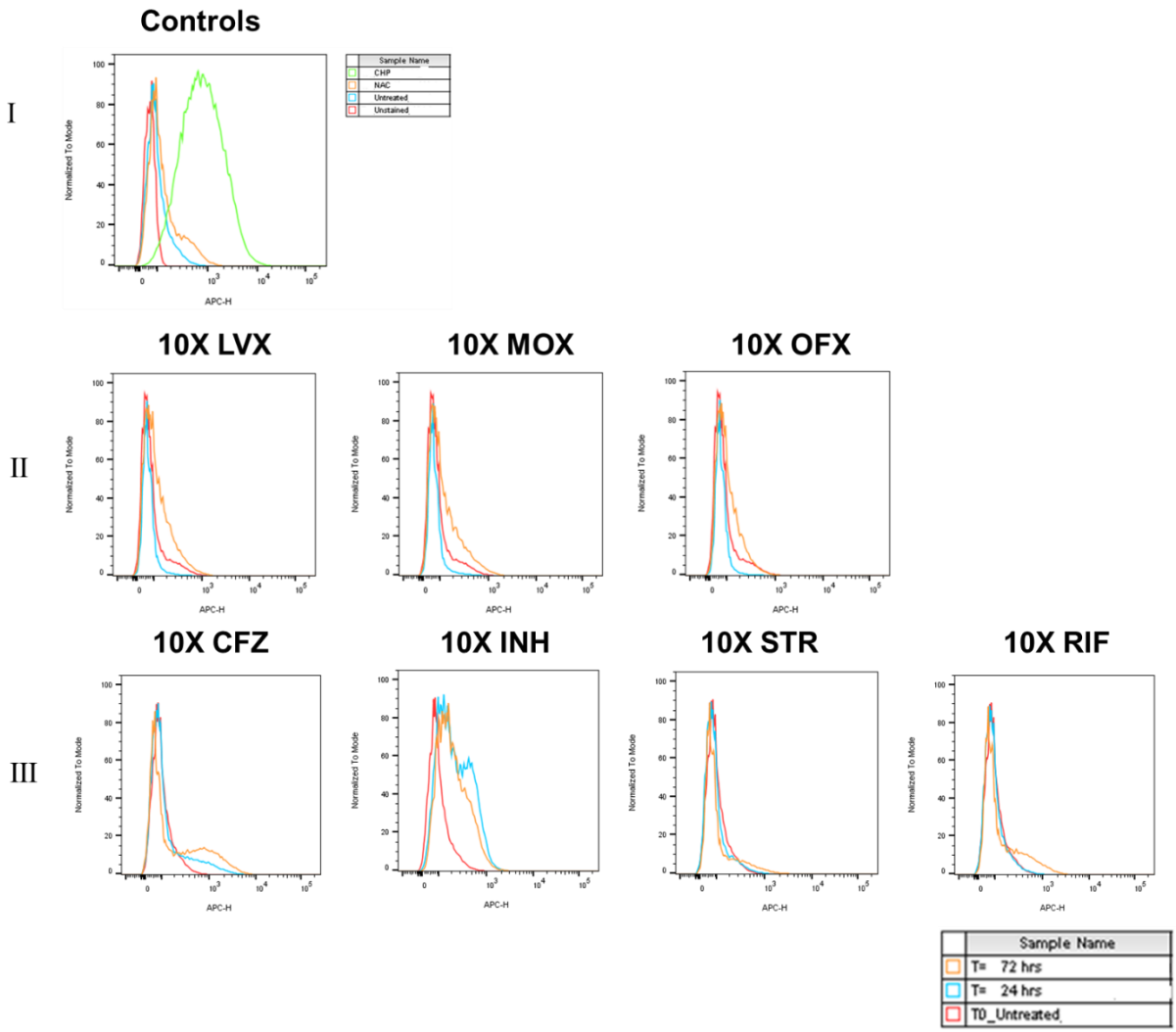

Figure 3.13. Evaluating ROS production by anti-TB drugs using CellROX Deep red. Cells were stained in triplicate with CellROX Deep red to measure ROS production after 24 and 72 hours of drug treatment. **(I)** The overlay shows the high fluorescent intensity observed with CHP the positive control. **(II)** The histograms show that there were very subtle changes in the fluorescence intensity after treatment with fluoroquinolones (LVX, MOXI and OFX). **(III)** There was a great increase in the CellROX Deep red fluorescence intensity after CFZ and INH treatment. There were minimal changes in the fluorescence intensity after STR and RIF treatment. The y axis shows the percentage of cells normalised to mode. The x axis shows the CellROX Deep red fluorescence intensity measured with the APC filter.

We then evaluated the generation of ROS after antibiotic treatment. Cells were stained at earlier time points i.e. 3 and 6 hours after addition of drugs but there were no changes in the signal intensity relative to baseline therefore we only presented data for the 24 and 72 hour time points. Treatment of *M. tuberculosis* with the fluoroquinolones resulted in very subtle changes in the CellROX Deep red fluorescence intensity which suggested that these antibiotics may not result in the production of ROS (Figure 3.13.II, Appendix E). The signal intensity increased after 24 hours in CFZ and INH treated

cultures suggesting that ROS were formed in a time dependant manner (Figure 3.13.III, Appendix E). This suggests that these antibiotics might produce ROS as part of their bactericidal activity. There were minimal changes in the fluorescence intensity of CellROX Deep red staining after STR and RIF treatment.

3.5. Multi-parameter analysis

3.5.1. Dual staining: Esterase activity and membrane integrity stains

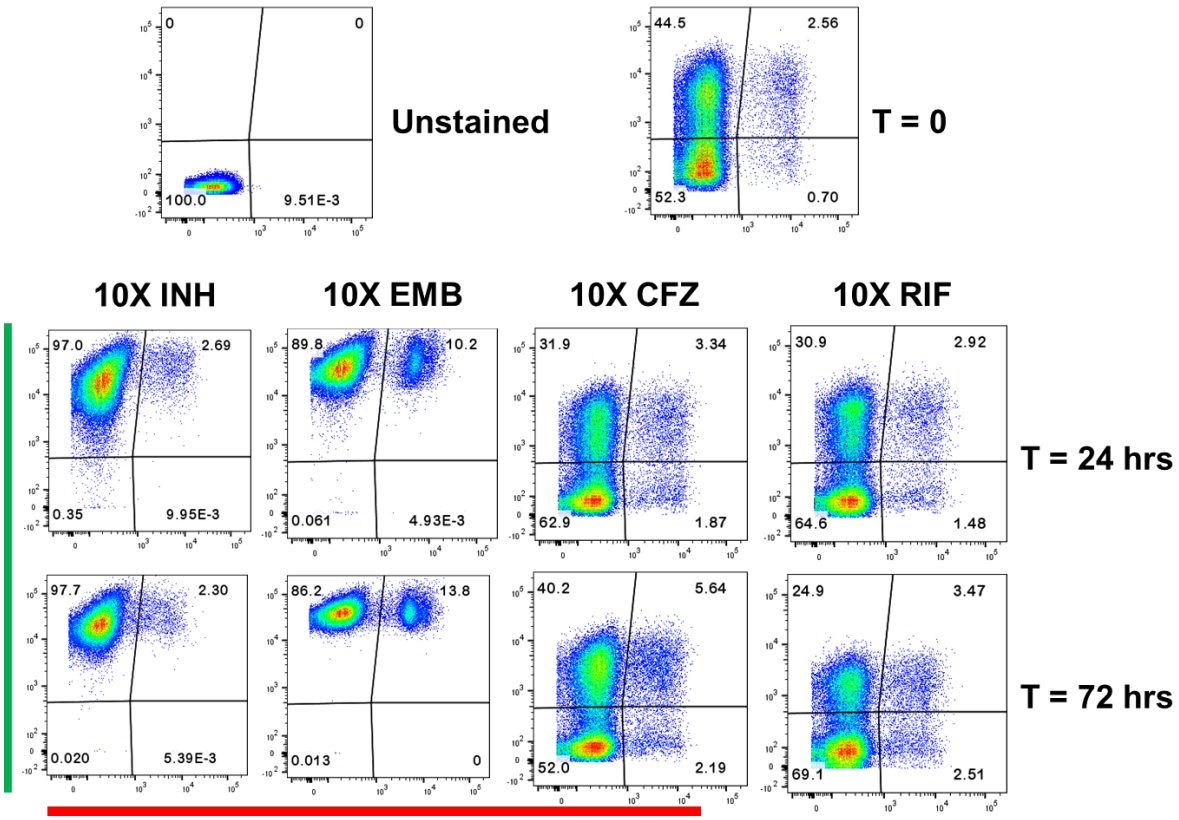

Figure 3.14. Dual staining with calcein green and PI. Cells were stained in triplicate with calcein green and PI to evaluate esterase activity and membrane integrity after 24 and 72 hours of drug treatment. The dot plots show that all cells are calcein green positive after INH and EMB treated cultures. However, an increase in the dual positive subpopulation was only observed in EMB treated cells. CFZ and RIF treated cells produced similar staining patterns with approximately 50% of the population being calcein green and PI negative. There was a slight increase in the PI positive subpopulation. The y axis shows calcein green fluorescence intensity and the x axis shows PI fluorescence intensity. Gates were based on the unstained control. The numbers show the percentages of cells in the respective gates.

In order to increase our ability to identify subpopulations of potentially viable organisms we then decided to combine stains. We reasoned that if high PI staining and reduced esterase activity were associated with reduced viability, at least with drugs that didn't interfere with the bacterial cell wall,

then there may be an enrichment of high PI staining in the calcein negative population. Dual staining of antibiotic treated cells with fluorescent dyes that detect esterase activity and membrane integrity was carried out using the same protocols as before. The results were similar with single staining. In the case of INH and EMB we observed high calcein staining and a small subpopulation of 2.3% and 13.8 that were dual stain with each drug respectively. In contrast with CFZ and RIF there 4 distinct populations after drug treatment with double positive and negative staining as well as staining for either calcein or PI. These observations were similar for cells stained with either calcein green and PI (Figure 3.14) and calcein blue and Sytox red (Figure 3.15). The presence of a PI or Sytox red positive population that were negatively stained for calcein suggested these may be a marker of non-viability, although this population was very small. The marked differences in staining after treatment with different drugs also suggests that the mechanisms of antibiotic survival may differ depending on the antibiotic used for treatment. The marked heterogeneity of staining may also indicate that many distinct subpopulations of bacteria are selected after antibiotic therapy.

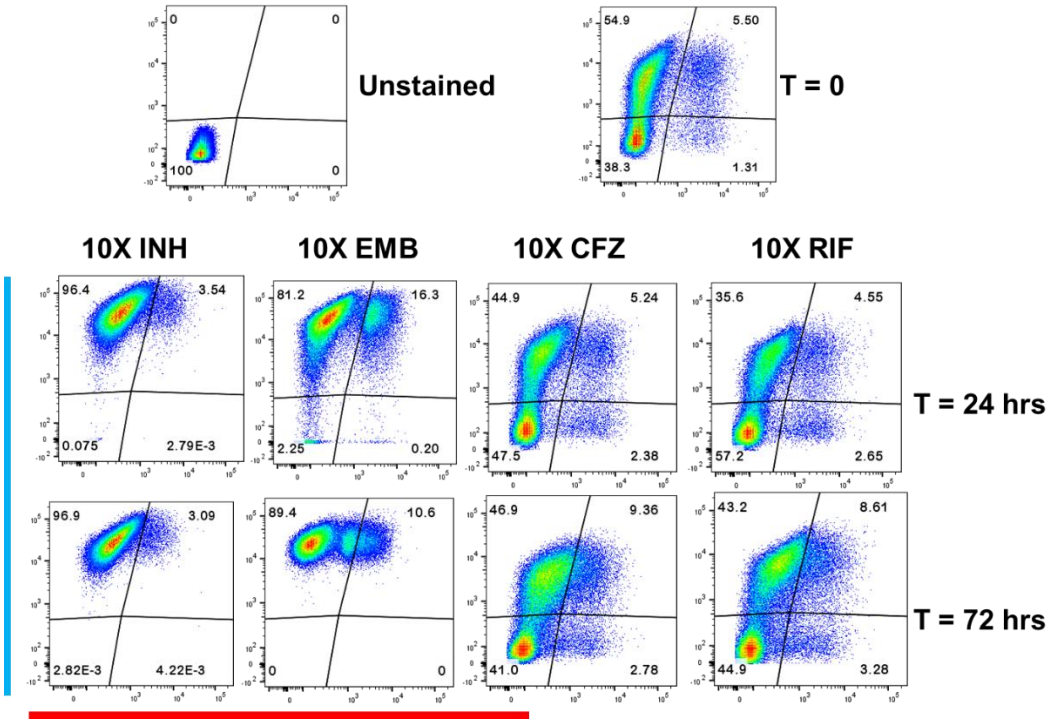

Figure 3.15. Dual staining with calcein blue and Sytox red. Cells were stained in triplicate with calcein blue and Sytox red to evaluate esterase activity and membrane integrity after 24 and 72 hours of drug treatment. All cells were positive for calcein blue after INH and EMB treated cultures. Only EMB treated cells resulted in an increase in the dual positive population. CFZ and RIF treated cells produced similar staining patterns with approximately equal distribution of the cells in calcein blue negative and calcein blue positive subpopulations. Approximately 10% of the cells were Sytox red positive after 72 hours of drug treatment. The y axis shows calcein blue fluorescence intensity and the x axis shows Sytox red fluorescence intensity. Gates were based on the untreated control (T = 0). The numbers show the percentages of cells in the respective gates.

3.6. Evaluation of fluorescent stains as viability markers

3.6.1. The effect of fluorescent stains on viability.

Having defined subpopulations of differentially stained bacteria after antibiotic treatment we then decided to assess if there would be any differences in the survival of the different subpopulations. Before evaluating the differences in survival between stained subpopulations from treated cells, we sought to verify the effect of fluorescent dyes on the viability of untreated cells. Figure 3.16 shows that there were no significant differences in the viability of the stained versus the unstained cells.

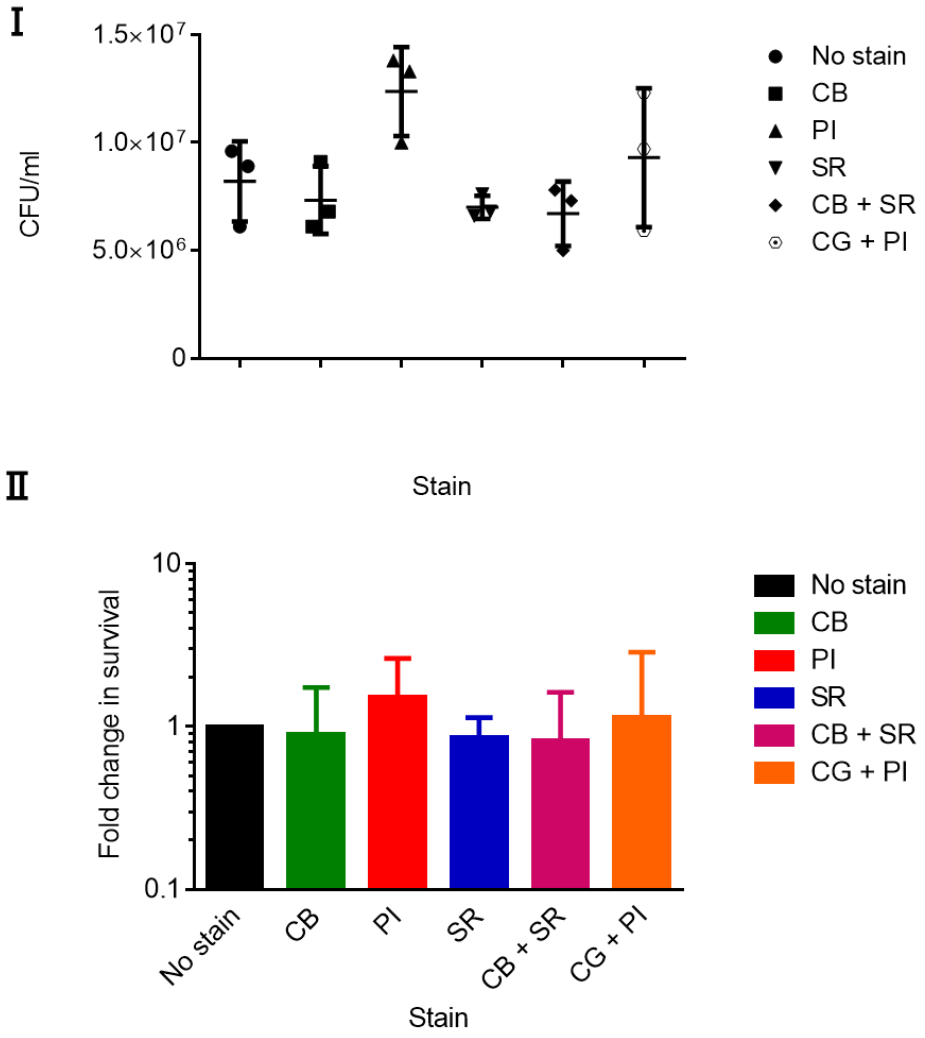

Figure 3.16. Analysing the effect of fluorescent dyes on the viability of untreated cells. Cells were stained in triplicate with fluorescent dyes for 1 hour then plated for CFU using the dilution method. There was no significant difference ($P > 0.05$) between the survival of the stained cells and the unstained cells. The fold change in survival was calculated by dividing the mean of the stained by the unstained. CB – Calcein blue, PI – Propidium iodide, SR – Sytox red. Error bars represent standard deviation.

3.6.2. Evaluating membrane integrity stains as viability markers

In our first experiment, we evaluated if bacteria that were positive for PI staining have reduced culturability. After treating with antibiotics for 72 and 168 hours bacteria were stained with PI and sorted on the basis of two gates corresponding to PI negative and positive. The gating for the negative population was based on the staining prior to treatment. Sorted bacteria were plated and the CFU was calculated. We then calculated a survival ratio for PI positive cells to PI negative cells. Despite the variation in staining patterns, mechanism of action and kill kinetics of the different antibiotics, we observed similar results when we evaluated the survival of the different subpopulations. There were no statistically significant differences in survival between the PI positive and PI negative subpopulations (Figure 3. 17). However, after 168 hours there was a trend towards less survival in the treatment with RIF and INH, the PI negative subpopulations but not with OFX. These results suggest that PI staining, suggestive of loss of membrane integrity does not correlate with culturability after 1 week of treatment.

I

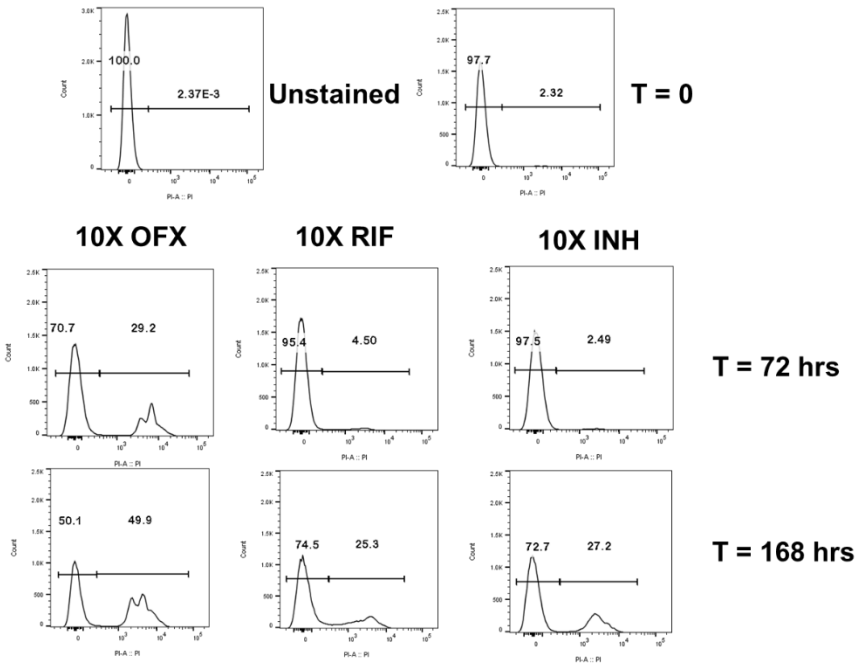

II

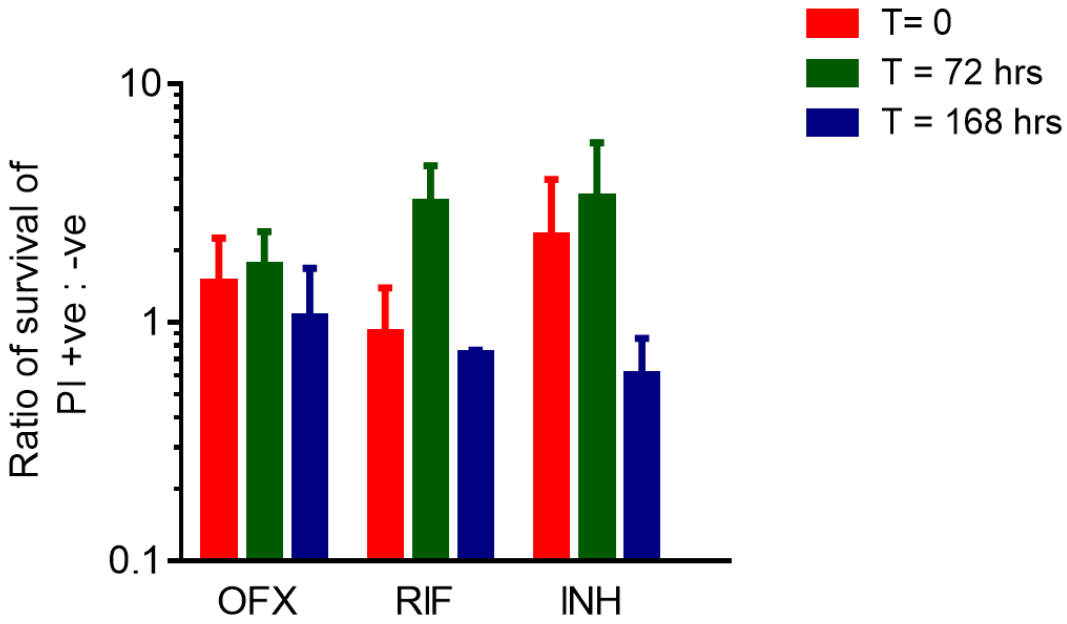

Figure 3.17. Evaluating Propidium iodide as a viability marker. Cells were stained in triplicate with PI to measure membrane integrity after 72 and 168 hours of antibiotic treatment. Equal numbers of events were sorted from the PI negative and PI positive subpopulations and plated for CFU. **(I)** The percentage of cells in the PI positive subpopulation increased with antibiotic treatment. Approximately 50% of the cells were PI positive after 168 hours of OFX treatment. **(II)**There were no significant differences between the survival of cells from the PI negative and PI positive subpopulations. P values > 0.05. Error bars represent standard deviation.

We then repeated the experiment with Sytox red. We observed similar results for both RIF and OFX treated cultures (Figure 3. 18). This observation supports our interpretation that dye uptake does not solely depend on membrane integrity.

I

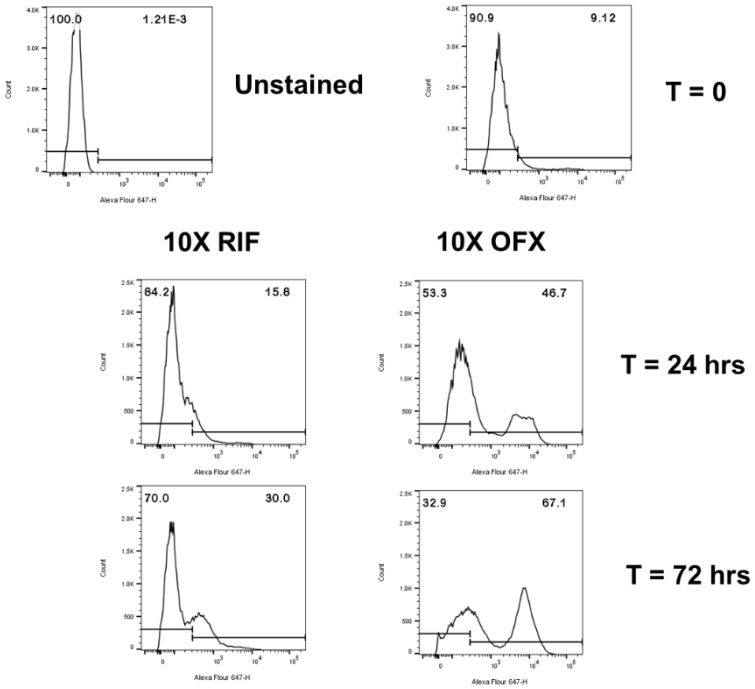

II

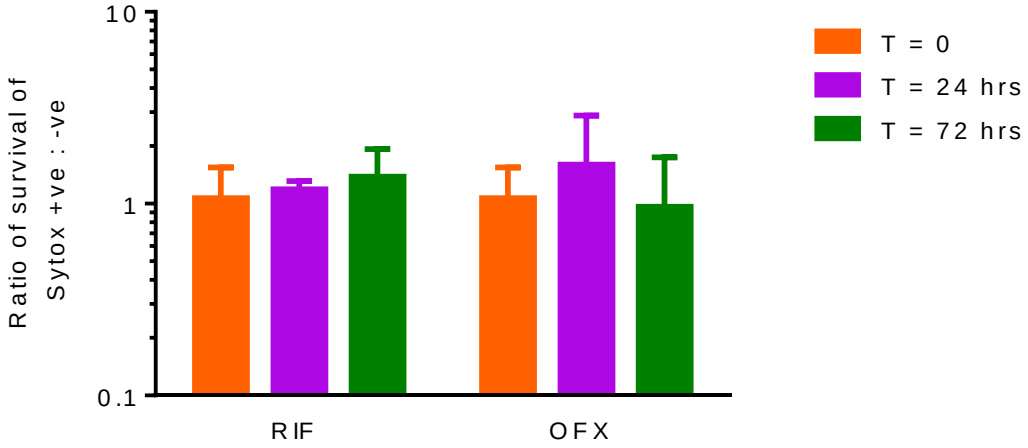

Figure 3.18. Evaluating Sytox red as a viability marker. Cells were stained in triplicate with Sytox red to measure membrane integrity after 24 and 72 hours of antibiotic treatment. Equal numbers of events were sorted from the Sytox red negative and Sytox red positive subpopulations and plated for CFU. **(I)** The percentage of cells in the Sytox red positive subpopulation increased with time. The percentage of cells that were PI positive after OFX treatment was twice that of RIF treated cells. **(II)** At baseline both subpopulations are equally enriched for survivors. After 24 and 72 hours of drug treatment, there were no significant differences between the survival of Sytox red positive and negative subpopulations. P values > 0.05. Error bars represent standard deviation.

3.6.3. Evaluating Calcein blue as a viability marker

We next employed the same strategy to determine if different degrees of calcein staining associated with culturability after antibiotic treatment. We compared the difference in survival between calcein blue positive and calcein blue negative subpopulations. We observed that at baseline, both populations had equal numbers of survivors. After 24 hours of treatment there were no significant differences in the survival of the calcein blue stained subpopulations nor after 72 hours of treatment (Figure 3.19).

I

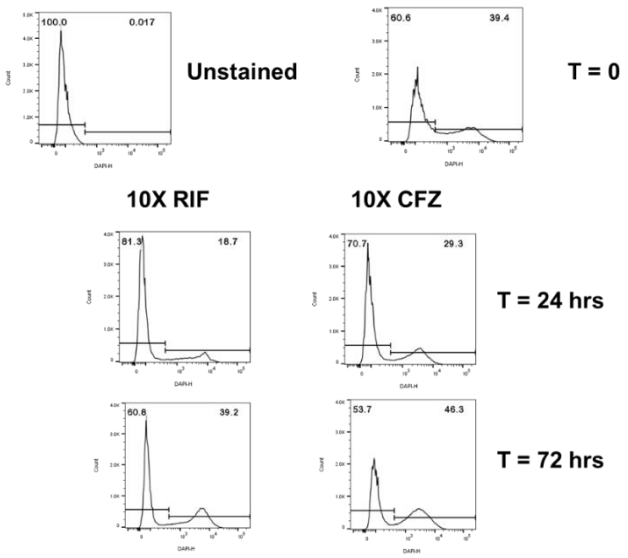

II

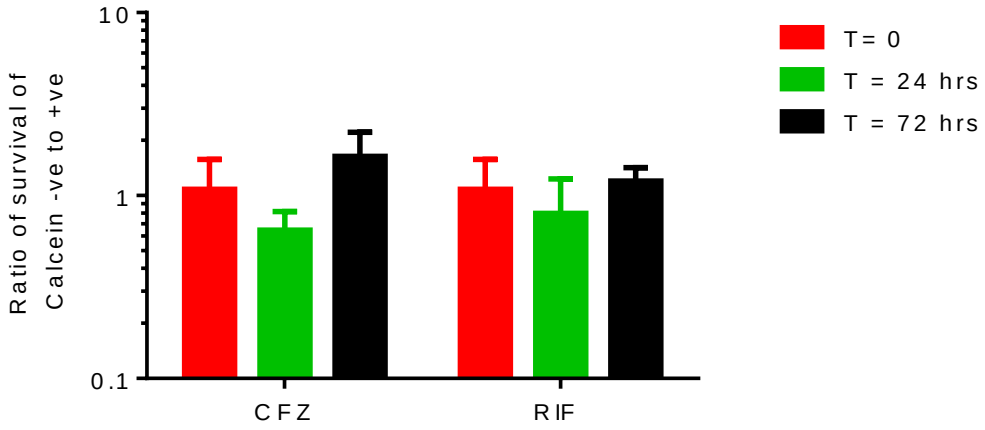

Figure 3.19. Evaluating calcein blue as a viability marker. Cells were stained in triplicate with calcein blue to measure esterase activity after 24 and 72 hours of antibiotic treatment. Equal numbers of events were sorted from the calcein blue negative and calcein blue positive subpopulations and plated for CFU. **(I)** There was a lot of heterogeneity in calcein blue staining and most of the cells were negative for calcein blue at all timepoints after RIF and CFZ treatment. **(II)** At baseline, there were equal chances of survival between the calcein blue positive and calcein blue negative population. There was no significant difference between the survival of the calcein blue negative and positive subpopulations after CFZ and RIF treatment. P values > 0.05. Error bars represent standard deviation.

3.6.4. Evaluating CellROX as a viability marker

We compared the survival between CellROX Deep red low and high staining bacteria by sorting and plating. These we classified as CellROX negative and CellROX positive respectively based on the stained baseline cells. Just like we observed with PI and Sytox red staining at baseline there was more survival in the CellROX positive subpopulation (Figure 3.20). Similar results were observed in RIF treated cells at all timepoints. However, after 24 hours of CFZ treatment there was a slight difference in the survival of the CellROX negative subpopulation as determined by comparing the survival ratios at baseline and after 24 hours.

I

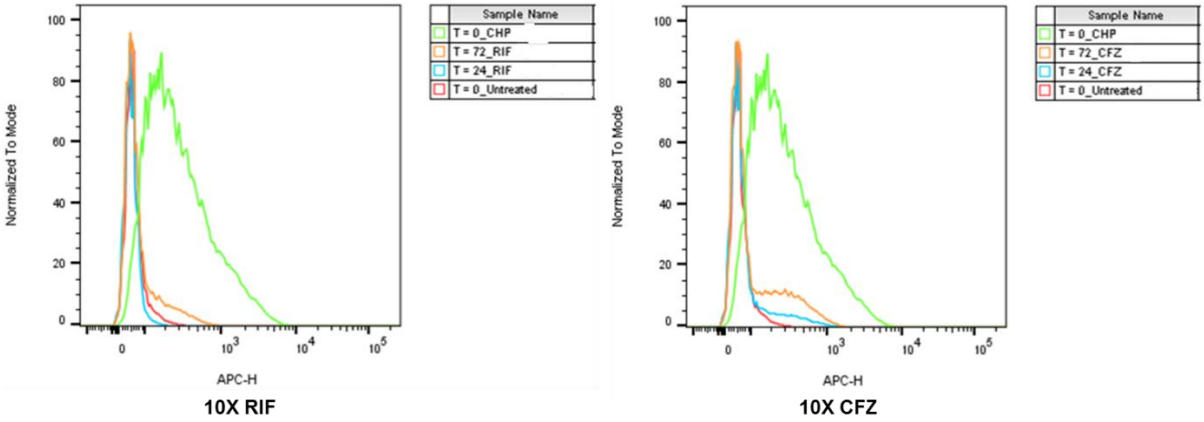

II

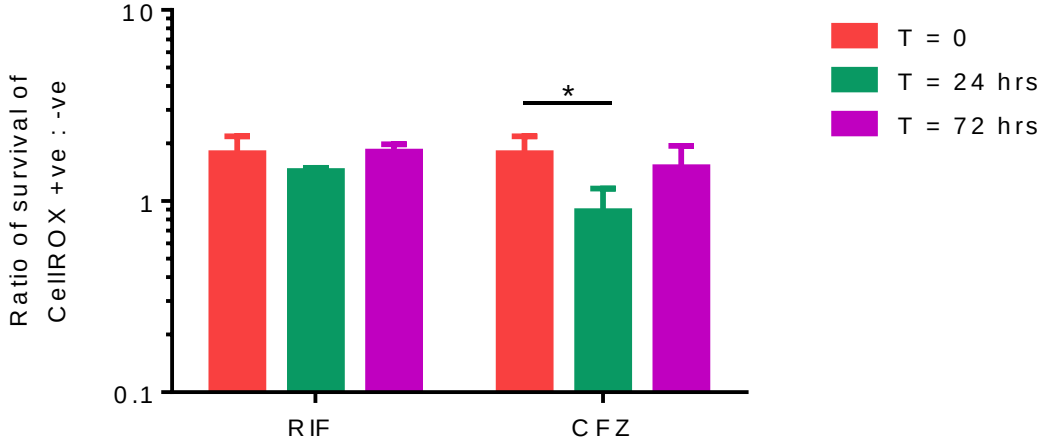

Figure 3.20. Evaluating CellROX Deep red as a marker of viability. Cells were stained in triplicate with CellROX Deep red to measure esterase activity after 24 and 72 hours of antibiotic treatment. Equal numbers of events were sorted from the CellROX deep red negative and CellROX deep red positive subpopulations and plated for CFU. **(I)**The staining patterns were drug dependant with the major increase in signal intensity occurring after 72 hours of antibiotic treatment. **(II)** At baseline and after 72 hours of antibiotic treatment, there were no significant differences (P > 0.05) in survival between the CellROX negative and positive subpopulations. However, after 24 hours of CFZ treatment, the CellROX negative subpopulation was enriched for survivors. * significant, P = 0.033. Error bars represent standard deviation.

CHAPTER 4

DISCUSSION

It has been proposed that the prolonged chemotherapy for drug susceptible TB is due in part to a rare *M. tuberculosis* subpopulation which is drug tolerant (Keren *et al.*, 2011). It is still not clear how a small fraction of bacteria (antibiotic survivors) can evade lengthy exposure to anti-TB drugs. Characterisation of this phenotype will require the identification and isolation of these antibiotic survivors. We hypothesised that FACS can be used to identify and isolate this subpopulation and this would eventually lead to the identification of cellular mechanisms responsible for the formation of this phenotype. In our approach, we first sought to identify fluorescent dyes which would distinguish viable from non-viable bacteria after antibiotic treatment. This was done by staining antibiotic treated *M. tuberculosis* with fluorescent dyes which measure different aspects of cell viability including enzyme activity, membrane integrity and membrane polarity.

We observed that staining patterns were drug specific and there was a phenotypic heterogeneity in the treated and untreated populations. Phenotypic heterogeneity refers to marked variability in phenotypic traits among a population of genetically identical microorganisms (Ackermann, 2015). We observed both aspects for most of the dyes that we tested regardless of the physiological aspect they were measuring.

The evaluation of esterase dyes for viability staining showed that at baseline, most cells were calcein positive suggesting esterase activity was present however a significant proportion of the cells were calcein negative (Figures 3.3 and 3.4). This could have been due to reduced cell wall permeability to calcein dyes or efflux activity. The latter is likely to be the cause since the *M. tuberculosis* genome is known to encode for many efflux pumps which are actively involved in the extrusion of a wide variety of chemical compounds (Cole *et al.*, 1998;De Rossi *et al.*, 2006;Viveiros *et al.*, 2012). This has implications for the staining patterns we observed because we were not sure if the cells that were staining negative for the cell permeant calcein dyes indicated lack of esterase activity or efflux activity. However, with FDA, which also requires esterase activity for fluorescence, we found that a greater proportion of cells stained positive which would suggest that variable esterase activity is not the driver of the heterogeneity we saw with calcein stains in untreated populations. Our results are different from Hendon-Dunn *et al.* (2016) who observed that all cells were calcein violet positive at baseline. This could be due to the differences in staining protocols i.e. concentrations of the dyes, duration of staining and formaldehyde fixing of cells. Formaldehyde fixing has been shown to cause changes in cell membrane which may cause the membrane to be more permeable (Günther *et al.*, 2008;Bullock, 1984). Our approach was to develop stains for detecting viability so we were not interested in using formaldehyde fixed cells in our staining protocols. Technical aspects pertaining to flow cytometer

settings and differences in hardware associated variables also present a challenge when comparing results across platforms and biological samples (Maecker and Trotter, 2006).

After INH and EMB treatment all cells still had a paradoxical increase in esterase activity with all cells staining positive with calcein blue and calcein green. In contrast, for RIF and CFZ treatment a large proportion of cells stained negative for both calcein dyes (Figure 3.3 and Figure 3.4). We were not surprised to see that all cells stained positive for calcein after INH and EMB treatment since these drugs target the cell wall. This could have resulted in increased permeability of the cell wall to the dyes. Apart from the differences at baseline, Hendon-Dunn *et al.* (2016) also observed that a proportion of cells remained calcein positive in the first 72 hours of INH and RIF treatment. Based on the assumption that cells lacking esterase activity (calcein negative) will not be viable, we sorted calcein blue negative and positive subpopulations to compare their survival. We observed that were no differences in the survival of both subpopulations before and after antibiotic treatment (Figure 3.19). The heterogeneity we observed with the calcein dyes and FDA staining (Figure 3.5) is a phenomenon which has been observed in many bacteria and eukaryotes. This variation is thought to arise due to differences in protein expression and function (Newman *et al.*, 2006). Further studies are required to understand the molecular mechanisms of variation in calcein staining and to determine if the differences are due to gene or protein expression. The heterogeneity in staining we report here highlights the challenges of understanding processes at the single cell level and emphasizes that limitations of analysis at the population level largely ignore such variability (Honeyborne *et al.*, 2016;Kaern *et al.*, 2005).

When we stained with PI and Sytox red we also observed drug specific staining patterns. It was encouraging to note that most cells were negative for these dyes at baseline because they are cell impermeant dyes which measure membrane integrity (Bunthof *et al.*, 2001;Khan *et al.*, 2010). The small number of cells that were positive in the absence of drug could be due to some cell death during logarithmic growth or that different stages of the cell division may be associated with changes in membrane permeability.

After INH treatment there were slight changes in the proportion of cells that stained positive with PI. Although many cells stained negative for PI and Sytox, there was an increase in the number of cells that stained positive after EMB, RIF and CFZ treatment (Figure 3.4 and Figure 3.5). This suggested that most of the cells had intact cell membranes after 72 hours of drug treatment. Another explanation would be reduced cell membrane permeability to these dyes because as cells enter a state with changes to the cell wall. Stationary phase and stressed *M. tuberculosis* cells have been shown to exhibit changes in cell wall metabolism which may result in thickening and reduced permeability to antibiotics (Betts *et al.*, 2002;Xie *et al.*, 2005;Bhamidi *et al.*, 2012;Sarathy *et al.*, 2013;Boutte *et al.*, 2016).

When we compared the different PI and Sytox red subpopulations, there were no significant differences in the survival of the negative and positive subpopulations (Figure 3.16 and Figure 3.17) indicating both

dyes are not viability markers. PI may be a good dye for identifying cell damage (Soejima *et al.*, 2009) but a poor indicator of cell death. It has been shown previously in some other bacteria which were stained with PI that there was no difference in survival between PI positive and PI negative subpopulations (Amor *et al.*, 2002). We have also shown that this observation is true with *M. tuberculosis* at least after 72 hours of treatment.

$DiOC_2$ (3) and $DiBAC_4$ (3) gave poor signals of depolarisation so we were not able to distinguish cells with depolarised membranes from those with hyperpolarised membranes (Figure 3.8 and Figure 3.11). Antibiotic treatment caused the red: green ratio to increase suggesting that cell membrane was still hyperpolarised (Figure 3.9) although we cannot rule out that drugs may have altered the interaction of the dyes with the cell membrane independently of polarisation. The sensitivity of the assay using these dyes, as determined in our control experiments, may also have been too low to detect subtle changes in membrane polarity. Antibiotics may also cause the cells to become more permeable to the dye hence the increase in the red: green ratio with INH producing a highest increase.

$DiOC_2$ (3) and $DiBAC_4$ (3) have been successfully used to differentiate depolarised cells from hyperpolarised cells in Gram positive bacteria (David *et al.*, 2012;Neumeyer *et al.*, 2013;Nuding and Zabel, 2013). We confirmed this as *S. aureus*, a Gram positive bacteria produced a remarkable shift in the red: green fluorescence ratio compared to the Gram negative *E. coli* and *M. tuberculosis* when treated with CCCP as also noted by Chawla and Singh (2013). In another study, it has also been shown that anti-tubercular drugs bedaquiline and Q203 do not depolarise the *M. tuberculosis* membrane (Lamprecht *et al.*, 2016). Based on these observations the outer membrane on *E. coli* and *M. tuberculosis* seems to affect dye activity showing that using fluorescent dyes may not be ideal for tracking membrane potential as a marker of viability in such bacteria.

Grant *et al.* (2012) has shown that bacterial persisters can be eradicated using hydroxyl radicals generated by antibiotics. We evaluated production of ROS by anti-TB drugs using CellROX dyes. Although both CellROX Deep red and CellROX green detect hydroxyl and superoxide radicals, CellROX deep red gave the strongest signal with CHP treatment suggesting it was the best of our stains for detecting ROS in *M. tuberculosis* (Figure 3.11 and Figure 3.12). According to Dwyer *et al.* (2009), some antibiotics induce the formation of ROS in their bactericidal activity. We observed that CFZ and INH result in the production of ROS in a time dependant manner (Figure 3.13). This has been observed previously by staining with hydroxyphenyl fluorescein after INH treatment of *M. tuberculosis* and DHE after CFZ treatment (Kim *et al.*, 2012;Goletti *et al.*, 2013;Yano *et al.*, 2011;Lamprecht *et al.*, 2016). However, RIF treatment did not produce ROS as shown by Piccaro *et al.* (2014) who used electron paramagnetic resonance spin trapping to identify hydroxyl radical formation by RIF. Based on our results, the fluoroquinolones and STR did not seem to produce ROS (Figure 3.13). When we evaluated CellROX Deep red as marker of viability, we observed that after 24 hours of CFZ treatment the

CellROX negative subpopulation was slightly enriched for survival. This suggests that at early time points in CFZ treatment the staining patterns could be used to predict viability using CellROX Deep red. Unfortunately, this does not apply for RIF at early and later time points. Further work is ongoing to determine if CellROX can detect survival at lower drug concentrations.

Our main challenge has been identifying a stain which predicts viability. This could have been due to the fact that we used the plating method to verify viability. Unfortunately this is the only method we could use because the CFU plating method remains the gold standard for measuring viability, and so we cannot rule out the presence of viable but not culturable cells. Repeating the experiments using liquid media to recover persistors could result in us recovering a greater proportion of this poorly culturable subpopulation. It will be interesting to compare the transcription and proteomic profiles of different subpopulations to identify what drives differences in staining. Our antibiotic treatment was done using cells in early log phase and lasted for at least 72 hours because we wanted to identify a biomarker which could work both in the early stages of growth and later stages of growth.

Unlike other researchers who use heat killed controls, our gates were based on the unstained control and stained pre-treatment control as we were interested in evaluating changes in staining induced by antibiotics. We evaluated single stains for viability because before we could evaluate dually stained populations it was important to know the if single staining could predict viability after treatment with any of the antibiotics. It would be interesting to further evaluate the dually stained subpopulations from RIF and CFZ treated cells as well as from other antibiotics. Ultimately, we would like to test our techniques on bacteria that have been sorted directly from sputum samples, especially as staining of sputum with FDA has been associated with monitoring treatment outcome (Schramm *et al.*, 2012;Kanade *et al.*, 2016).

We treated for only 72 hours in the majority of our experiments and it could be argued that true persisters, especially in the case of slow growing organisms, only emerge after longer periods of treatment. To some extent this is supported by an increase in PI staining after one week and at later timepoints in the work of others (Hendon-Dunn *et al.*, 2016). However at the concentrations of drug used we found at least a 10-fold reduction in culturable bacteria (Appendix F). So what is the state of the 90% of bacteria that are not culturable? Are they truly dead, or dying or in a potentially resuscitable state given the right conditions? It is our belief that the majority of them are in fact dead and it is for this reason we selected early timepoints based on the kill kinetics of some of these antibiotics (Keren et al., 2011), in order to maximise the chances of finding survivors. However from the results we observed here it may be advantegeous to treat for a longer time, at least 168 hours or even longer. For treatment longer than 168 hours there will be a need to add more antibiotic depending on the stability and adopt strategies to flow many millions of bacteria to detect the anticipated <1% of culturable organisms present at later times. Another option would be to use a lower concentration of antibitoics assuming that

the tolerant phenotype is subtle and is only apparent at concentrations lower than the 10X MIC we used. However lower concentrations may not be relevant clinically and run the risk of selecting for resistance.

Müller and Nebe-von-Caron (2010) stated that the suitability of fluorescent dyes and staining protocols can only be understood by optimising for each bacterial species. Here we showed the challenges of using FACS in monitoring survival during antibiotic treatment in *M. tuberculosis*. We observed that the fluorescent dyes cannot be applied to all antibiotics and the interpretation of the staining patterns is not universal. This suggests that for *M. tuberculosis*, the dye to be used depends on the antibiotic and the mechanism of action. The application of fluorescent dyes to *M. tuberculosis* may be also be problematic due to the nature of the cell wall which acts as a barrier to antibiotics and dyes (Sarathy *et al.*, 2013;Rodrigues *et al.*, 2015) . If FACS is to be used to monitor survival during antibiotic treatment a newer generation of stains may need to be developed. Reporter strains which express fluorescent proteins can also be used to monitor the expression of specific metabolic pathways or stress response proteins such as IniBAC response in cells exposed to antibiotic treatment (Tan and Russell, 2015;Boot *et al.*, 2016;Liu *et al.*, 2016). These would overcome the membrane barrier which effects the uptake of fluorescent dyes.

In conclusion we observed drug specific staining patterns with marked heterogeneity for most of the stains and antibiotics tested. Amongst the stains evaluated we found that after 24 hours of CFZ treatment, CellROX Deep red negative cells were enriched for viable bacteria. Further work is now underway to characterise the mechanisms which are responsible for this phenotype.

REFERENCES

Ackermann, M. (2015). A functional perspective on phenotypic heterogeneity in microorganisms. *Nature Reviews Microbiology,* **13** (8)**,** 497-508.

Amann, R. I., Binder, B. J., Olson, R. J., Chisholm, S. W., Devereux, R. & Stahl, D. A. (1990). Combination of 16S rRNA-targeted oligonucleotide probes with flow cytometry for analyzing mixed microbial populations. *Applied and Environmental Microbiology,* **56** (6)**,** 1919-1925.

Amann, R. I., Ludwig, W. & Schleifer, K.-H. (1995). Phylogenetic identification and in situ detection of individual microbial cells without cultivation. *Microbiological Reviews,* **59** (1)**,** 143-169.

Ambriz-Aviña, V., Contreras-Garduño, J. A. & Pedraza-Reyes, M. (2014). Applications of Flow Cytometry to Characterize Bacterial Physiological Responses. *BioMed Research International,* **2014,** 1-14.

Amor, K. B., Breeuwer, P., Verbaarschot, P., Rombouts, F. M., Akkermans, A. D., De Vos, W. M. & Abee, T. (2002). Multiparametric flow cytometry and cell sorting for the assessment of viable, injured, and dead Bifidobacterium cells during bile salt stress. *Applied and Environmental Microbiology,* **68** (11)**,** 5209-5216.

Arndt-Jovin, D. J. & Jovin, T. M. (1989). Fluorescence labeling and microscopy of DNA. *Methods in Cell Biology,* **30,** 417-448.

Balaban, N. Q., Merrin, J., Chait, R., Kowalik, L. & Leibler, S. (2004). Bacterial persistence as a phenotypic switch. *Science,* **305** (5690)**,** 1622-1625.

Barer, M. (1997). Viable but non-culturable and dormant bacteria: time to resolve an oxymoron and a misnomer? *Journal of Medical Microbiology,* **46** (8)**,** 629-631.

Becker Cl, Jw, P. & Mk, H. 2002. Is Forward Scatter Monotonic on Commercial Flow Cytometers? *The International Society for Advancement of Cytometry XXI Congress.* San Diego, CA.

Belenky, P., Jonathan, D. Y., Porter, C. B., Cohen, N. R., Lobritz, M. A., Ferrante, T., Jain, S., Korry, B. J., Schwarz, E. G. & Walker, G. C. (2015). Bactericidal Antibiotics Induce Toxic Metabolic Perturbations that Lead to Cellular Damage. *Cell Reports,* **13** (5)**,** 968-980.

Betts, J. C., Lukey, P. T., Robb, L. C., Mcadam, R. A. & Duncan, K. (2002). Evaluation of a nutrient starvation model of *Mycobacterium tuberculosis* persistence by gene and protein expression profiling. *Molecular Microbiology,* **43** (3)**,** 717-731.

Bhamidi, S., Shi, L., Chatterjee, D., Belisle, J. T., Crick, D. C. & Mcneil, M. R. (2012). A bioanalytical method to determine the cell wall composition of *Mycobacterium tuberculosis* grown in vivo. *Analytical Biochemistry,* **421** (1)**,** 240-249.

Bigger, J. W. (1944). Treatment of staphylococcal infections with penicillin. *Lancet,* **244,** 497-500.

Boeree, M. J., Diacon, A. H., Dawson, R., Narunsky, K., Du Bois, J., Venter, A., Phillips, P. P., Gillespie, S. H., Mchugh, T. D. & Hoelscher, M. (2015). A dose-ranging trial to optimize the dose of rifampin in the treatment of tuberculosis. *American Journal of Respiratory and Critical Care Medicine,* **191** (9)**,** 1058-1065.

Boot, M., Sparrius, M., Jim, K. K., Commandeur, S., Speer, A., Van De Weerd, R. & Bitter, W. (2016). iniBAC induction Is Vitamin B12- and MutAB-dependent in *Mycobacterium marinum*. *The Journal of Biological Chemistry,* **291** (38)**,** 19800-12.

Boutte, C. C., Baer, C. E., Papavinasasundaram, K., Liu, W., Chase, M. R., Meniche, X., Fortune, S. M., Sassetti, C. M., Ioerger, T. R. & Rubin, E. J. (2016). A cytoplasmic peptidoglycan amidase homologue controls mycobacterial cell wall synthesis. *eLife,* **5,** e14590.

Breeuwer, P. & Abee, T. (2000). Assessment of viability of microorganisms employing fluorescence techniques. *International Journal of Food Microbiology,* **55** (1)**,** 193-200.

Bryk, R., Gold, B., Venugopal, A., Singh, J., Samy, R., Pupek, K., Cao, H., Popescu, C., Gurney, M. & Hotha, S. (2008). Selective killing of nonreplicating mycobacteria. *Cell Host & Microbe,* **3** (3)**,** 137-145.

Bullock, G. R. (1984). The current status of fixation for electron microscopy: a review. *Journal of Microscopy,* **133** (1)**,** 1-15.

Bunthof, C. J., Bloemen, K., Breeuwer, P., Rombouts, F. M. & Abee, T. (2001). Flow cytometric assessment of viability of lactic acid bacteria. *Applied and Environmental Microbiology,* **67** (5)**,** 2326-2335.

Button, D. & Robertson, B. R. (2001). Determination of DNA content of aquatic bacteria by flow cytometry. *Applied and Environmental Microbiology,* **67** (4)**,** 1636-1645.

Cabiscol, E., Tamarit, J. & Ros, J. (2010). Oxidative stress in bacteria and protein damage by reactive oxygen species. *International Microbiology,* **3** (1)**,** 3-8.

Caugant, D., Sandven, P., Eng, J., Jeque, J. & Tønjum, T. (1995). Detection of rifampin resistance among isolates of *Mycobacterium tuberculosis* from Mozambique. *Microbial Drug Resistance,* **1** (4)**,** 321-326.

CDC, Centers For Disease Control and Prevention. (2006). Notice to readers : Revised definition of XDR-TB. *Morbidity and Mortality Weekly Report,* **55,** 1176.

Chan, E., Chatterjee, D., Iseman, M. & Heifets, L. (2003). Pyrazinamide, ethambutol, ethionamide, and aminoglycosides. *Tuberculosis.* Lippincott Williams & Wilkins Philadelphia, PA.

Chan, E. D., Laurel, V., Strand, M. J., Chan, J. F., Huynh, M.-L. N., Goble, M. & Iseman, M. D. (2004). Treatment and outcome analysis of 205 patients with multidrug-resistant tuberculosis. *American Journal of Respiratory and Critical Care Medicine,* **169** (10)**,** 1103-1109.

Chan, L. L., Wilkinson, A. R., Paradis, B. D. & Lai, N. (2012). Rapid image-based cytometry for comparison of fluorescent viability staining methods. *Journal of Fluorescence,* **22** (5)**,** 1301-1311.

Chawla, M. & Singh, A. (2013). Detection of Membrane Potential in *Mycobacterium tuberculosis*. *Bioprotocol,* **3** (11)**,** 1-3.

Chengalroyen, M. D., Beukes, G. M., Gordhan, B. G., Streicher, E. M., Churchyard, G., Hafner, R., Warren, R., Otwombe, K., Martinson, N. & Kana, B. D. (2016). Detection and Quantification

of Differentially Culturable Tubercle Bacteria in Sputum from Tuberculosis Patients. *American Journal of Respiratory and Critical Care Medicine*.

Clarke, J. M., Gillings, M. R., Altavilla, N. & Beattie, A. J. (2001). Potential problems with fluorescein diacetate assays of cell viability when testing natural products for antimicrobial activity. *Journal of Microbiological Methods,* **46** (3)**,** 261-267.

Cogan, N. G. (2006). Effects of persistor formation on bacterial response to dosing. *Journal of Theoretical Biology,* **238,** 694-703.

Cohen, K., Bishai, W. & Pym, A. (2014). Molecular Basis of Drug Resistance in *Mycobacterium tuberculosis*. *In:* Hatfull, G. F. & Jacobs, W. R. J. (eds.) *Molecular Genetics of Mycobacteria.* Washington DC, USA: ASM Press.

Cole, S., Brosch, R., Parkhill, J., Garnier, T., Churcher, C., Harris, D., Gordon, S., Eiglmeier, K., Gas, S. & Barry, C. R. (1998). Deciphering the biology of *Mycobacterium tuberculosis* from the complete genome sequence. *Nature,* **393** (6685)**,** 537-544.

Comas, J. & Vives-Rego, J. (1997). Assessment of the effects of gramicidin, formaldehyde, and surfactants on *Escherichia coli* by flow cytometry using nucleic acid and membrane potential dyes. *Cytometry,* **29** (1)**,** 58-64.

Comas, J. & Vives-Rego, J. (1998). Enumeration, viability and heterogeneity in *Staphylococcus aureus* cultures by flow cytometry. *Journal of Microbiological Methods,* **32** (1)**,** 45-53.

Cooper, S. (1969). Cell division and DNA replication following a shift to a richer medium. *Journal of Molecular Biology,* **43** (1)**,** 1-11.

Cooper, S. (2006). Regulation of DNA synthesis in bacteria: analysis of the Bates/Kleckner licensing/initiation - mass model for cell cycle control. *Molecular Microbiology,* **62** (2)**,** 303-307.

Czechowska, K., Johnson, D. R. & Van Der Meer, J. R. (2008). Use of flow cytometric methods for single-cell analysis in environmental microbiology. *Current Opinion in Microbiology,* **11** (3)**,** 205-212.

Dahl, J. L., Kraus, C. N., Boshoff, H. I., Doan, B., Foley, K., Avarbock, D., Kaplan, G., Mizrahi, V., Rubin, H. & Barry, C. E. (2003). The role of RelMtb-mediated adaptation to stationary phase in long-term persistence of *Mycobacterium tuberculosis* in mice. *Proceedings of the National Academy of Sciences,* **100** (17)**,** 10026-10031.

Dartois, V. & Barry, C. E. (2010). Clinical pharmacology and lesion penetrating properties of second- and third-line antituberculous agents used in the management of multidrug-resistant (MDR) and extensively-drug resistant (XDR) tuberculosis. *Current Clinical Pharmacology,* **5** (2)**,** 96-114.

Davey, H. M., Weichart, D. H., Kell, D. B. & Kaprelyants, A. S. (2004). Estimation of microbial viability using flow cytometry. *Current Protocols in Cytometry*, **11** (11.3)**,** 1-44.

David, F., Hebeisen, M., Schade, G., Franco- Lara, E. & Di Berardino, M. (2012). Viability and membrane potential analysis of *Bacillus megaterium* cells by impedance flow cytometry. *Biotechnology and Bioengineering,* **109** (2)**,** 483-492.

De Rossi, E., Aínsa, J. A. & Riccardi, G. (2006). Role of mycobacterial efflux transporters in drug resistance: an unresolved question. *FEMS Microbiology Reviews,* **30** (1)**,** 36-52.

Deb, C., Lee, C.-M., Dubey, V. S., Daniel, J., Abomoelak, B., Sirakova, T. D., Pawar, S., Rogers, L. & Kolattukudy, P. E. (2009). A novel in vitro multiple-stress dormancy model for *Mycobacterium tuberculosis* generates a lipid-loaded, drug-tolerant, dormant pathogen. *PLoS One,* **4** (6)**,** e6077.

Decamp, O. & Warren, A. (2001). Abundance, biomass and viability of bacteria in wastewaters: impact of treatment in horizontal subsurface flow constructed wetlands. *Water Research,* **35** (14)**,** 3496-3501.

Dhandayuthapani, S., Via, L., Thomas, C., Horowitz, P., Deretic, D. & Deretic, V. (1995). Green fluorescent protein as a marker for gene expression and cell biology of mycobacterial interactions with macrophages. *Molecular Microbiology,* **17** (5)**,** 901-912.

Dhar, N. & Mckinney, J. D. (2010). *Mycobacterium tuberculosis* persistence mutants identified by screening in isoniazid treated mice. *Proceedings of the National Academy of Sciences,* **107,** 12275-12280.

Drlica, K. (1999). Mechanism of flouroquinolone action. *Current Opinion in Microbiology,* **2,** 504 - 508.

Dwyer, D. J., Belenky, P. A., Yang, J. H., Macdonald, I. C., Martell, J. D., Takahashi, N., Chan, C. T., Lobritz, M. A., Braff, D. & Schwarz, E. G. (2014). Antibiotics induce redox-related physiological alterations as part of their lethality. *Proceedings of the National Academy of Sciences,* **111** (20)**,** E2100-E2109.

Dwyer, D. J., Kohanski, M. A. & Collins, J. J. (2009). Role of reactive oxygen species in antibiotic action and resistance. *Current Opinion in Microbiology,* **12** (5)**,** 482-489.

Epps, D. E., Wolfe, M. L. & Groppi, V. (1994). Characterization of the steady-state and dynamic fluorescence properties of the potential-sensitive dye bis-(1, 3-dibutylbarbituric acid) trimethine oxonol ($DiBAC_4(3)$) in model systems and cells. *Chemistry and Physics of Lipids,* **69** (2)**,** 137-150.

Foladori, P., Bruni, L. & Tamburini, S. (2015). Bacteria viability and decay in water and soil of vertical subsurface flow constructed wetlands. *Ecological Engineering,* **82,** 49-56.

Fouchet, P., Jayat, C., Héchard, Y., Ratinaud, M.-H. & Frelat, G. (1993). Recent advances of flow cytometry in fundamental and applied microbiology. *Biology of the Cell,* **78** (1-2)**,** 95-109.

Fox, W. (1981). Whither short-course chemotherapy? *British Journal of Diseases of the Chest,* **75** (4)**,** 331-357.

Gillespie, S. H., Crook, A. M., Mchugh, T. D., Mendel, C. M., Meredith, S. K., Murray, S. R., Pappas, F., Phillips, P. P. & Nunn, A. J. (2014). Four-month moxifloxacin-based regimens for drug-sensitive tuberculosis. *New England Journal of Medicine,* **371** (17)**,** 1577-1587.

Glickman, M. S., Cox, J. S. & Jacobs, W. R. (2000). A novel mycolic acid cyclopropane synthetase is required for cording, persistence, and virulence of *Mycobacterium tuberculosis*. *Molecular Cell,* **5** (4)**,** 717-727.

Golchin, S. A., Stratford, J., Curry, R. J. & Mcfadden, J. A microfluidic system for long-term time-lapse microscopy studies of mycobacteria. *Tuberculosis,* **92** (6)**,** 489-496.

Goletti, D., Petruccioli, E., Romagnoli, A., Piacentini, M. & Fimia, G. M. (2013). Autophagy in *Mycobacterium tuberculosis* infection: a passepartout to flush the intruder out? *Cytokine & Growth Factor Reviews,* **24** (4)**,** 335-343.

Grant, S. S., Kaufmann, B. B., Chand, N. S., Haseley, N. & Hung, D. T. (2012). Eradication of bacterial persisters with antibiotic-generated hydroxyl radicals. *Proceedings of the National Academy of Sciences,* **109** (30)**,** 12147-12152.

Günther, S., Hübschmann, T., Rudolf, M., Eschenhagen, M., Röske, I., Harms, H. & Müller, S. (2008). Fixation procedures for flow cytometric analysis of environmental bacteria. *Journal of Microbiological Methods,* **75** (1)**,** 127-134.

Hammes, F. & Egli, T. (2010). Cytometric methods for measuring bacteria in water: advantages, pitfalls and applications. *Analytical and Bioanalytical Chemistry,* **397** (3)**,** 1083-1095.

Helaine, S., Cheverton, A. M., Watson, K. G., Faure, L. M., Matthews, S. A. & Holden, D. W. (2014). Internalization of *Salmonella* by macrophages induces formation of nonreplicating persisters. *Science,* **343** (6167)**,** 204-8.

Helb, D., Jones, M., Story, E., Boehme, C., Wallace, E., Ho, K., Kop, J., Owens, M. R., Rodgers, R. & Banada, P. (2010). Rapid detection of *Mycobacterium tuberculosis* and rifampin resistance by use of on-demand, near-patient technology. *Journal of Clinical Microbiology,* **48** (1)**,** 229-237.

Hendon-Dunn, C. L., Doris, K. S., Thomas, S. R., Allnutt, J. C., Marriott, A. a. N., Hatch, K. A., Watson, R. J., Bottley, G., Marsh, P. D. & Taylor, S. C. (2016). A flow cytometry method for rapidly assessing *M. tuberculosis* responses to antibiotics with different modes of action. *Antimicrobial Agents and Chemotherapy***,** AAC. 02712-15.

Heym, B., Zhang, Y., Poulet, S., Young, D. & Cole, S. (1993). Characterization of the *katG* gene encoding a catalase-peroxidase required for the isoniazid susceptibility of *Mycobacterium tuberculosis*. *Journal of Bacteriology,* **175** (13)**,** 4255-4259.

Hobby, G. L., Meyer, K. & Chaffee, E. (1942). Observations on the Mechanism of Action of Penicillin. *Experimental Biology and Medicine,* **50** (2)**,** 281-285.

Honeyborne, I., Mchugh, T. D., Kuittinen, I., Cichonska, A., Evangelopoulos, D., Ronacher, K., Van Helden, P. D., Gillespie, S. H., Fernandez-Reyes, D. & Walzl, G. (2016). Profiling persistent

tubercule bacilli from patient sputa during therapy predicts early drug efficacy. *BMC Medicine,* **14** (68)**,** 1-13.

Horobin, R. W., Stockert, J. C. & Rashid-Doubell, F. (2006). Fluorescent cationic probes for nuclei of living cells: why are they selective? A quantitative structure–activity relations analysis. *Histochemistry and Cell Biology,* **126** (2)**,** 165-175.

Jain, P., Weinrick, B. C., Kalivoda, E. J., Yang, H., Munsamy, V., Vilcheze, C., Weisbrod, T. R., Larsen, M. H., O'donnell, M. R. & Pym, A. (2016). Dual-Reporter Mycobacteriophages (Φ2DRMs) Reveal Preexisting *Mycobacterium tuberculosis* Persistent Cells in Human Sputum. *mBio,* **7** (5)**,** e01023-16.

Ji, B., Lounis, N., Maslo, C., Truffot-Pernot, C., Bonnafous, P. & Grosset, J. (1998). In vitro and in vivo activities of moxifloxacin and clinafloxacin against *Mycobacterium tuberculosis*. *Antimicrobial Agents and Chemotherapy,* **42** (8)**,** 2066-2069.

Jindani, A., Doré, C. J. & Mitchison, D. A. (2003). Bactericidal and sterilizing activities of antituberculosis drugs during the first 14 days. *American Journal of Respiratory and Critical Care Medicine,* **167** (10)**,** 1348-1354.

Johnson, I. (2010). *The Molecular Probes Handbook: A Guide to Fluorescent Probes and Labeling Technologies,* U.S.A, Life Technologies Corporation.

Joux, F. & Lebaron, P. (2000). Use of fluorescent probes to assess physiological functions of bacteria at single-cell level. *Microbes and Infection,* **2** (12)**,** 1523-1535.

Kaern, M., Elston, T. C., Blake, W. J. & Collins, J. J. (2005). Stochasticity in gene expression: from theories to phenotypes. *Nature Reviews Genetics,* **6** (6)**,** 451-464.

Kanade, S., Nataraj, G., Ubale, M. & Mehta, P. (2016). Fluorescein diacetate vital staining for detecting viability of acid-fast bacilli in patients on antituberculosis treatment. *International Journal of Mycobacteriology,* **5** (3)**,** 294-298.

Keren, I., Kaldalu, N., Spoering, A., Wang, Y. & Lewis, K. (2004). Persister cells and tolerance to antimicrobials. *FEMS Microbiology Letters,* **230** (1)**,** 13-18.

Keren, I., Minami, S., Rubin, E. & Lewis, K. (2011). Characterization and transcriptome analysis of *Mycobacterium tuberculosis* persisters. *mbio,* **2** (3)**,** e00100-11.

Keren, I., Wu, Y., Inocencio, J., Mulcahy, L. R. & Lewis, K. (2013). Killing by bactericidal antibiotics does not depend on reactive oxygen species. *Science,* **339** (6124)**,** 1213-1216.

Khan, M. M. T., Pyle, B. H. & Camper, A. K. (2010). Specific and Rapid Enumeration of Viable but Nonculturable and Viable-Culturable Gram-Negative Bacteria by Using Flow Cytometry. *Applied Environmental Microbiology,* **76** (15)**,** 5088-96.

Kim, J.-J., Lee, H.-M., Shin, D.-M., Kim, W., Yuk, J.-M., Jin, H. S., Lee, S.-H., Cha, G.-H., Kim, J.-M. & Lee, Z.-W. (2012). Host cell autophagy activated by antibiotics is required for their effective antimycobacterial drug action. *Cell Host & Microbe,* **11** (5)**,** 457-468.

Kirk, S. M., Schell, R. F., Moore, A. V., Callister, S. M. & Mazurek, G. H. (1998). Flow Cytometric Testing of Susceptibilities of *Mycobacterium tuberculosis* Isolates to Ethambutol, Isoniazid, and Rifampin in 24 Hours. *Journal of Clinical Microbiology,* **36** (6)**,** 1568-1573.

Knox, R., King, M. & Woodroffe, R. (1952). *In-vitro* action of isoniazid on *Mycobacterium tuberculosis*. *The Lancet,* **260** (6740)**,** 854-858.

Kohanski, M. A., Dwyer, D. J., Hayete, B., Lawrence, C. A. & Collins, J. J. (2007). A common mechanism of cellular death induced by bactericidal antibiotics. *Cell,* **130** (5)**,** 797-810.

Korshunov, S. & Imlay, J. A. (2006). Detection and quantification of superoxide formed within the periplasm of *Escherichia coli*. *Journal of Bacteriology,* **188** (17)**,** 6326-6334.

Krämer, C. E., Singh, A., Helfrich, S., Grünberger, A., Wiechert, W., Nöh, K. & Kohlheyer, D. (2015). Non-invasive microbial metabolic activity sensing at single cell level by perfusion of calcein acetoxymethyl ester. *PLoS One,* **10** (10)**,** e0141768.

Lagman, M., Ly, J., Saing, T., Singh, M. K., Tudela, E. V., Morris, D., Chi, P.-T., Ochoa, C., Sathananthan, A. & Venketaraman, V. (2015). Investigating the causes for decreased levels of glutathione in individuals with type II diabetes. *PLoS One,* **10** (3)**,** e0118436.

Lamprecht, D. A., Finin, P. M., Rahman, M. A., Cumming, B. M., Russell, S. L., Jonnala, S. R., Adamson, J. H. & Steyn, A. J. (2016). Turning the respiratory flexibility of *Mycobacterium tuberculosis* against itself. *Nature Communications,* **7**.

Lewis, K. (2007). Persister cells, dormancy and infectious disease. *Nature Reviews Microbiology,* **5** (1)**,** 48-56.

Lewis, K. (2010). Persister cells. *Annual Review of Microbiology,* **64,** 357-372.

Lin, P. L., Ford, C. B., Coleman, M. T., Myers, A. J., Gawande, R., Ioerger, T., Sacchettini, J., Fortune, S. M. & Flynn, J. L. (2014). Sterilization of granulomas is common in active and latent tuberculosis despite within-host variability in bacterial killing. *Nature Medicine,* **20** (1)**,** 75-79.

Liu, Y., Tan, S., Huang, L., Abramovitch, R. B., Rohde, K. H., Zimmerman, M. D., Chen, C., Dartois, V., Vanderven, B. C. & Russell, D. G. (2016). Immune activation of the host cell induces drug tolerance in *Mycobacterium tuberculosis* both in vitro and in vivo. *The Journal of Experimental Medicine,* **213** (5)**,** 809-25.

Lobritz, M. A., Belenky, P., Porter, C. B., Gutierrez, A., Yang, J. H., Schwarz, E. G., Dwyer, D. J., Khalil, A. S. & Collins, J. J. (2015). Antibiotic efficacy is linked to bacterial cellular respiration. *Proceedings of the National Academy of Sciences,* **112** (27)**,** 8173-8180.

Loontiens, F. G., Regenfuss, P., Zechel, A., Dumortier, L. & Clegg, R. M. (1990). Binding characteristics of Hoechst 33258 with calf thymus DNA, poly [d (AT)] and d (CCGGAATTCCGG): multiple stoichiometries and determination of tight binding with a wide spectrum of site affinities. *Biochemistry,* **29** (38)**,** 9029-9039.

Machado, D., Couto, I., Perdigao, J., Rodrigues, L., Portugal, I., Baptista, P., Veigas, B., Amaral, L. & Viveiros, M. (2012). Contribution of efflux to the emergence of isoniazid and multidrug resistance in *Mycobacterium tuberculosis*. *PLoS One,* **7** (4)**,** e34538.

Maecker, H. T. & Trotter, J. (2006). Flow cytometry controls, instrument setup, and the determination of positivity. *Cytometry Part A,* **69** (9)**,** 1037-1042.

Maglica, Ž., Özdemir, E. & Mckinney, J. D. (2015). Single-Cell Tracking Reveals Antibiotic-Induced Changes in Mycobacterial Energy Metabolism. *mbio,* **6** (1)**,** e02236-14.

Maher, K. J. & Fletcher, M. A. (2005). Quantitative flow cytometry in the clinical laboratory. *Clinical and Applied Immunology Reviews,* **5** (6)**,** 353-372.

Maisonneuve, E. & Gerdes, K. (2014). Molecular mechanisms underlying bacterial persisters. *Cell,* **157** (3)**,** 539-548.

Manina, G., Dhar, N. & Mckinney, J. D. (2015). Stress and host immunity amplify *Mycobacterium tuberculosis* phenotypic heterogeneity and induce nongrowing metabolically active forms. *Cell Host & Microbe,* **17** (1)**,** 32-46.

Manina, G. & Mckinney, J. D. (2013). A single-cell perspective on non-growing but metabolically active (NGMA) bacteria. *In:* Pieters, J., Mckinney, John D (ed.) *Pathogenesis of Mycobacterium tuberculosis and its Interaction with the Host Organism.* Heidelberg, Berlin Springer.

Mason, D., Lopéz- Amorós, R., Allman, R., Stark, J. & Lloyd, D. (1995). The ability of membrane potential dyes and calcafluor white to distinguish between viable and non- viable bacteria. *Journal of Applied Bacteriology,* **78** (3)**,** 309-315.

Mc Dermott, W. (1958). Microbial persistence. *Yale Journal of Biology and Medicine,* **30,** 257-291.

Mikusová, K., Slayden, R. A., Besra, G. S. & Brennan, P. J. (1995). Biogenesis of the mycobacterial cell wall and the site of action of ethambutol. *Antimicrobial Agents and chemotherapy,* **39** (11)**,** 2484-2489.

Miller, L. P., Crawford, J. T. & Shinnick, T. M. (1994). The *rpoB* gene of *Mycobacterium tuberculosis*. *Antimicrobial Agents and Chemotherapy,* **38** (4)**,** 805-811.

Mitchison, D. & Davies, G. (2012). The chemotherapy of tuberculosis: past, present and future [State of the art]. *The International Journal of Tuberculosis and Lung Disease,* **16** (6)**,** 724-732.

Moore, A. V., Kirk, S. M., Callister, S. M., Mazurek, G. H. & Schell, R. F. (1999). Safe determination of susceptibility of *Mycobacterium tuberculosis* to antimycobacterial agents by flow cytometry. *Journal of Clinical Microbiology,* **37** (3)**,** 479-483.

Mouton, J. M., Helaine, S., Holden, D. W. & Sampson, S. L. (2016). Elucidating population-wide mycobacterial replication dynamics at the single-cell level. *Microbiology,* **162** (6)**,** 966-78.

Müller, S. & Nebe-Von-Caron, G. (2010). Functional single-cell analyses: Flow cytometry and cell sorting of microbial populations and communities. *FEMS Microbiology Reviews,* **34** (4)**,** 554-587.

Nair, J., Rouse, D. A., Bai, G. H. & Morris, S. L. (1993). The *rpsL* gene and streptomycin resistance in single and multiple drug-resistant strains of *Mycobacterium tuberculosis*. *Molecular Microbiology,* **10** (3)**,** 521-527.

Nebe-Von-Caron, G., Stephens, P., Hewitt, C., Powell, J. & Badley, R. (2000). Analysis of bacterial function by multi-colour fluorescence flow cytometry and single cell sorting. *Journal of Microbiological Methods,* **42** (1)**,** 97-114.

Nettmann, E., Fröhling, A., Heeg, K., Klocke, M., Schlüter, O. & Mumme, J. (2013). Development of a flow-fluorescence in situ hybridization protocol for the analysis of microbial communities in anaerobic fermentation liquor. *BMC Microbiology,* **13** (1)**,** 1.

Neumeyer, A., Hübschmann, T., Müller, S. & Frunzke, J. (2013). Monitoring of population dynamics of *Corynebacterium glutamicum* by multiparameter flow cytometry. *Microbial Biotechnology,* **6** (2)**,** 157-167.

Newman, J. R., Ghaemmaghami, S., Ihmels, J., Breslow, D. K., Noble, M., Derisi, J. L. & Weissman, J. S. (2006). Single-cell proteomic analysis of *S. cerevisiae* reveals the architecture of biological noise. *Nature,* **441** (7095)**,** 840-846.

Norden, M. A., Kurzynski, T. A., Bownds, S. E., Callister, S. M. & Schell, R. F. (1995). Rapid susceptibility testing of *Mycobacterium tuberculosis* (H37Ra) by flow cytometry. *Journal of Clinical Microbiology,* **33** (5)**,** 1231-1237.

Novo, D., Perlmutter, N. G., Hunt, R. H. & Shapiro, H. M. (1999). Accurate flow cytometric membrane potential measurement in bacteria using diethyloxacarbocyanine and a ratiometric technique. *Cytometry,* **35** (1)**,** 55-63.

Novo, D. J., Perlmutter, N. G., Hunt, R. H. & Shapiro, H. M. (2000). Multiparameter Flow Cytometric Analysis of Antibiotic Effects on Membrane Potential, Membrane Permeability, and Bacterial Counts of *Staphylococcus aureus* and *Micrococcus luteus*. *Antimicrobial Agents and Chemotherapy,* **44** (4)**,** 827-834.

Nuding, S. & Zabel, L. T. (2013). Detection, identification, and susceptibility testing of bacteria by flow cytometry. *Journal of Bacteriology & Parasitology,* **2013**.

O'donnell, M. R., Pym, A., Jain, P., Munsamy, V., Wolf, A., Karim, F., Jacobs, W. R. & Larsen, M. H. (2015). A Novel Reporter Phage To Detect Tuberculosis and Rifampin Resistance in a High-HIV-Burden Population. *Journal of Clinical Microbiology,* **53** (7)**,** 2188-2194.

Paixão, L., Rodrigues, L., Couto, I., Martins, M., Fernandes, P., De Carvalho, C. C., Monteiro, G. A., Sansonetty, F., Amaral, L. & Viveiros, M. (2009). Fluorometric determination of ethidium bromide efflux kinetics in *Escherichia coli*. *Journal of Biological Engineering,* **3** (18)**,** 1- 13.

Patterson, G. H. & Lippincott-Schwartz, J. (2002). A photoactivatable GFP for selective photolabeling of proteins and cells. *Science,* **297** (5588)**,** 1873-1877.

Piccaro, G., Pietraforte, D., Giannoni, F., Mustazzolu, A. & Fattorini, L. (2014). Rifampin induces hydroxyl radical formation in *Mycobacterium tuberculosis*. *Antimicrobial Agents and Chemotherapy,* **58** (12)**,** 7527-7533.

Piddock, L. J. (2006). Multidrug-resistance efflux pumps? not just for resistance. *Nature Reviews Microbiology,* **4** (8)**,** 629-636.

Postgate, J. R. (1969). Viable counts and viability. *Journal of Microbiological Methods,* **1,** 611-628.

Probes, M. (2010). *Acetoxymethyl (AM) and acetate esters,* U.S.A, Life Technologies Incorporation.

Rehse, M. A., Corpuz, S., Heimfeld, S., Minie, M. & Yachimiak, D. (1995). Use of fluorescence threshold triggering and high- speed flow cytometry for rare event detection. *Cytometry,* **22** (4)**,** 317-322.

Rodrigues, L., Viveiros, M. & Ainsa, J. A. (2015). Measuring efflux and permeability in mycobacteria. *Methods in Molecular Biology,* **1285,** 227-39.

Roth, B. L., Poot, M., Yue, S. T. & Millard, P. J. (1997). Bacterial viability and antibiotic susceptibility testing with SYTOX green nucleic acid stain. *Applied and Environmental Microbiology,* **63** (6)**,** 2421-2431.

Rusconi, R., Garren, M. & Stocker, R. (2014). Microfluidics expanding the frontiers of microbial ecology. *Annual Review of Biophysics,* **43,** 65-91.

Sabban, S. (2011). *Development of an in vitro model system for studying the interaction of Equus caballus lgE with its high-affinity Fc receptor.* Doctorate of Philosophy, The University of Sheffield.

Sarathy, J., Dartois, V., Dick, T. & Gengenbacher, M. (2013). Reduced drug uptake in phenotypically resistant nutrient-starved nonreplicating *Mycobacterium tuberculosis*. *Antimicrobial Agents and Chemotherapy,* **57** (4)**,** 1648-1653.

Schramm, B., Hewison, C., Bonte, L., Jones, W., Camelique, O., Ruangweerayut, R., Swaddiwudhipong, W. & Bonnet, M. (2012). Field evaluation of a simple fluorescence method for detection of viable *Mycobacterium tuberculosis* in sputum specimens during treatment follow-up. *Journal of Clinical Microbiology,* **50** (8)**,** 2788-90.

Shapiro, H. M. (2003). *Practical flow cytometry,* New Jersey, USA, John Wiley & Sons.

Shapiro, H. M. (2005). *Practical flow cytometry,* John Wiley & Sons.

Shapiro, H. M. (2015). Microbial cytometry: What it was, Is and Maybe. *In:* Wilkinson, M. G. (ed.) *Flow cytometry in Microbiology : Technology and Applications.* England: Caister Academic Press.

Shapiro, H. M. & Nebe-Von-Caron, G. (2004). Multiparameter flow cytometry of bacteria. *In:* Hawley, T. S. & Hawley, R. G. (eds.) *Flow Cytometry Protocols.* 2nd ed. New York, USA: Humana Press.

Shapiro, H. M. & Perlmutter, N. G. (2001). Violet laser diodes as light sources for cytometry. *Cytometry,* **44** (2)**,** 133-136.

Shu, Z., Weigel, K. M., Soelberg, S. D., Lakey, A., Cangelosi, G. A., Lee, K. H., Chung, J. H. & Gao, D. (2012). Cryopreservation of *Mycobacterium tuberculosis* complex cells. *Journal of Clinical Microbiology,* **50** (11)**,** 3575-80.

Singh, R., Barry, C. E. I. & Boshoff, H. I. (2010). The three RelE homologs of *Mycobacterium tuberculosis* have individual drug-specific effects on bacterial antibiotic tolerance. *Journal of Bacteriology,* **192,** 1279-1291.

Soejima, T., Iida, K., Qin, T., Taniai, H. & Yoshida, S. (2009). Discrimination of live, anti-tuberculosis agent-injured, and dead *Mycobacterium tuberculosis* using flow cytometry. *FEMS Microbiology Letters,* **294** (1)**,** 74-81.

Southward, C. M. & Surette, M. G. (2002). The dynamic microbe: green fluorescent protein brings bacteria to light. *Molecular Microbiology,* **45** (5)**,** 1191 - 1195.

Sträuber, H. & Müller, S. (2010). Viability states of bacteria—specific mechanisms of selected probes. *Cytometry Part A,* **77** (7)**,** 623-634.

Strober, W. (2001). Monitoring cell growth. *Current Protocols in Immunology,* **Appendix 3A,** A. 3A. 1-A. 3A. 2.

Szumowski, J. D., Adams, K. N., Edelstein, P. H. & Ramakrishnan, L. (2012). Antimicrobial efflux pumps and *Mycobacterium tuberculosis* drug tolerance: evolutionary considerations. *In:* Pieters, J. & Mckinney, J. D. (eds.) *Pathogenesis of Mycobacterium tuberculosis and its Interaction with the Host Organism.* Berlin: Springer.

Takayama, K. & Kilburn, J. O. (1989). Inhibition of synthesis of arabinogalactan by ethambutol in *Mycobacterium smegmatis*. *Antimicrobial Agents and Chemotherapy,* **33** (9)**,** 1493-1499.

Tan, S. & Russell, D. G. (2015). Trans- species communication in the *Mycobacterium tuberculosis*-infected macrophage. *Immunological Reviews,* **264** (1)**,** 233-248.

Telford, W. G., Shcherbakova, D. M., Buschke, D., Hawley, T. S. & Verkhusha, V. V. (2015). Multiparametric flow cytometry using near-infrared fluorescent proteins engineered from bacterial phytochromes. *PLoS One,* **10** (3)**,** e0122342.

Timmins, G. S. & Deretic, V. (2006). Mechanisms of action of isoniazid. *Molecular Microbiology,* **62** (5)**,** 1220-1227.

Tracy, B. P., Gaida, S. M. & Papoutsakis, E. T. (2010). Flow cytometry for bacteria: enabling metabolic engineering, synthetic biology and the elucidation of complex phenotypes. *Current Opinion in Biotechnology,* **21** (1)**,** 85-99.

Trouillon, R. L., Passarelli, M. K., Wang, J., Kurczy, M. E. & Ewing, A. G. (2012). Chemical analysis of single cells. *Analytical Chemistry,* **85** (2)**,** 522-542.

Tudó, G., Laing, K., Mitchison, D. A., Butcher, P. D. & Waddell, S. J. (2010). Examining the basis of isoniazid tolerance in nonreplicating *Mycobacterium tuberculosis* using transcriptional profiling. *Future Medicinal Chemistry,* **2** (8)**,** 1371-1383.

Tzur, A., Moore, J. K., Jorgensen, P., Shapiro, H. M. & Kirschner, M. W. (2011). Optimizing optical flow cytometry for cell volume-based sorting and analysis. *PLoS One,* **6** (1)**,** e16053.

Valdivia, R. H. & Falkow, S. (1997). Fluorescence-based isolation of bacterial genes expressed within host cells. *Science,* **277** (5334)**,** 2007-2011.

Veal, D., Deere, D., Ferrari, B., Piper, J. & Attfield, P. (2000). Fluorescence staining and flow cytometry for monitoring microbial cells. *Journal of Immunological Methods,* **243** (1)**,** 191-210.

Virgo, P. F. & Gibbs, G. J. (2012). Flow cytometry in clinical pathology. *Annals of Clinical Biochemistry,* **49** (1)**,** 17-28.

Viveiros, M., Martins, M., Rodrigues, L., Machado, D., Couto, I., Ainsa, J. & Amaral, L. (2012). Inhibitors of mycobacterial efflux pumps as potential boosters for anti-tubercular drugs. *Expert Review of Anti-infective therapy,* **10** (9)**,** 983-998.

Vives-Rego, J., Lebaron, P. & Nebe-Von Caron, G. (2000). Current and future applications of flow cytometry in aquatic microbiology. *FEMS Microbiology Reviews,* **24** (4)**,** 429-448.

Völsch, A., Nader, W., Geiss, H., Nebe, G. & Birr, C. (1990). Detection and analysis of two serotypes of ammonia-oxidizing bacteria in sewage plants by flow cytometry. *Applied and Environmental Microbiology,* **56** (8)**,** 2430-2435.

Vromman, F., Laverrière, M., Perrinet, S., Dufour, A. & Subtil, A. (2014). Quantitative monitoring of the *Chlamydia trachomatis* developmental cycle using GFP-expressing bacteria, microscopy and flow cytometry. *PLoS One,* **9** (6)**,** e99197.

Wakamoto, Y., Dhar, N., Chait, R., Schneider, K., Signorino-Gelo, F., Leibler, S. & Mckinney, J. D. (2013). Dynamic persistence of antibiotic-stressed mycobacteria. *Science,* **339** (6115)**,** 91-95.

Wang, Y., Hammes, F., De Roy, K., Verstraete, W. & Boon, N. (2010). Past, present and future applications of flow cytometry in aquatic microbiology. *Trends in Biotechnology,* **28** (8)**,** 416-424.

Waring, M. (1965). Complex formation between ethidium bromide and nucleic acids. *Journal of Molecular Biology,* **13** (1)**,** 269-282.

Wayne, L. G. & Hayes, L. G. (1996). An in vitro model for sequential study of shiftdown of *Mycobacterium tuberculosis* through two stages of nonreplicating persistence. *Infection and Immunity,* **64** (6)**,** 2062-2069.

WHO, World Health Organisation (2015). Global Tuberculosis Report 2015. Available: http://apps.who.int/iris/bitstream/10665/191102/1/9789241565059_eng.pdf?ua=1 [Accessed 28/01/2016].

Wickens, H., Pinney, R., Mason, D. & Gant, V. (2000). Flow cytometric investigation of filamentation, membrane patency, and membrane potential in *Escherichia coli* following ciprofloxacin exposure. *Antimicrobial Agents and Chemotherapy,* **44** (3)**,** 682-687.

Wolfe, A., Shimer Jr, G. H. & Meehan, T. (1987). Polycyclic aromatic hydrocarbons physically intercalate into duplex regions of denatured DNA. *Biochemistry,* **26** (20)**,** 6392-6396.

Wu, L., Wang, S., Song, Y., Wang, X. & Yan, X. (2016). Applications and challenges for single-bacteria analysis by flow cytometry. *Science China Chemistry,* **59** (1)**,** 30-39.

Xie, Z., Siddiqi, N. & Rubin, E. J. (2005). Differential antibiotic susceptibilities of starved *Mycobacterium tuberculosis* isolates. *Antimicrobial Agents and Chemotherapy,* **49** (11)**,** 4778-4780.

Yamaguchi, N. & Nasu, M. (1997). Flow cytometric analysis of bacterial respiratory and enzymatic activity in the natural aquatic environment. *Journal of Applied Microbiology,* **83** (1)**,** 43-52.

Yano, T., Kassovska-Bratinova, S., Teh, J. S., Winkler, J., Sullivan, K., Isaacs, A., Schechter, N. M. & Rubin, H. (2011). Reduction of clofazimine by mycobacterial Type 2 NADH: Quinone oxidoreductase a pathway for the generation of bactericidal levels of reactive oxygen species. *Journal of Biological Chemistry,* **286** (12)**,** 10276-10287.

Zhang, Y. (2005). The magic bullets and tuberculosis drug targets. *Annual Reviews of Pharmacology and Toxicology,* **45,** 529-564.

Zhang, Y., Garbe, T. & Young, D. (1993). Transformation with katG restores isoniazid- sensitivity in *Mycobacterium tuberculosis* isolates resistant to a range of drug concentrations. *Molecular Microbiology,* **8** (3)**,** 521-524.

Zhang, Y. & Mitchison, D. (2003). The curious characteristics of pyrazinamide: a review. *The International Journal of Tuberculosis and Lung Disease,* **7** (1)**,** 6-21.

Zhang, Y., Yew, W. W. & Barer, M. R. (2012). Targeting persisters for tuberculosis control. *Antimicrobial Agents and Chemotherapy,* **56** (5)**,** 2223-2230.

Zhao, B. Y., Pine, R., Domagala, J. & Drlica, K. (1999). Fluoroquinolone Action against Clinical Isolates of M*ycobacterium tuberculosis*: Effects of a C-8 Methoxyl Group on Survival in Liquid Media and in Human Macrophages. *Antimicrobial Agents and Chemotherapy,* **43** (3)**,** 661-666.

APPENDIX A

Preparation of media

Middlebrook 7H9 media

- Middlebrook 7H9 broth base (Becton Dickinson) 4.9 g per litre.
- Powder dissolved in 900 mL deionised water.
- 10mL of 50% glycerol, 2.5 mL of 80% Tween and 100 mL oleic -albumin- dextrose -catalase (OADC) enrichment (Becton Dickinson) added.
- Media filter sterilised (Sigma 1 L filter systems) and stored at 4 ºC

Middlebrook 7H10 Agar plates

- Middlebrook 7H10 agar base (Becton Dickinson) 19 g per litre. Dissolved in 9000 mL deionised water.
- 10 mL of 50% glycerol added.
- Agar autoclaved at 121 ºC for 15 minutes.
- Allowed to cool to 65 °C then 100 mL OADC enrichment added
- Poured 25 mL into petri dish and allowed to set
- Plates stored at 4 ºC

APPENDIX B

Preparation of Antimicrobial stock solutions

- Antimicrobial powder (Sigma Aldrich) was dissolved in respective solvent to make 10 mg/mL stock solution immediately before use.
- This was the working concentration for most antibiotics except INH, EMB and CFZ.
- The working concentration for INH, EMB and CFZ was 1 mg/mL.

Solvents used to dissolve antibiotics and concentrations of antibiotic used.

Antibiotic	**Solvent**	**MIC concentration (µg/mL)**	**10X MIC concentration (µg/mL)**
INH	Sterile deionised water	0.1	1
RIF	Dimethyl sulfoxide	0.4	4
EMB	Sterile deionised water	0.1	1
Fluoroquinolones (OFX, LVX, MOX)	0.1M NaOH	1 – LVX and OFX 0.5 - MOX	10 – LVX and OFX 5 - MOX
STR	Sterile deionised water	0.1	1
CFZ	Dimethyl sulfoxide	0.1	1

APPENDIX C

Properties of the fluorescent dyes and cytometer settings

Fluorescent dye / Parameter	**Filter**	**PMT voltage**
Calcein blue	DAPI	425
Calcein green	FITC	450
FDA	FITC	450
PI	PI	550
Sytox red	Alexa Fluor 647	522
$DiOC_2$ (3) – green fluorescence	Alexa Fluor 488	444
$DiOC_2$ (3) – red fluorescence	PerCP-Cy5.5	511
$DiBAC_4$ (3)	FITC	450
CellROX Green	FITC	450
CellROX Deep red	APC	400
CellROX Orange	PE	438
DHE	PerCP-Cy5.5	511
FSC	FSC	100
SSC	SSC	200

APPENDIX D

Final concentrations of fluorescent dyes

Fluorescent dye	**Final concentration**
Calcein blue	5 µg/mL
Calcein green	5 µg/mL
FDA	2.5 µg/mL
PI	2 µg/mL
Sytox red	5 µg/mL
$DiOC_2$ (3)	15 µM
$DiBAC_4$ (3)	0.05 µg/mL
CellROX Green	5 µM
CellROX Deep red	5 µM
CellROX Orange	5 µM

APPENDIX E

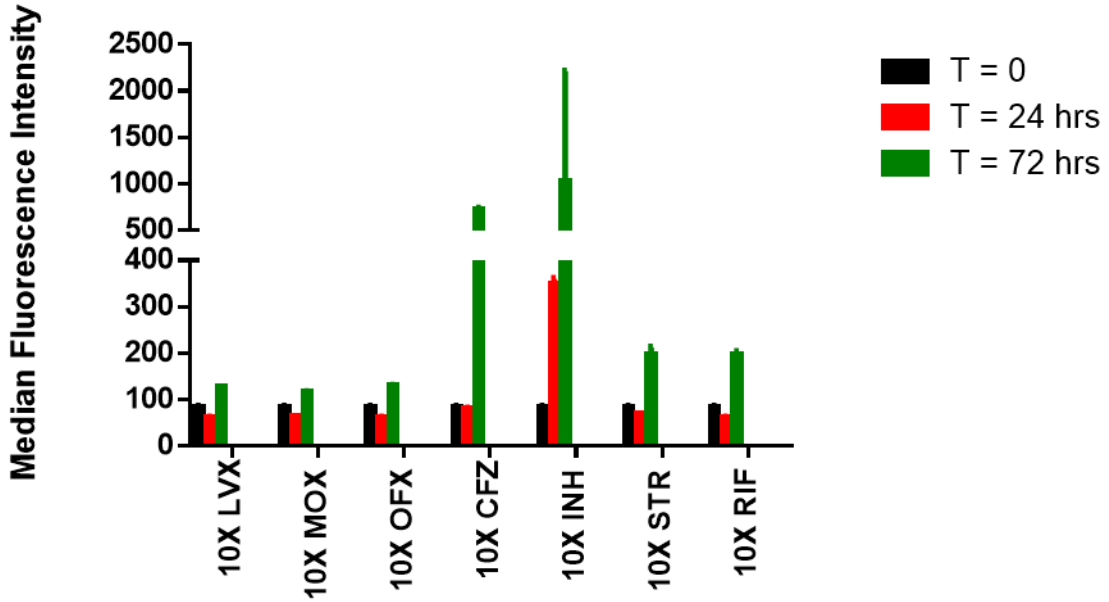

Figure A1. Evaluating ROS production by anti-TB drugs using CellROX deep red. Cells were stained in triplicate with CellROX Deep red to measure ROS production after 24 and 72 hours of drug treatment. The histograms show that there were very subtle changes in the fluorescence intensity after treatment with fluoroquinolones (LVX, MOXI and OFX). There was a great increase in the CellROX Deep red fluorescence intensity after CFZ and INH treatment. There were minimal changes in the fluorescence intensity after STR and RIF treatment. The y axis shows the median fluorescence intensity. The x axis shows the different antibiotic treatments. Error bars represent standard deviation.

APPENDIX F

I

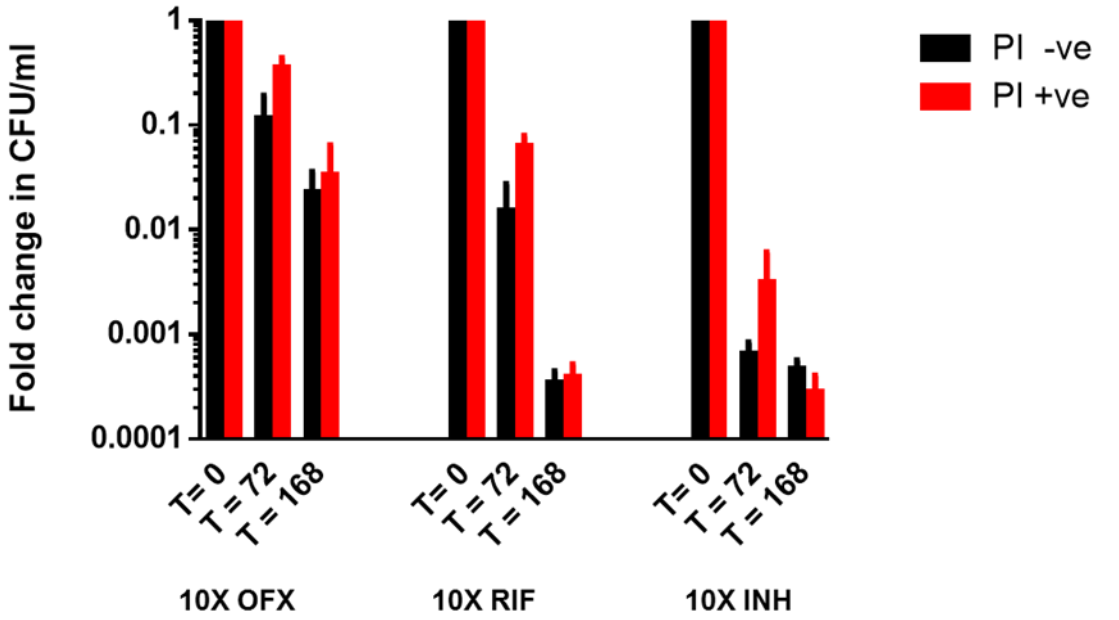

II

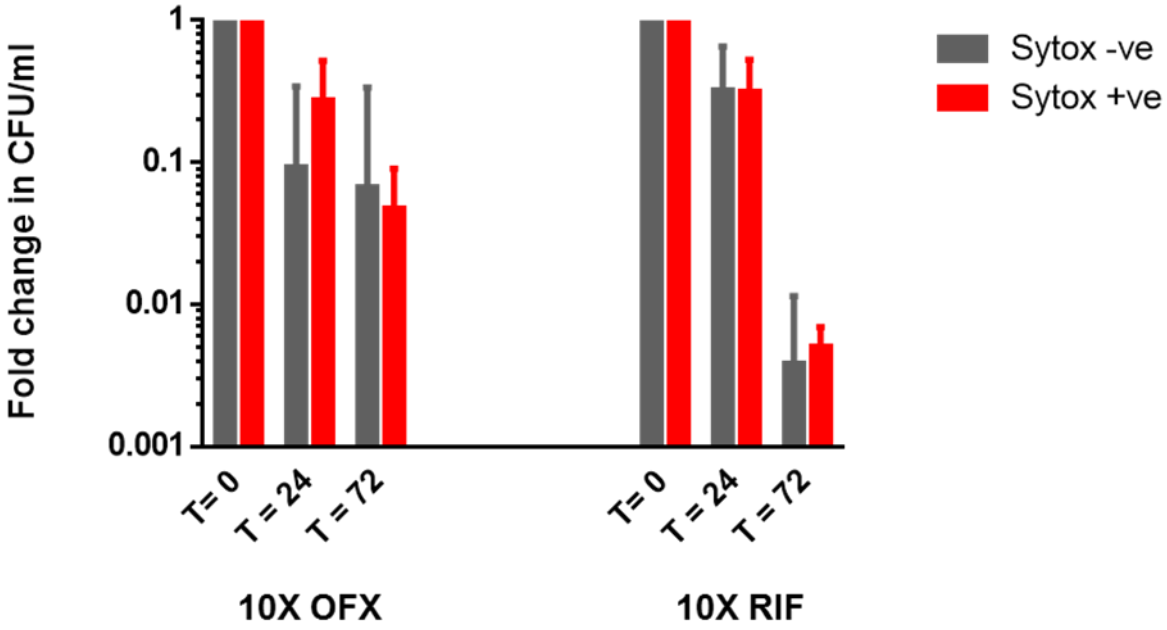

III

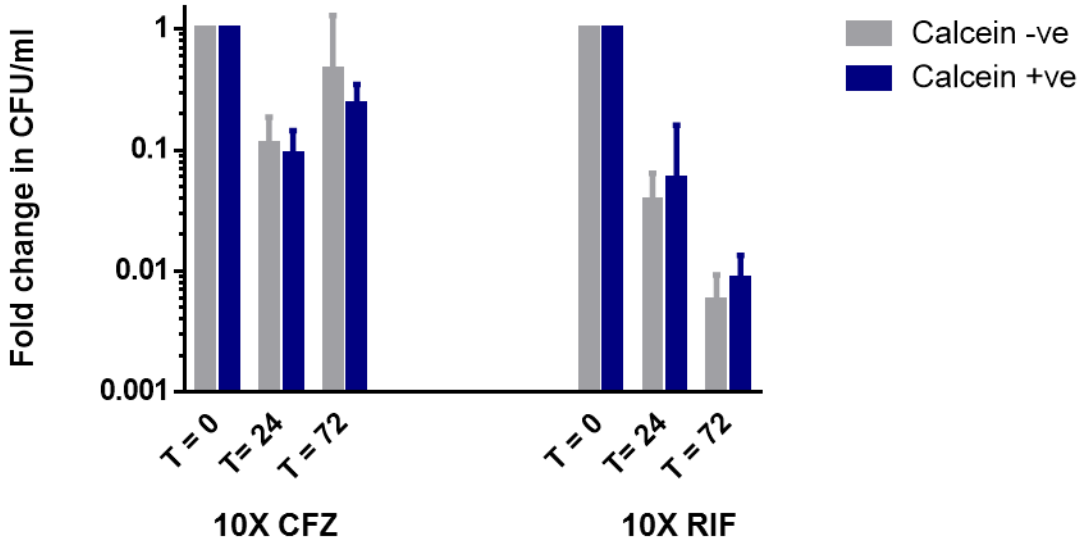

IV

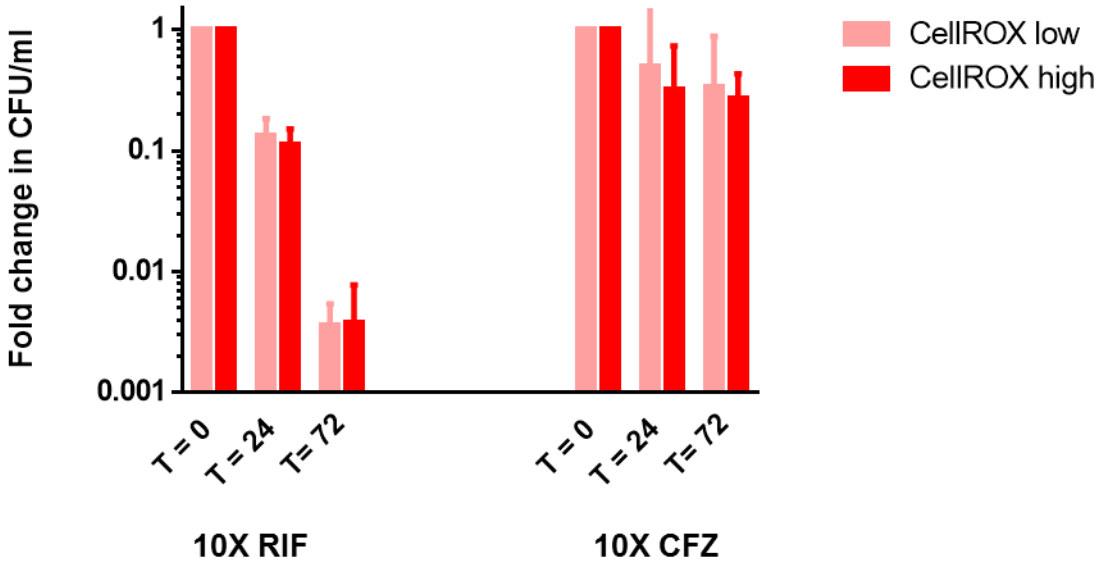

Figure A2. Killing kinetics during treatment with different antibiotics. Cells were stained in triplicate with different fluorescent stains after antibiotic treatment. A specific number of events was sorted from different subpopulations and plated for CFU. The observed CFU was used to calculate the CFU/ml. I – PI staining, II – sytox red, III – calcein blue and IV – CellROX deep red. There was approximately 90% killing after 72 hours of OFX and more than 90% killing after RIF and INH treatment. CFZ treatment however showed about 50% killing after 72 hours. There were very minimal differences between the negative and positive subpopulations from the different subpopulations. Error bars represent standard deviation.